Row-stochastic matrices can provably outperform doubly stochastic matrices in decentralized learning

Bing Liu 1 Boao Kong 2 Limin Lu 1 Kun Yuan 3 Chengcheng Zhao 1

Abstract

Decentralized learning often involves a weighted global loss with heterogeneous node weights λ . We revisit two natural strategies for incorporating these weights: (i) embedding them into the local losses to retain a uniform weight (and thus a doubly stochastic matrix), and (ii) keeping the original losses while employing a λ -induced rowstochastic matrix. Although prior work shows that both strategies yield the same expected descent direction for the global loss, it remains unclear whether the Euclidean-space guarantees are tight and what fundamentally differentiates their behaviors. To clarify this, we develop a weighted Hilbert-space framework $L^2(\lambda; \mathbb{R}^d)$ and obtain convergence rates that are strictly tighter than those from Euclidean analysis. In this geometry, the row-stochastic matrix becomes self-adjoint whereas the doubly stochastic one does not, creating additional penalty terms that amplify consensus error, thereby slowing convergence. Consequently, the difference in convergence arises not only from spectral gaps but also from these penalty terms. We then derive sufficient conditions under which the row-stochastic design converges faster even with a smaller spectral gap. Finally, by using a Rayleigh-quotient and Loewnerorder eigenvalue comparison, we further obtain topology conditions that guarantee this advantage and yield practical topology-design guidelines.

1. Introduction

The ever-increasing scale of data and models has made distributed learning a central paradigm for large-scale optimization. Among its variants, decentralized learning has attracted growing attention for its robustness to single-point failures, low communication overhead, and strong scalability. Most existing analyses, however, assume uniform node weights and symmetric, doubly stochastic mixing (Lian et al., 2017; Alghunaim & Yuan, 2022; Koloskova et al., 2020). In practical systems, nodes often possess unequal data volumes and computational capacities, making heterogeneous weighting a more practical choice.

Therefore, we study decentralized learning over a network of n nodes with heterogeneous weights $\lambda = [\lambda_1, \dots, \lambda_n]^{\top}$. Each node i accesses its local data distribution \mathcal{D}_i and collaboratively solves the weighted optimization problem

$$\min_{\theta \in \mathbb{R}^d} F(\theta) = \frac{1}{n} \sum_{i=1}^n \lambda_i \left[F_i(\theta) := \mathbb{E}_{\xi_{i,j} \sim \mathcal{D}_i} \left[f_i(\theta, \xi_{i,j}) \right] \right], \tag{1}$$

where $\lambda_i > 0$ and $\sum_{i=1}^n \lambda_i = n$, and $f_i(\theta, \xi_{i,j})$ denotes the instantaneous loss of sample $\xi_{i,j}$ evaluated at θ .

Two natural decentralized designs arise to solve problem (1).

- **Strategy I** absorbs the weights into the local losses, i.e., each F_i is replaced by $\lambda_i F_i$. This transformation recovers uniform node weights (1/n) and leads to the standard framework with a doubly stochastic mixing.
- Strategy II, in contrast, keeps the original losses and incorporates λ into a row-stochastic mixing matrix whose stationary distribution equals λ/n .

Existing analyses show that the two strategies share the same expected descent direction and both converge to first-order stationary points (Sayed, 2014). However, several fundamental questions remain open:

- (Q1) Does the convergence rate obtained under standard Euclidean framework remain tight under heterogeneous node weights?
- (Q2) Do the differences between the two strategies arise solely from the spectral gaps of their mixing matrices, or also from other key factors?
- (Q3) Given a weight vector λ , under what conditions should we prefer one strategy over the other?

¹College of Control Science and Engineering, Zhejiang University ²Center for Data Science, Peking University ³Center for Machine Learning Research, Peking University. Correspondence to: Chengcheng Zhao <Chengchengzhao@zju.edu.cn>.

Main contributions. This work advances the understanding of decentralized learning with heterogeneous weights by addressing the open questions above. Our main contributions are summarized as follows:

- (C1) We develop a new analytical framework built upon a weighted Hilbert space $L^2(\lambda;\mathbb{R}^d)$. Because of the heterogeneous node weights, the error recursions of both strategies naturally reside in this weighted space rather than in the standard Euclidean one (Appendix B.2). Within this framework, we derive tight convergence rates for decentralized stochastic gradient tracking under both strategies and show that the Euclidean analysis leads to strictly looser bounds.
- (C2) Within the $L^2(\lambda;\mathbb{R}^d)$ space, the λ -induced row-stochastic matrix becomes self-adjoint, whereas the doubly stochastic matrix does not. This lack of self-adjointness generates additional *penalty terms* in the convergence rates, increasing the consensus error and tightening the admissible step-size range of Strategy I. Consequently, the difference between the two strategies is determined not only by their spectral gaps but also by these penalty terms. Hence, Strategy II can converge faster even when its spectral gap is smaller.
- (C3) From the derived convergence rates, we first obtain spectral-gap conditions under which Strategy II converges strictly faster than Strategy I. We then use Rayleigh-quotient and Loewner-order arguments to express these conditions as degree—weight constraints on the topology. These constraints further yield simple topology-design guidelines: node degrees should scale proportionally with their associated weights.

2. Related Works

Decentralized learning with uniform weights. Early work in optimization study decentralized gradient descent with diminishing step sizes, time-varying directed graphs, and later fixed-step convergence guarantees (Nedic & Ozdaglar, 2009; Nedić & Olshevsky, 2014; Yuan et al., 2016). In machine learning, Lian et al. (2017) initiate the study of decentralized stochastic gradient descent (SGD), showing linear speedup comparable to centralized SGD while substantially reducing communication. Subsequent research improves robustness to data heterogeneity via gradient tracking and related techniques (Yuan et al., 2023; Pu & Nedić, 2021), accelerates convergence with first-order momentum (Assran et al., 2019; Ying et al., 2021), and reduces communication costs through more efficient protocols (Tang et al., 2018; Koloskova et al., 2019). Nevertheless, most existing analyses assume uniform node weights and thus rely on doubly stochastic mixing matrices, leaving the heterogeneous-weight setting relatively less understood.

Decentralized learning with heterogeneous weights. In federated learning, heterogeneous weights are standard (McMahan et al., 2017; Li et al., 2020) because a server can directly implement weighted aggregation. In decentralized settings, however, the lack of a global server makes weighting more challenging, and only a few works treat it directly (Chen & Sayed, 2013; Yuan et al., 2018a;b; Cyffers et al., 2024; Zhu et al., 2025). Cyffers et al. (2024) encode weights via the stationary distribution of random walks to strengthen differential privacy, but the convergence analysis remains in a standard (uniform-weight) framework. Zhu et al. (2025) introduce a *Data Influence Cascade* metric to quantify node impact, without rate analysis. The diffusion framework (Sayed, 2014; Chen & Sayed, 2013; 2015) handles heterogeneous node weights either via row-stochastic mixing or by folding the weights into the local losses, reducing the problem to uniform weights. Exact diffusion (Yuan et al., 2018a;b) further removes the bias introduced by leftstochastic mixing and constant step sizes through additional communication and computation. Both diffusion and exact diffusion are developed for strongly convex losses. In contrast, we study when row-stochastic mixing with heterogeneous weights can outperform doubly stochastic mixing without extra steps, and we introduce a new framework for comparing their convergence rates.

Column-/row-stochastic mixing under uniform weights. On directed graphs, nodes may only know in- or out-degrees, enabling only column- or row-stochastic matrices and introducing bias. For column-stochastic mixing, the bias and rates have been extensively characterized (Nedić & Olshevsky, 2014; Xi & Khan, 2017; Assran et al., 2019; Liang et al., 2025b), with Liang et al. (2025b) giving effective metrics, tight bounds, and showing that multiple communication rounds can mitigate asymmetry and recover optimal rates. For row-stochastic mixing, most prior results focus on deterministic, strongly convex problems (Mai & Abed, 2016; Xin et al., 2019a;b; Ghaderyan et al., 2023). In the stochastic, non-convex setting, Liang et al. (2025a) propose effective metrics, establish a lower bound, and show that with multiple communication per iteration the upper bound matches the lower bound up to logarithmic factors, yielding near-optimal rates.

3. Preliminaries

3.1. Notations

Let \mathbb{R}^d denote the d-dimensional Euclidean space and $\mathbb{R}^{m \times d}$ the set of real $m \times d$ matrices. For a vector x, $\|x\|_2$ and $\langle x,y \rangle$ denote its Euclidean norm and standard inner product, respectively. Let 1 denote the all-ones vector and I denote the identity matrix. For a matrix M, let $M_{i,j}$, M^{\top} , $\|M\|_2$, and $\|M\|_F$ denote its (i,j)-th entry, transpose, spectral norm, and Frobenius norm. A matrix M is row-

stochastic if $M_{i,j} \geq 0$ and $\sum_{i} M_{i,j} = 1$ for all i; if both M and M^{\top} are row-stochastic, it is doubly stochastic. For a square matrix $W \in \mathbb{R}^{m \times m}$, let $\sigma(W) = {\{\sigma_i(W)\}_{i=1}^m}$ denote its eigenvalues in non-increasing order, and define the spectral radius as $\rho(W) = \max_i |\sigma_i(W)|$. When W is row-stochastic, $\rho(W) = 1$, and its spectral gap is defined as $1 - \max\{|\sigma_2(W)|, |\sigma_n(W)|\}$. We define the filtration $\mathcal{F}^{(t)}$ as the filtration before the stochastic gradient evaluation in the t-th step. We use $a \lesssim_d b$ to indicate that there exists a $C \geq 0$ that is independent with d such that $a \leq Cb$.

3.2. Markov Chains

Consider a finite Markov chain with row-stochastic transition matrix P.

Irreducibility. The chain is *irreducible* if any two states communicate, i.e., there exists t > 0 such that $\Pr\{X_t = i \mid t = 1\}$ $X_0 = i$ > 0.

Aperiodicity. The period of a state i is the greatest common divisor of $\{t: \Pr\{X_t = i \mid X_0 = i\} > 0\}$. A chain is aperiodic if all states have period one, which is ensured when $P_{i,i} > 0$ for all i.

Stationary distribution. If the chain is irreducible and aperiodic, there exists a unique row-stochastic vector π such that $\pi \mathbf{1} = 1 \pi P = \pi$. The equality $\pi_i = \sum_{j=1}^n \pi_j P_{j,i}$ expresses the balance of probability flows, and the stronger detailed balance condition requires $\pi_i P_{i,j} = \pi_j P_{j,i}, \ \forall i, j$. Moreover, $P^t \to \mathbf{1}\pi$ as $t \to \infty$, and the convergence rate is governed by the spectral gap of P.

4. Algorithm Overview

We consider the decentralized optimization problem in (1) and employ decentralized stochastic gradient tracking to mitigate data heterogeneity. Our framework follows the standard GT structure (Xu et al., 2017), with two lightweight extensions to incorporate heterogeneous node weights. We consider learning over a network $\mathcal{G} = (\mathcal{V}, \mathcal{E})$, where $\mathcal{V} =$ $\{1,\ldots,n\}$ and \mathcal{E} denotes the edge set; each node i communicates only with its neighbors $\mathcal{N}_i = \{j : (i, j) \in \mathcal{E}\}.$ For brevity, we denote $g_i^{(t)} := \nabla f_i(\theta_i^{(t)}; \xi_i^{(t)})$. The overall procedure is summarized in Algorithm 1. Let $\Theta^{(t)} = [\theta_1^{(t)}, \dots, \theta_n^{(t)}]^\top$, $Y^{(t)} = [y_1^{(t)}, \dots, y_n^{(t)}]^\top$, and $\nabla F_{\xi}^{(t)} = [g_1^{(t)}, \dots, g_n^{(t)}]^\top$. The algorithm iterates as

Let
$$\Theta^{(t)} = [\theta_1^{(t)}, \dots, \theta_n^{(t)}]^\top$$
, $Y^{(t)} = [y_1^{(t)}, \dots, y_n^{(t)}]^\top$, and $\nabla F_{\xi}^{(t)} = [g_1^{(t)}, \dots, g_n^{(t)}]^\top$. The algorithm iterates as

$$\Theta^{(t+1)} = W_{\lambda}[\Theta^{(t)} - \alpha Y^{(t)}],$$

$$Y^{(t+1)} = W_{\lambda}Y^{(t)} + G_{\lambda}[\nabla F_{\xi}^{(t+1)} - \nabla F_{\xi}^{(t)}],$$
(2)

where $(W_{\lambda}, G_{\lambda})$ encode different weighting mechanisms:

Strategy I (Weighted loss, uniform mixing):

 $(W_{\lambda},G_{\lambda})=(W^{\mathrm{ds}},D_{\lambda}),$ where W^{ds} is symmetric and doubly stochastic, and $D_{\lambda} = \operatorname{diag}(\lambda_1, \dots, \lambda_n)$.

Algorithm 1 Weighted Decentralized Gradient Tracking

- 1: **Input:** step size α , batch sizes $\{b_i\}$, total iterations T, and system matrices W_{λ}, G_{λ} .
- 2: **Initialize:** the same initial state $\theta^{(0)}$; $y_i^{(0)} = g_i^{(0)}$ for Strategy II, or $y_i^{(0)} = \lambda_i g_i^{(0)}$ for Strategy I.
- 3: **for** t = 0 **to** T 1 **do**
- 4: for each node $i \in \mathcal{V}$ do
- Receive $\{\theta_j^{(t)}, y_j^{(t)}\}_{j \in \mathcal{N}_i}$ from neighbors. 5:
- 6:

$$\begin{aligned} \theta_i^{(t+1)} &= \sum_{j=1}^n [W_{\lambda}]_{i,j} (\theta_j^{(t)} - \alpha y_j^{(t)}). \\ \text{Tracker update:} \end{aligned}$$

7:

$$y_i^{(t+1)} = \sum_{j=1}^{n} [W_{\lambda}]_{i,j} y_j^{(t)} + [G_{\lambda}]_{i,i} (g_i^{(t+1)} - g_i^{(t)}).$$

- 9: end for

Strategy II (Uniform loss, weighted mixing):

 $(W_{\lambda}, G_{\lambda}) = (W, I)$, where W is row-stochastic with $\frac{\lambda^{\perp}}{n}$ being its stationary distribution, i.e., $\frac{\lambda^{\top}}{n}W = \frac{\lambda^{\top}}{n}$.

Under the initialization in Algorithm 1, the gradient-tracking property ensures that $\frac{\lambda^\top}{n}Y^{(t)}=\frac{1}{n}\sum_{i=1}^n\lambda_ig_i^{(t)}$ for Strategy II, and $\frac{\mathbf{1}^\top}{n}Y^{(t)}=\frac{1}{n}\sum_{i=1}^n\lambda_ig_i^{(t)}$ for Strategy I.

Remark 4.1. Using the same initialization across all nodes is standard in decentralized optimization (Lian et al., 2017; Koloskova et al., 2020) and we adopt it here for consistency with existing work and to simplify the analysis.

4.1. Problem of Interest

In fact, both strategies yield the same expected descent direction of the global loss (1).

Strategy I: Weighted local losses.

Each node scales its loss as $F'_i(\theta) = \lambda_i F_i(\theta)$, and uses a doubly stochastic matrix W^{ds} . The global average $\bar{\theta}^{(t)} =$ $\frac{1}{n} \sum_{i} \theta_{i}^{(t)}$ evolves as

$$\bar{\theta}^{(t+1)} = \frac{\mathbf{1}^{\top}}{n} W^{\text{ds}}[\Theta^{(t)} - \alpha Y^{(t)}] = \bar{\theta}^{(t)} - \frac{\alpha}{n} \sum_{i=1}^{n} \lambda_i g_i^{(t)},$$

which is an unbiased estimator of the global gradient.

Strategy II: Weighted mixing matrix.

Instead of modifying the local losses, we embed λ_i in a rowstochastic W such that $\frac{\lambda^\top}{n}W=\frac{\lambda^\top}{n}$. Defining the weighted average $\bar{\theta}_{\lambda}^{(t)}=\frac{1}{n}\sum_{i}\lambda_{i}\theta_{i}^{(t)}$, we have

$$\bar{\theta}_{\lambda}^{(t+1)} = \frac{\lambda^{\top}}{n} W[\Theta^{(t)} - \alpha Y^{(t)}] = \bar{\theta}_{\lambda}^{(t)} - \frac{\alpha}{n} \sum_{i=1}^{n} \lambda_i g_i^{(t)},$$

which is also an unbiased estimator of the global gradient.

We are interested in whether the two strategies, despite sharing the same descent direction, exhibit the same error recursion and convergence behavior, and what fundamentally distinguishes them. We address this question by introducing a new analytical framework and deriving the corresponding convergence rates for both strategies.

5. The $L^2(\lambda; \mathbb{R}^d)$ -Hilbert Space

This section gives a decentralized construction of a row-stochastic matrix W whose stationary distribution equals λ/n . We then develop the λ -weighted geometry that underlies our analysis and the spectral identities used later.

5.1. Constructing W from λ

The weighting vector is naturally encoded by the stationary distribution. Our goal is thus a decentralized row-stochastic W whose stationary distribution matches λ/n .

We adopt a modified Metropolis–Hastings rule (Chib & Greenberg, 1995) to construct a transition matrix P with stationary distribution λ/n :

$$P_{i,j} = \begin{cases} \frac{1}{d_i} \min\left(1, \frac{\lambda_j d_i}{\lambda_i d_j}\right), & \text{if } i \neq j \text{ and } j \in \mathcal{N}_i, \\ 1 - \sum_{k \in \mathcal{N}_i} P_{i,k}, & \text{if } i = j, \\ 0, & \text{otherwise.} \end{cases}$$

To preclude oscillations and ensure aperiodicity, we introduce a *laziness* parameter $\varepsilon \in (0,1)$:

$$W \leftarrow (1 - \varepsilon)P + \varepsilon I$$
.

The resulting entries are

$$W_{i,j} = \begin{cases} \frac{1-\varepsilon}{d_i} \min\left(1, \frac{\lambda_j d_i}{\lambda_i d_j}\right), & \text{if } i \neq j \text{ and } j \in \mathcal{N}_i, \\ 1 - \sum_{k \in \mathcal{N}_i} W_{i,k}, & \text{if } i = j, \\ 0, & \text{otherwise.} \end{cases}$$
 (3)

This procedure is fully distributed—each node needs only λ_i and the degrees of its neighbors—and the positive diagonal prevents periodicity. The doubly stochastic matrix W^{ds} is recovered from (3) by setting $\lambda \equiv 1$.

5.2. $L^2(\lambda; \mathbb{R}^d)$ -Hilbert Space

Heterogeneous node weights induce a non-Euclidean geometry (cf. Appendix B.2). We therefore introduce the vector-valued Hilbert space $L^2(\lambda; \mathbb{R}^d)$ endowed with the inner product

$$\langle X, Y \rangle_{\lambda, d} = \sum_{i=1}^{n} \lambda_i \langle x_i, y_i \rangle, \quad X, Y \in (\mathbb{R}^d)^n.$$

The induced the weighted Frobenius norm is $||X||_{\lambda,F} = (\sum_i \lambda_i ||x_i||^2)^{1/2}$, and for the matrix (linear map) W, we

use the corresponding weighted spectral norm $\|W\|_{\lambda} = \max_{\|X\|_{\lambda,F}=1} \|WX\|_{\lambda,F}$. Equivalently, $L^2(\lambda;\mathbb{R}^d) \cong L^2(\lambda) \widehat{\otimes} \mathbb{R}^d$. Under the construction (3), W is self-adjoint in this space, admits an orthogonal eigen-decomposition, and allows for standard spectral analysis.

Spectral relationships. For the symmetric, doubly stochastic case W^{ds} , let $J = \frac{\mathbf{1}\mathbf{1}^{\mathsf{T}}}{n}$ denote the projection onto its stationary distribution. Then

$$||W^{\mathrm{ds}} - J||_2 = \rho(W^{\mathrm{ds}} - J) = \rho_J,$$

where ρ_J is the second-largest eigenvalue magnitude of W.

For the λ -induced row-stochastic matrix W, its λ -weighted spectral norm satisfies

$$\|W - \Lambda\|_{\lambda} = \|D_{\lambda}^{1/2}(W - \Lambda)D_{\lambda}^{-1/2}\|_{2} = \|\widetilde{W}_{\Lambda}\|_{2},$$

where $\Lambda = \frac{\mathbf{1}\lambda^\top}{n}$ and \widetilde{W}_{Λ} is a symmetric similarity transform of W_{Λ} that preserves its eigenvalues. The detailed balance condition ensures $\widetilde{W}_{\Lambda} = \widetilde{W}_{\Lambda}^\top$ (Lemma B.4), implying

$$||W - \Lambda||_{\lambda} = \rho(\widetilde{W}_{\Lambda}) = \rho(W_{\Lambda}) := \rho_{\Lambda}.$$

Hence, the λ -weighted spectral norm coincides with ρ_{Λ} , i.e., the second-largest eigenvalue magnitude of W. We also consider the λ -weighted spectral norm of $W^{\mathrm{ds}} - J$:

$$\|W_J\|_{\lambda} = \|D_{\lambda}^{1/2} W_J D_{\lambda}^{-1/2}\|_2 \le \sqrt{\frac{\lambda_{\max}}{\lambda_{\min}}} \rho_J := \kappa_{\lambda} \rho_J.$$

Here $\kappa_{\lambda} > 1$ quantifies the metric distortion. Because a doubly stochastic matrix is non-self-adjoint in $L^2(\lambda; \mathbb{R}^d)$, this non-normality introduces a multiplicative penalty > 1. For more details of the space, we refer to Appendix A.

6. Convergence rate for Algorithm 1

In this section, we present our convergence rate for Algorithm 1 with different communication strategies.

6.1. Assumptions and Descent Lemma

To begin with, we present the following assumptions, which are commonly used in existing lectures.

Assumption 6.1 (β -smoothness). Each local loss $F_i(\theta)$ is differentiable and β -smooth, i.e.,

$$\|\nabla F_i(\theta_1) - \nabla F_i(\theta_2)\| \le \beta \|\theta_1 - \theta_2\|, \quad \forall \theta_1, \theta_2 \in \mathbb{R}^d.$$

Assumption 6.2 (Gradient oracles). For each node $i \in \mathcal{V}$ and all $\theta \in \mathbb{R}^d$, it holds that:

$$\mathbb{E}[\nabla f_i(\theta;\xi)] = \nabla F_i(\theta), \ \mathbb{E}[\|\nabla f_i(\theta;\xi) - \nabla F_i(\theta)\|^2] < v^2.$$

Assumption 6.3 (Connected graph). The communication graph $\mathcal G$ is connected. Hence, the matrices W and W^{ds} constructed via (3) are irreducible and aperiodic, and thus have positive spectral gaps: $\rho_\Lambda < 1$ and $\rho_J < 1$.

We now explain why the subsequent analysis is naturally carried out in the weighted Hilbert space $L^2(\lambda; \mathbb{R}^d)$. Under Assumptions 6.1–6.2 and a step size $\alpha \leq 1/\beta$, the descent lemma for Algorithm 1 yields (see Appendix B.2)

$$\begin{split} \mathbb{E}[F(\bar{\theta}_*^{(t+1)})] &\leq \mathbb{E}[F(\bar{\theta}_*^{(t)})] - \frac{\alpha}{2} \mathbb{E}\Big[\|\nabla F(\bar{\theta}_*^{(t)})\|^2\Big] \\ &\quad + \frac{\alpha\beta^2}{2n} \mathbb{E}\Big[\|(I - M_*)\Theta^{(t)}\|_{F,\lambda}^2\Big] + \frac{\alpha^2 c_\lambda \beta \upsilon^2}{2}, \end{split}$$

where $c_{\lambda}=n^{-2}\sum_{i=1}^{n}\lambda_{i}^{2}<1, \ \ {\rm and}\ \ (\bar{\theta}_{*}^{(t)},M_{*}) \ \ {\rm equals}$ $(\bar{\theta}^{(t)},J)$ in Strategy I and $(\bar{\theta}_{\lambda}^{(t)},\Lambda)$ in Strategy II.

The key observation is that the consensus error enters the inequality solely through the weighted term $\|(I-M_*)\Theta^{(t)}\|_{F,\lambda}^2$. This term is exactly the squared norm in $L^2(\lambda;\mathbb{R}^d)$, indicating that the geometry induced by the heterogeneous node weights is governed by this space. Consequently, $L^2(\lambda;\mathbb{R}^d)$ provides the appropriate functional setting for analyzing consensus under heterogeneous weights.

6.2. Consensus Error

In this subsection, we analyze the parameter and tracker consensus errors across all nodes and introduce the following notation to jointly characterize them for both strategies:

$$E_{\rm I}^{(t)} = \begin{bmatrix} (I-J)\Theta^{(t)} \\ \alpha(I-J)Y^{(t)} \end{bmatrix}, \qquad E_{\rm II}^{(t)} = \begin{bmatrix} (I-\Lambda)\Theta^{(t)} \\ \alpha(I-\Lambda)Y^{(t)} \end{bmatrix}.$$

Building on (Koloskova et al., 2021), we derive closed-form spectral norms for the matrices in the recursion, enabling direct computation of the consensus error at any iteration t without the window-averaging technique used in (Koloskova et al., 2021). This yields a simpler analysis and more transparent accumulated-error bounds:

Proposition 6.4. Under Assumptions 6.1–6.3, the following accumulated consensus error bounds hold (See proof in Appendix B.3.):

(Strategy I). If
$$\alpha < \frac{1}{2\lambda_{\max}\beta}\sqrt{\frac{1}{15B(\rho_J)}}$$
, then

$$\sum_{t=0}^{T-1} \mathbb{E}\left[\left\|E_{I}^{(t)}\right\|_{F,\lambda}^{2}\right]$$

$$\leq \left(\frac{\kappa_{\lambda}}{C_{1}'}\right) \frac{18(1-\rho_{J}^{2})^{2}+6\rho_{J}^{2}}{(1-\rho_{J}^{2})^{3}} \left\|E_{I}^{(0)}\right\|_{F,\lambda}^{2}$$

$$+ \left(\frac{\lambda_{\max}^{2}}{C_{1}'}\right) 2n\alpha^{2}B(\rho_{J}) \sum_{j=0}^{T-1} \mathbb{E}[\|\nabla F(\overline{\theta}^{(t)})\|^{2}]$$

$$+ \left(\frac{\lambda_{\max}^{2}}{C_{1}'}\right) 18n\alpha^{2}v^{2}T \left(A(\rho_{J}) + \frac{3}{2}c_{\lambda}\alpha^{2}\beta^{2}B(\rho_{J})\right),$$
(4)

where
$$A(\rho_J) := \frac{1+\rho_J^2}{(1-\rho_J^2)^3}$$
, $B(\rho_J) := \frac{2(1+3\rho_J^4)}{(1-\rho_J^2)^3(1-\rho_J)}$, $c_\lambda = \frac{1}{n^2} \sum_{i=1}^n \lambda_i^2 < 1$, and $C_1' = 1 - 60\lambda_{\max}^2 \alpha^2 \beta^2 B(\rho_J) > 0$.

(Strategy II). If
$$\alpha < \frac{1}{2\beta} \sqrt{\frac{1}{15B(\rho_{\Lambda})}}$$
, then
$$\sum_{t=0}^{T-1} \mathbb{E}\left[\left\|E_{\Pi}^{(t)}\right\|_{F,\lambda}^{2}\right] \qquad (5)$$

$$\leq \frac{1}{C_{1}} \frac{18(1-\rho_{\Lambda}^{2})^{2}+6\rho_{\Lambda}^{2}}{(1-\rho_{\Lambda}^{2})^{3}} \left\|E_{\Pi}^{(0)}\right\|_{F,\lambda}^{2}$$

$$+ \frac{1}{C_{1}} 2n\alpha^{2}B(\rho_{\Lambda}) \sum_{j=0}^{T-1} \mathbb{E}[\|\nabla F(\overline{\theta}_{\lambda}^{(t)})\|^{2}]$$

$$+ \frac{1}{C_{1}} 18n\alpha^{2}v^{2} \left(A(\rho_{\Lambda}) + \frac{3}{2}c_{\lambda}\alpha^{2}\beta^{2}B(\rho_{\Lambda})\right) T,$$

where
$$A(\rho_{\Lambda}):=\frac{1+\rho_{\Lambda}^2}{(1-\rho_{\Lambda}^2)^3},\ B(\rho_{\Lambda}):=\frac{2(1+3\rho_{\Lambda}^4)}{(1-\rho_{\Lambda}^2)^3(1-\rho_{\Lambda})},\ c_{\lambda}=\frac{1}{n^2}\sum_{i=1}^n\lambda_i^2<1,\ and\ C_1=1-60\alpha^2\beta^2B(\rho_{\Lambda})>0.$$

We observe that Strategy I introduces several multiplicative constants exceeding unity, notably κ_{λ} and λ_{\max}^2 , which are absent in Strategy II. The constant κ_{λ} originates from the non-self-adjoint property of W^{ds} , while the λ_{\max}^2 factor emerges from the combined effect of the gradient-related matrix D_{λ} and the non-self-adjoint nature of W^{ds} , collectively amplifying the consensus error. For comparative analysis, we present the corresponding spectral norms below (detailed derivations are provided as Proposition B.14):

$$||A_{\mathrm{I}}^t||_{\lambda}^2 = \frac{2+t+t\sqrt{t^2+4}}{2} \, \kappa_{\lambda} \rho_J^{2t}, \quad ||A_{\mathrm{II}}^t||_{\lambda}^2 = \frac{2+t+t\sqrt{t^2+4}}{2} \, \rho_{\Lambda}^{2t}.$$

and

$$||W(I-\Lambda)||_{\lambda}^2 \le \rho_{\Lambda}^2, \qquad ||W^{\mathrm{ds}}(I-J)D_{\lambda}||_{\lambda}^2 \le \lambda_{\mathrm{max}}^2 \rho_J^2.$$

Thus, under comparable spectral gaps ($\rho_J \approx \rho_{\Lambda}$), **Strategy II** yields strictly smaller consensus error.

6.3. Convergence rate

With the consensus error analysis, we now derive the convergence rates of Algorithm 1 under both strategies, summarized in the following theorem.

Theorem 6.5. *Under Assumptions 6.1–6.3, the following convergence rates hold (See proof in Appendix B.4.):*

$$(Strategy I). \quad If \alpha < \frac{1}{\lambda_{\max}\beta} \sqrt{\frac{1}{62B(\rho_J)}}, then$$

$$\frac{1}{T} \sum_{t=0}^{T-1} \mathbb{E} \left[\|\nabla F(\overline{\theta}^{(t)})\|^2 \right]$$

$$\leq \left(\frac{1}{C_2'} \right) \frac{2[F(\overline{\theta}^{(0)}) - F(\theta^{\star})]}{\alpha T} + \left(\frac{1}{C_2'} \right) \alpha c_{\lambda} \beta v^2$$

$$+ \left(\frac{\kappa_{\lambda}}{C_1' C_2'} \right) \frac{6[3(1 - \rho_J^2)^2 + \rho_J^2]\beta^2}{(1 - \rho_J^2)^3 n T} \left\| E_I^{(0)} \right\|_{F,\lambda}^2$$

$$+ \left(\frac{\lambda_{\max}^2}{C_1' C_2'} \right) 18\alpha^2 \beta^2 v^2 \left(A(\rho_J) + \frac{3}{2} c_{\lambda} \alpha^2 \beta^2 B(\rho_J) \right),$$

$$where C_2' = 1 - \frac{2\lambda_{\max}^2 \alpha^2 \beta^2 B(\rho_J)}{C_1'} > 0.$$

(Strategy II). If
$$\alpha < \frac{1}{\beta} \sqrt{\frac{1}{62B(\rho_{\Lambda})}}$$
, then
$$\frac{1}{T} \sum_{t=0}^{T-1} \mathbb{E} \left[\|\nabla F(\overline{\theta}_{\lambda}^{(t)})\|^{2} \right]$$

$$\leq \frac{1}{C_{2}} \frac{2[F(\overline{\theta}_{\lambda}^{(0)}) - F(\theta^{*})]}{\alpha T} + \frac{1}{C_{2}} \alpha c_{\lambda} \beta v^{2}$$

$$+ \frac{1}{C_{1}C_{2}} \frac{6[3(1 - \rho_{\Lambda}^{2})^{2} + \rho_{\Lambda}^{2}]\beta^{2}}{(1 - \rho_{\Lambda}^{2})^{3}nT} \left\| E_{\text{II}}^{(0)} \right\|_{F,\lambda}^{2}$$

$$+ \frac{1}{C_{1}C_{2}} 18\alpha^{2}\beta^{2}v^{2} \left(A(\rho_{\Lambda}) + \frac{3}{2}c_{\lambda}\alpha^{2}\beta^{2}B(\rho_{\Lambda}) \right),$$
where $C_{2} = 1 - \frac{2\alpha^{2}\beta^{2}B(\rho_{\Lambda})}{C_{1}} > 0$.

Impact of multiplicative constants on convergence. Both strategies achieve the same asymptotic convergence rate of $\mathcal{O}(1/T)$, yet exhibit significant differences in their constant factors. This performance discrepancy is consistent with the consensus error analysis presented in Section 6.2. Although the two strategies share identical convergence order, Strategy I introduces additional multiplicative constants $\kappa_{\lambda} > 1$ and $\lambda_{\rm max}^2 > 1$ that adversely affect its non-asymptotic performance. These factors emerge from the non-self-adjoint nature of W^{ds} and the joint effect of the gradient-related matrix D_{λ} , as established in our earlier analysis. Consequently, even in scenarios where W^{ds} benefits from a more favorable spectral gap, Strategy II demonstrates superior convergence efficiency owing to its tighter constant factors and the absence of these performance-degrading multiplicative penalty terms.

Recovery of linear-speedup under uniform weighting.

Our framework demonstrates consistency with established results in the uniform-weight setting. When the optimization problem (1) reduces to the uniform-weight scenario (i.e., $\lambda \equiv 1$), both Strategy I and Strategy II become equivalent, corresponding to classical decentralized SGD with doubly-stochastic mixing and Euclidean-space analysis. In this degenerate case, c_{λ} simplifies to $\frac{1}{n}$, yielding the asymptotic convergence rate established in the following corollary.

Corollary 6.6. Under uniform weighting ($\lambda \equiv 1$), Algorithm 1 achieves the following asymptotic convergence rate:

$$\frac{1}{T} \sum_{t=0}^{T-1} \mathbb{E}\left[\|\nabla F(\overline{\theta}^{(t)})\|^2 \right] \lesssim_{n,T} \frac{1}{\sqrt{nT}}.$$

This result precisely matches the asymptotic linear speedup convergence established in prior work (Lian et al., 2017), confirming the consistency of our generalized framework with classical analysis in the uniform-weight setting.

6.4. Limitations of the Standard Euclidean Framework.

To ensure analytical rigor, the convergence rate for **Strategy I** presented in our main results is derived within the Hilbert

space $L^2(\lambda; \mathbb{R}^d)$ framework. This approach exposes fundamental limitations in conventional Euclidean space analysis (Chen & Sayed, 2013), which does not fully capture the intrinsic geometric structure of decentralized learning with heterogeneous node weights.

While the standard Euclidean framework can be applied to **Strategy I** through rescaling of smoothness and noise constants, it produces much looser convergence bounds. Specifically, by considering the rescaled loss $F'_i(\theta) = \lambda_i F_i(\theta)$, we obtain the following conservative estimates:

$$\|\nabla F_i'(\theta_1) - \nabla F_i'(\theta_2)\| \le \lambda_{\max} \beta \|\theta_1 - \theta_2\|,$$

$$\mathbb{E}\left[\|\nabla f_i'(\theta; \xi) - \nabla F_i'(\theta)\|^2\right] \le \lambda_{\max}^2 v^2.$$

Within this conventional analytical framework, the convergence rate becomes:

If
$$\alpha < \frac{1}{\lambda_{\max}\beta} \sqrt{\frac{1}{62B(\rho_J)}}$$
, then
$$\frac{1}{T} \sum_{t=0}^{T-1} \mathbb{E}[\|\nabla F(\overline{\theta}^{(t)})\|^2] \qquad (8)$$

$$\leq \left(\frac{1}{C_2'}\right) \frac{2[F(\overline{\theta}^{(0)}) - F(\theta^*)]}{\alpha C_2' T} + \left(\frac{\lambda_{\max}^3}{n C_2'}\right) \alpha \beta v^2$$

$$+ \left(\frac{\lambda_{\max}^2}{C_1' C_2'}\right) \frac{6[3(1 - \rho_J^2)^2 + \rho_J^2]\beta^2}{(1 - \rho_J^2)^3 n T} \left\|E_{\mathrm{I}}^{(0)}\right\|_{F,\lambda}^2$$

$$+ \left(\frac{\lambda_{\max}^4}{C_1' C_2'}\right) 18\alpha^2 \beta^2 v^2 \left(A(\rho_J) + \left(\lambda_{\max}^2\right) \frac{3}{2} c_\lambda \alpha^2 \beta^2 B(\rho_J)\right).$$

When compared with our refined result in Theorem 6.5, the differences are highlighted in brackets. The standard analysis introduces multiple $\lambda_{\rm max}$ factors (up to the sixth power) that substantially inflate the error bounds, clearly demonstrating the superiority of our Hilbert space framework in delivering significantly tighter convergence guarantees. *Remark* 6.7. We do not provide a convergence rate for Strategy II under the Euclidean framework. Since the row-stochastic matrix W is non-self-adjoint in this space, additional penalty terms arise, making its rate strictly worse

7. Head-to-Head Convergence: Spectral Conditions, Topology Design, and Step Sizes

than Strategy I (8), as established in prior work (Liang et al.,

2025a). Hence, the convergence rate derived in $L^2(\lambda; \mathbb{R}^d)$ provides the tightest characterization of Strategy II.

Theorem 6.5 provides convergence rates for both strategies. A direct comparison at fixed α and T is obscured by higher-order terms and constants. We therefore begin by deriving a sufficient spectral condition under which Strategy II achieves strictly faster convergence, then translate it into topological condition, highlight its step-size advantage, and finally provide corresponding topology-design guidelines.

7.1. Spectral and Topological Conditions for Faster Convergence and Step Size Advantage

Strategy II can outperform Strategy I even when $\rho_{\Lambda} > \rho_{J}$, due to the self-adjointness of the λ -induced operator. This phenomenon is formalized below.

Theorem 7.1. Let $\eta = 1.8 \times 10^{-3}$. If the spectral gaps satisfy

$$1 - \rho_{\Lambda} \ge \max\left\{ (1 + \eta) \kappa_{\lambda}^{-1/3}, \ \lambda_{\max}^{-1/2} \right\} (1 - \rho_J),$$

then Strategy II converges strictly faster.

We denote $R = \max\left\{(1+\eta)\kappa_{\lambda}^{-1/3}, \lambda_{\max}^{-1/2}\right\} \in (0,1)$. Because spectral gaps of W and W^{ds} are often difficult to interpret directly, we next translate the condition in Theorem 7.1 into a more transparent relationship between the network topology and the weight vector λ . Closed-form expressions for the spectral gaps are generally unavailable in high dimensions (Horn & Johnson, 2012); we therefore compare ρ_{Λ} and ρ_{J} via Rayleigh quotients (Golub & Van Loan, 2013).

Theorem 7.2. A necessary and sufficient condition for Theorem 7.1 is that the weight vector λ satisfies

$$R \inf_{\substack{z' \neq 0 \\ \langle z', \mathbf{1} \rangle = 0}} \frac{\sum_{i,j} \min\left\{\frac{1}{d_i}, \frac{1}{d_j}\right\} (z'_i - z'_j)^2}{\|z'\|_2^2} \tag{9}$$

$$\leq \inf_{\substack{z\neq 0\\(z,D^{1/2}\mathbf{1})=0}} \frac{\sum_{i,j} \min\left\{\frac{1}{d_i} \sqrt{\frac{\lambda_i}{\lambda_j}}, \frac{1}{d_j} \sqrt{\frac{\lambda_j}{\lambda_i}}\right\} (z_i - z_j)^2}{\|z\|_2^2}.$$

As condition (9) is difficult to evaluate directly, we also provide a simple sufficient condition.

Corollary 7.3. If the weight vector λ satisfies

$$R \min \left\{ \frac{d_i}{d_j}, 1 \right\} \le \sqrt{\frac{\lambda_i}{\lambda_j}} \le R^{-1} \max \left\{ \frac{d_i}{d_j}, 1 \right\} \quad \forall i, j, \quad (10)$$

then Theorem 7.1 holds. When the total degree is fixed, ρ_{Λ} is maximized when $\lambda \propto d$, i.e.,

$$\tfrac{\lambda_i}{\lambda_j} = \tfrac{d_i}{d_j} \text{ for all } i,j \quad \big(\exists \ c>0: \lambda=cd\big).$$

Remark 7.4. Under condition (10), the Laplacians satisfy $\mathcal{L}(\lambda) \succeq R \mathcal{L}(1)$ in the Loewner order (Horn & Johnson, 2012), implying $\sigma_i(\mathcal{L}(\lambda)) \geq R \sigma_i(\mathcal{L}(1))$ for all i.

Step-size advantage of Strategy II. The step-size bounds in Theorem 6.5 further imply that

$$1 - \rho_{\Lambda} \ge \lambda_{\max}^{-1/2} (1 - \rho_J) \implies \alpha_{\max}^{\text{II}} \ge \alpha_{\max}^{\text{I}}.$$

Thus, even when $1-\rho_{\Lambda}$ is smaller, Strategy II still admits larger step sizes. In practice, a broader admissible step size range allows more aggressive learning rates with faster per-iteration decrease, and further enhances robustness to stochastic noise and generalization performance (Ghadimi & Lan, 2013; Wu et al., 2022).

7.2. Design Principles and Degree Allocation

From Corollary 7.3, on regular graphs the uniform weight $\lambda \equiv 1$ maximizes the spectral gap; with heterogeneous weights, regularity is suboptimal.

Design intuition. Corollary 7.3 suggests matching degrees to λ : nodes with larger λ_i should have higher connectivity for more frequent exchange—consistent with practice when some nodes hold more data or compute.

Therefore, we propose Algorithm 2^1 , which constructs a connected simple graph whose degree sequence is as close as possible to being proportional to the weights λ .

Algorithm 2 Build Graph From Weights

Require: Node weight vector λ , target average degree \bar{d} **Ensure:** A connected simple graph \mathcal{G}_{λ} whose degrees are as proportional as possible to the weights.

- 1: $d \leftarrow \text{SCALEToDEGREES}(\lambda_1, \dots, \lambda_n, \bar{d})$
- 2: **for** trial = 1, 2, ..., K **do**
- 3: success, $\mathcal{G}_{\lambda} \leftarrow \text{HAVELHAKIMICONSTRUCT}(d)$
- 4: **if not** success **then**
- 5: **continue** {go to next trial}
- 6: end if
- 7: $\mathcal{G}_{\lambda} \leftarrow \text{MakeConnected}(\mathcal{G}_{\lambda})$
- 8: **if** \mathcal{G}_{λ} is connected and $\deg_{\mathcal{G}_{\lambda}}(i) = d_i$ for all i **then**
- 9: **return** \mathcal{G}_{λ}
- 10: **end if**
- 11: **end for**
- 12: $\mathcal{G}_{\lambda} \leftarrow \text{FallbackConnectedGraph}(d)$
- 13: **return** \mathcal{G}_{λ}

Algorithm 2 first rescales λ into an integer degree sequence d with even total sum and bounded degrees $d_i \in [1, n-1]$ using the subroutine SCALETODEGREES. It then repeatedly attempts to realize d as a simple graph via a Havel–Hakimi procedure (HAVELHAKIMICONSTRUCT) (Hakimi, 1962), and applies a degree-preserving edge-swap routine (MAKECONNECTED) to merge disconnected components until a connected realization is obtained. If no connected realization with $\deg_{\mathcal{G}_{\lambda}}(i) = d_i$ for all i is found in K trials, the algorithm falls back to a simple scheme that first builds a ring and then greedily adds edges to match d as closely as

 $^{^1}$ For n nodes, Algorithm 2 runs in $O(n^2 \log n)$ time in typical cases and in $O(n^3)$ time in the worst case, and always returns a connected simple graph due to the fallback construction.

possible (FALLBACKCONNECTEDGRAPH). Detailed pseudocode for the subroutines is provided in Appendix D.

8. Experiments

We now empirically validate the theoretical findings using both a synthetic least-squares task and a deep learning task on CIFAR-10. All experiments are conducted on a 16-node network with two distinct weight vectors λ_A and λ_B , across standard benchmark topologies as well as the tailored graphs \mathcal{G}_{λ_A} and \mathcal{G}_{λ_B} generated by Algorithm 2. Detailed experimental settings are in Appendix E.

8.1. Least-Squares Quadratic Experiment

Following the setup of Koloskova et al. (2020), we conduct decentralized least-squares experiments with minor modifications, as detailed in Section E.3. Each local loss is augmented with an ℓ_2 regularization term, and stochastic gradients are simulated by injecting zero-mean Gaussian noise into the true gradients. The results, averaged over ten random seeds, are presented in Figure 1, which shows the norm of the weighted average gradient $\left\|\sum_{i=1}^n \frac{\lambda_i}{n} F_i(\theta_i^{(t)})\right\|$.

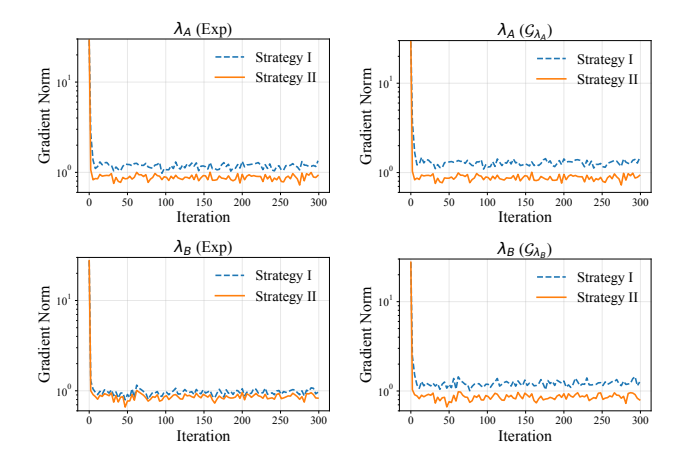


Figure 1. Weighted gradient norms for least-squares experiment.

As evident from Figure 1, Strategy II consistently achieves faster convergence across all scenarios. Notably, even when W exhibits a smaller spectral gap than W^{ds} (e.g., in the exponential graph), Strategy II still converges more rapidly. This suggests that the dominant factor influencing convergence is the non-self-adjointness of the matrix—captured by λ_{max} and κ_{λ} —rather than the spectral gap alone.

8.2. Deep Learning on CIFAR-10

To further validate these findings, we evaluate the strategies on a deep learning task using the ResNet-18 model (He et al., 2016) on the CIFAR-10 dataset. The performance of Strategy I and Strategy II in Algorithm 1 is measured by the

weighted average instantaneous loss $\sum_{i=1}^{n} \frac{\lambda_i}{n} f_i(\theta_i^{(t)}; \xi_i^{(t)})$ across nodes. The loss curves are smoothed using a 30-iteration moving average (interval loss) and averaged over six random seeds, as shown in Figures 2 and 3.

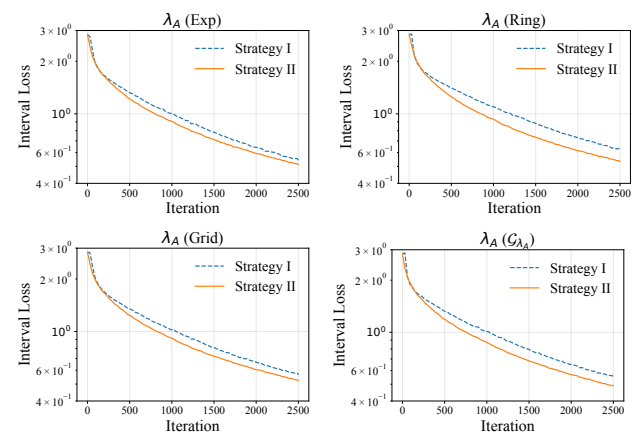


Figure 2. Interval losses for CIFAR-10 experiment under λ_1 .

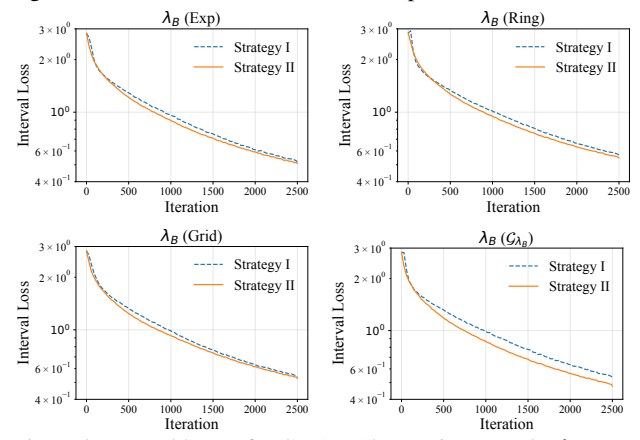


Figure 3. Interval losses for CIFAR-10 experiment under λ_2 .

We observe that Strategy II consistently outperforms Strategy I across different network topologies: even in cases where the doubly stochastic matrix W^{ds} has a larger spectral gap. This highlights the dominant impact of non-self-adjointness on the convergence rate. Under various weights and topologies, Strategy II maintains its advantage over Strategy I. Complete test accuracies and additional results on other topologies are provided in Appendix E.4.

9. Conclusion

We revisit decentralized learning with heterogeneous node weights and show that the standard Euclidean framework, due to a coarse rescaling argument, leads to loose convergence rates. In contrast, a proposed weighted Hilbert-space analysis yields tighter convergence rates and reveals that the row-stochastic matrix is self-adjoint while the doubly stochastic one is not, introducing penalty terms that slow convergence and tighten step sizes. These insights show that performance gaps are not dictated by spectral gaps alone and lead to degree—weight guidelines for topology design.

Impact Statement

This work focuses on improving our basic understanding of machine learning methods. Although the ideas presented here could have broader practical effects, we are not aware of any direct or significant societal impacts that require specific mention at this time.

References

- Alghunaim, S. A. and Yuan, K. A unified and refined convergence analysis for non-convex decentralized learning. *IEEE Transactions on Signal Processing*, 70:3264–3279, 2022.
- Assran, M., Loizou, N., Ballas, N., and Rabbat, M. Stochastic gradient push for distributed deep learning. In *International Conference on Machine Learning*, pp. 344–353. PMLR, 2019.
- Beveridge, A. and Youngblood, J. The best mixing time for random walks on trees. *Graphs and Combinatorics*, 32 (6):2211–2239, 2016.
- Boyd, S. P., Ghosh, A., Prabhakar, B., and Shah, D. Mixing times for random walks on geometric random graphs. In *ALENEX/ANALCO*, pp. 240–249, 2005.
- Chen, J. and Sayed, A. H. Distributed pareto optimization via diffusion strategies. *IEEE Journal of Selected Topics* in Signal Processing, 7(2):205–220, 2013.
- Chen, J. and Sayed, A. H. On the learning behavior of adaptive networks—part i: Transient analysis. *IEEE Transactions on Information Theory*, 61(6):3487–3517, 2015.
- Chib, S. and Greenberg, E. Understanding the metropolishastings algorithm. *The American Statistician*, 49(4): 327–335, 1995.
- Chung, F. R. *Spectral graph theory*, volume 92. American Mathematical Soc., 1997.
- Cyffers, E., Bellet, A., and Upadhyay, J. Differentially private decentralized learning with random walks. In *Proceedings of the 41st International Conference on Machine Learning (ICML)*, volume 235, pp. 9762–9783. PMLR, 2024.
- Fan, K. On a theorem of weyl concerning eigenvalues of linear transformations i. *Proceedings of the National Academy of Sciences*, 35(11):652–655, 1949.
- Ghaderyan, D., Aybat, N. S., Aguiar, A. P., and Pereira, F. L. A fast row-stochastic decentralized method for distributed optimization over directed graphs. *IEEE Transactions on Automatic Control*, 69(1):275–289, 2023.

- Ghadimi, S. and Lan, G. Stochastic first-and zeroth-order methods for nonconvex stochastic programming. *SIAM Journal on Optimization*, 23(4):2341–2368, 2013.
- Golub, G. H. and Van Loan, C. F. *Matrix computations*. Johns Hopkins University Press, 2013.
- Hakimi, S. L. On realizability of a set of integers as degrees of the vertices of a linear graph. i. *Journal of the Society for Industrial and Applied Mathematics*, 10(3):496–506, 1962.
- He, K., Zhang, X., Ren, S., and Sun, J. Deep residual learning for image recognition. In *Proceedings of the IEEE Conference on Computer Vision and Pattern Recognition*, pp. 770–778, 2016.
- Horn, R. A. and Johnson, C. R. *Matrix analysis*. Cambridge University Press, 2012.
- Koloskova, A., Stich, S., and Jaggi, M. Decentralized stochastic optimization and gossip algorithms with compressed communication. In *International Conference on Machine Learning*, pp. 3478–3487. PMLR, 2019.
- Koloskova, A., Loizou, N., Boreiri, S., Jaggi, M., and Stich, S. A unified theory of decentralized sgd with changing topology and local updates. In *International Conference* on *Machine Learning*, pp. 5381–5393. PMLR, 2020.
- Koloskova, A., Lin, T., and Stich, S. U. An improved analysis of gradient tracking for decentralized machine learning. Advances in Neural Information Processing Systems, 34:11422–11435, 2021.
- Krizhevsky, A., Hinton, G., et al. Learning multiple layers of features from tiny images. *Master's Thesis*, 2009.
- Levin, D. A. and Peres, Y. *Markov chains and mixing times*, volume 107. American Mathematical Soc., 2017.
- Li, T., Sahu, A. K., Talwalkar, A., and Smith, V. Federated learning: Challenges, methods, and future directions. *IEEE Signal Processing Magazine*, 37(3):50–60, 2020.
- Lian, X., Zhang, C., Zhang, H., Hsieh, C.-J., Zhang, W., and Liu, J. Can decentralized algorithms outperform centralized algorithms? a case study for decentralized parallel stochastic gradient descent. Advances in Neural Information Processing Systems, 30, 2017.
- Liang, L., Chen, X., Luo, G., and Yuan, K. Achieving linear speedup and near-optimal complexity for decentralized optimization over row-stochastic networks. In *International Conference on Machine Learning*. PMLR, 2025a.

- Liang, L., Huang, X., Xin, R., and Yuan, K. Understanding the influence of digraphs on decentralized optimization: Effective metrics, lower bound, and optimal algorithm. SIAM Journal on Optimization, 35(3):1570–1600, 2025b.
- Mai, V. S. and Abed, E. H. Distributed optimization over weighted directed graphs using row stochastic matrix. In 2016 American Control Conference (ACC), pp. 7165– 7170. IEEE, 2016.
- McMahan, B., Moore, E., Ramage, D., Hampson, S., and Aguera y Arcas, B. Communication-efficient learning of deep networks from decentralized data. In *Artificial Intelligence and Statistics*, pp. 1273–1282. PMLR, 2017.
- Mohar, B., Alavi, Y., Chartrand, G., and Oellermann, O. The laplacian spectrum of graphs. *Graph Theory, Combinatorics, and Applications*, 2(871-898):12, 1991.
- Nedić, A. and Olshevsky, A. Distributed optimization over time-varying directed graphs. *IEEE Transactions on Au*tomatic Control, 60(3):601–615, 2014.
- Nedic, A. and Ozdaglar, A. Distributed subgradient methods for multi-agent optimization. *IEEE Transactions on Automatic Control*, 54(1):48–61, 2009.
- Pu, S. and Nedić, A. Distributed stochastic gradient tracking methods. *Mathematical Programming*, 187(1):409–457, 2021.
- Sayed, A. H. Adaptive networks. *Proceedings of the IEEE*, 102(4):460–497, 2014.
- Tang, H., Gan, S., Zhang, C., Zhang, T., and Liu, J. Communication compression for decentralized training. Advances in Neural Information Processing Systems, 31, 2018.
- Wu, L., Wang, M., and Su, W. The alignment property of sgd noise and how it helps select flat minima: A stability analysis. Advances in Neural Information Processing Systems, 35:4680–4693, 2022.
- Xi, C. and Khan, U. A. Dextra: A fast algorithm for optimization over directed graphs. *IEEE Transactions on Automatic Control*, 62(10):4980–4993, 2017.
- Xin, R., Jakovetić, D., and Khan, U. A. Distributed nesterov gradient methods over arbitrary graphs. *IEEE Signal Processing Letters*, 26(8):1247–1251, 2019a.
- Xin, R., Xi, C., and Khan, U. A. Frost—fast row-stochastic optimization with uncoordinated step-sizes. *EURASIP Journal on Advances in Signal Processing*, 2019(1):1, 2019b.

- Xu, J., Zhu, S., Soh, Y. C., and Xie, L. Convergence of asynchronous distributed gradient methods over stochastic networks. *IEEE Transactions on Automatic Control*, 63(2):434–448, 2017.
- Ying, B., Yuan, K., Chen, Y., Hu, H., Pan, P., and Yin, W. Exponential graph is provably efficient for decentralized deep training. *Advances in Neural Information Process*ing Systems, 34:13975–13987, 2021.
- Yuan, K., Ling, Q., and Yin, W. On the convergence of decentralized gradient descent. SIAM Journal on Optimization, 26(3):1835–1854, 2016.
- Yuan, K., Ying, B., Zhao, X., and Sayed, A. H. Exact diffusion for distributed optimization and learning—part i: Algorithm development. *IEEE Transactions on Signal Processing*, 67(3):708–723, 2018a.
- Yuan, K., Ying, B., Zhao, X., and Sayed, A. H. Exact diffusion for distributed optimization and learning-part ii: Convergence analysis. *IEEE Transactions on Signal Processing*, 67(3):724–739, 2018b.
- Yuan, K., Alghunaim, S. A., and Huang, X. Removing data heterogeneity influence enhances network topology dependence of decentralized sgd. *Journal of Machine Learning Research*, 24(280):1–53, 2023.
- Zhang, H., Dauphin, Y. N., and Ma, T. Fixup initialization: Residual learning without normalization. In *International Conference on Learning Representations*, 2019.
- Zhu, T., Li, W., Wang, C., and He, F. Dice: Data influence cascade in decentralized learning. *International Conference on Learning Representations*, 2025.

A. More details on the $L^2(\lambda; \mathbb{R}^d)$ -Hilbert Space

A.1. Definition of $L^2(\lambda)$ **space**

Let S denote the index set of nodes and let

$$\lambda = (\lambda_i)_{i \in S}, \qquad \lambda_i > 0, \qquad \sum_{i \in S} \lambda_i = n > 1,$$

be the vector of heterogeneous node weights used in the decentralized optimization problem (1). Here λ should be regarded as a *positive weight vector* associated with the network nodes, rather than a probability distribution.

The weighted Hilbert space $L^2(\lambda)$ is defined as

$$L^{2}(\lambda) := \left\{ \phi : S \to \mathbb{R} \middle| \sum_{i \in S} |\phi(i)|^{2} \lambda_{i} < \infty \right\},\,$$

with inner product and induced norm

$$\langle \phi_1, \phi_2 \rangle_{\lambda} := \sum_{i \in S} \lambda_i \phi_1(i) \phi_2(i), \qquad \|\phi\|_{\lambda} := \left(\langle \phi, \phi \rangle_{\lambda}\right)^{1/2}.$$

If λ is replaced by $c\lambda$ for any constant c>0, then

$$\langle \phi_1, \phi_2 \rangle_{c\lambda} = c \langle \phi_1, \phi_2 \rangle_{\lambda}, \qquad \|\phi\|_{c\lambda} = \sqrt{c} \|\phi\|_{\lambda}.$$

Hence the element set of $L^2(\lambda)$ is unchanged, and the geometry of the Hilbert space is preserved up to a scaling factor.

In this paper, we focus on the matrix W introduced in (3), which is constructed to satisfy the detailed balance condition with respect to λ :

$$\lambda_i W_{ij} = \lambda_j W_{ji}, \quad \forall i, j \in S.$$

As a result, W is self-adjoint with respect to $\langle \cdot, \cdot \rangle_{\lambda}$, and its spectral properties are invariant to rescaling of λ . Equivalently, under the λ -similarity transform, $\widetilde{W} := D_{\lambda}^{1/2}WD_{\lambda}^{-1/2}$ is symmetric, which can be readily verified from its expression:

$$\widetilde{W}_{i,j} = \begin{cases} (1-\varepsilon) \min\left(\frac{1}{d_i}\sqrt{\frac{\lambda_i}{\lambda_j}}, \frac{1}{d_j}\sqrt{\frac{\lambda_j}{\lambda_i}}\right) & \text{if } i \neq j \text{ and } j \in \mathcal{N}_i \\ 1 - \sum_{k \in \mathcal{N}_i} \widetilde{W}_{i,k} & \text{if } i = j \\ 0 & \text{otherwise.} \end{cases}$$

Remark. It is worth emphasizing that λ in our setting is not required to be the stationary distribution of a Markov chain. Instead, it is a user-defined weight vector that induces the reversibility condition for W. While stationary distributions are a special case where λ is normalized to sum to one, our construction applies more generally and does not rely on probabilistic normalization.

A.2. $L^2(\lambda; \mathbb{R}^d)$ -Hilbert space.

In addition to the scalar-valued space $L^2(\lambda)$, it is often convenient to consider its vector-valued extension

$$L^{2}(\lambda; \mathbb{R}^{d}) := \left\{ \phi : S \to \mathbb{R}^{d} \middle| \sum_{i \in S} \lambda_{i} ||\phi(i)||^{2} < \infty \right\}.$$

This space can be identified with the tensor product

$$L^2(\lambda; \mathbb{R}^d) \cong L^2(\lambda) \widehat{\otimes} \mathbb{R}^d.$$

This identification simply reflects that an element of $L^2(\lambda; \mathbb{R}^d)$ consists of n vectors in \mathbb{R}^d , with geometry determined independently by the weighted node index $(L^2(\lambda))$ and the feature dimension (\mathbb{R}^d) .

The inner product between $\phi_1, \phi_2 \in L^2(\lambda; \mathbb{R}^d)$ is given by

$$\langle \phi_1, \phi_2 \rangle_{\lambda, d} = \sum_{i \in S} \lambda_i \langle \phi_1(i), \phi_2(i) \rangle,$$

where $\langle \cdot, \cdot \rangle$ denotes the standard Euclidean inner product in \mathbb{R}^d . The induced norm reads

$$\|\phi\|_{\lambda,d}^2 = \sum_{i \in S} \lambda_i \|\phi(i)\|^2,$$

This vector-valued extension inherits all Hilbert space properties of $L^2(\lambda)$ and is particularly useful when analyzing multi-dimensional signals or operator dynamics with matrix-valued actions. Equivalently, if ϕ is arranged as a $|S| \times d$ matrix with $\phi(i)$ as its i-th row, then $\|\phi\|_{\lambda,d}^2$ coincides with the λ -weighted Frobenius norm of this matrix, i.e., $\|\phi\|_{F,\lambda}^2$.

A.3. Why introduce the $L^2(\lambda; \mathbb{R}^d)$ space?

The motivation for introducing this space is twofold. First, under heterogeneous weights, the tightest result from the descent lemma is naturally expressed in the $L^2(\lambda; \mathbb{R}^d)$ norm; using the standard Euclidean space instead would introduce looser bounds. Second, the matrix W is generally not symmetric under the standard Euclidean inner product, so its eigenvectors are not orthogonal. Analyzing in the Euclidean space thus inevitably requires coarse bounding, leading to convergence results that are not sufficiently tight.

By introducing the weighted Hilbert space $L^2(\lambda)$, endowed with the inner product

$$\langle \phi_1, \phi_2 \rangle_{\lambda} = \sum_{i \in S} \lambda_i \phi_1(i) \phi_2(i),$$

we recover orthogonality of eigenvectors when W is reversible with respect to λ , i.e., when the detailed balance condition $\lambda_i W_{ij} = \lambda_j W_{ji}$ holds. In this case W is self-adjoint with respect to $\langle \cdot, \cdot \rangle_{\lambda}$, and thus admits an orthogonal spectral decomposition in $L^2(\lambda)$. This structure enables the use of Hilbert space techniques, such as Pythagorean identities and spectral gap estimates, to quantify the rate at which the dynamics defined by W converge to equilibrium.

Even when $\sum_i \lambda_i \neq 1$, the space $L^2(\lambda)$ remains well defined, since normalization of λ only rescales the inner product without altering the spectral properties of W or the convergence rate analysis.

B. Proof for the convergence rate

In this section, we present the proof of convergence for the proposed algorithms.

B.1. Technical lemmas

To begin with, we introduce some technical lemmas.

The following lemma provides the eigenvalue of the row-stochastic matrix.

Lemma B.1. Suppose $P \in \mathbb{R}^{n \times n}$ is a row-stochastic matrix and π is its stationary distribution, then the eigenvalue of the matrix $P - \mathbf{1}^{\top} \pi$ can be given by:

$$\sigma(P - \mathbf{1}^{\top} \pi) = \{0, \sigma_2(P), \dots, \sigma_n(P)\}.$$

Proof. As P is a row-stochastic matrix with stationary distribution π , then it holds that $P\mathbf{1}=\mathbf{1}, \pi P=\pi$, and $\pi\mathbf{1}=1$. Denote $\Pi=\mathbf{1}\pi$, then $(P-\Pi)\mathbf{1}=P\mathbf{1}-\mathbf{1}(\pi\mathbf{1})=\mathbf{1}-\mathbf{1}=0$. Thus 0 is an eigenvalue of $P-\Pi$ with eigenvector $\mathbf{1}$.

Moreover, if $\sigma \neq 1$ is an eigenvalue of P with respect to the vector v, it holds from $\pi P = \pi$ and $Pv = \sigma v$ that $\pi v = \pi(Pv) = \sigma \pi v$. Thus $(\sigma - 1)\pi v = 0$ and $\pi v = 0$ holds. Consequently, it holds that $\Pi v = \mathbf{1}\pi v = 0$, and $(P - \Pi)v = Pv = \sigma v$.

Therefore, combining the two aspects yields $\sigma(P - 1\pi) = \{0, \sigma_2(P), \dots, \sigma_n(P)\}.$

Lemma B.2. Suppose $\omega_1, \ldots, \omega_n > 0$, and let $x_1, \ldots, x_n \in \mathbb{R}^d$ be independent random vectors with zero expectation. Then, we have

$$\mathbb{E}\left[\left\|\sum_{i=1}^{n}\omega_{i}x_{i}\right\|^{2}\right] = \sum_{i=1}^{n}\omega_{i}^{2}\mathbb{E}\left[\left\|x_{i}\right\|^{2}\right] = \sum_{i=1}^{n}\omega_{i}^{2}\operatorname{var}(x_{i}).$$

Proof. As the independence among x_1, \ldots, x_n and the zero-mean property, we can derive that:

$$\mathbb{E}\left[\left\|\sum_{i=1}^{n}\omega_{i}x_{i}\right\|^{2}\right] = \mathbb{E}\left[\left\langle\sum_{i=1}^{n}\omega_{i}x_{i},\sum_{j=1}^{n}\omega_{j}x_{j}\right\rangle\right] = \mathbb{E}\left[\sum_{i=1}^{n}\sum_{j=1}^{n}\omega_{i}\omega_{j}\langle x_{i},x_{j}\rangle\right]$$
$$= \mathbb{E}\left[\sum_{i=1}^{n}\omega_{i}^{2}\langle x_{i},x_{i}\rangle\right] = \sum_{i=1}^{n}\omega_{i}^{2}\mathbb{E}\left[\left\|x_{i}\right\|^{2}\right] = \sum_{i=1}^{n}\omega_{i}^{2}\operatorname{var}(x_{i}).$$

Thus we finish the proof of this lemma.

The following lemma can be obtained from Young's inequality:

Lemma B.3. Given two matrices $A, B \in \mathbb{R}^{m \times d}$, for any a > 0, the following inequality holds:

$$||A + B||_{F,\lambda}^2 \le (1+a)||A||_{F,\lambda}^2 + \left(1 + \frac{1}{a}\right)||B||_{F,\lambda}^2.$$

Lemma B.4. Let W be the matrix constructed in (3). Under the λ -similarity transform $\widetilde{W} = D_{\lambda}^{1/2}WD_{\lambda}^{-1/2}$, the transformed matrix \widetilde{W} is symmetric.

Proof. From the definition in (3), the entries of W are given by

$$W_{i,j} = \begin{cases} \frac{1-\varepsilon}{d_i} \min\left(1, \frac{\lambda_j d_i}{\lambda_i d_j}\right), & \text{if } i \neq j \text{ and } j \in \mathcal{N}_i, \\ 1-\sum_{k \in \mathcal{N}_i} W_{i,k}, & \text{if } i = j, \\ 0, & \text{otherwise.} \end{cases}$$

Applying the similarity transformation $\widetilde{W} = D_{\lambda}^{1/2} W D_{\lambda}^{-1/2}$ yields

$$[\widetilde{W}]_{i,j} = \begin{cases} \min\left(\frac{1-\varepsilon}{d_i}\sqrt{\frac{\lambda_i}{\lambda_j}}, \frac{1-\varepsilon}{d_j}\sqrt{\frac{\lambda_j}{\lambda_i}}\right), & \text{if } i \neq j \text{ and } j \in \mathcal{N}_i, \\ 1-\sum_{k \in \mathcal{N}_i} [\widetilde{W}]_{i,k}, & \text{if } i = j, \\ -\sqrt{\lambda_i\lambda_j}, & \text{otherwise.} \end{cases}$$

By construction, $[\widetilde{W}]_{i,j} = [\widetilde{W}]_{j,i}$ for all i,j. Therefore, \widetilde{W} is symmetric under the λ -similarity transform.

Lemma B.5. Let $W_J := W^{\mathrm{ds}} - J$, $J = \frac{\mathbf{1}\mathbf{1}^{\top}}{n}$, and $D_{\lambda} = \mathrm{diag}(\lambda_1, \dots, \lambda_n)$. Then the λ -weighted spectral norm of $(W_J)^t(I-J)D_{\lambda}$ satisfies that:

$$\|W_I^t(I-J)D_\lambda\|_{\lambda} \leq \lambda_{\max}\rho_I^t$$

where $\lambda_{\max} = \max_i \lambda_i$ and $\rho_J = \|W^{ds} - J\|_2 < 1$ denotes the spectral radius of $W^{ds} - J$.

Proof. Note that W^{ds} is a doubly stochastic matrix, we have

$$W^{\mathrm{ds}}J = JW^{\mathrm{ds}} = J$$

Hence,

$$(W_J)^t(I-J) = (W^{ds}-J)^t(I-J) = [(W^{ds})^t - J](I-J) = (W^{ds})^t - J.$$

Thus we consider the λ -weighted spectral norm of $(I-J)D_{\lambda}$:

$$\begin{aligned} \|(W_J)^t (I - J) D_{\lambda} \|_{\lambda} &= \|D_{\lambda}^{1/2} [(W^{\mathrm{ds}})^t - J] D_{\lambda} D_{\lambda}^{-1/2} \|_2 \\ &= \|D_{\lambda}^{1/2} [(W^{\mathrm{ds}})^t - J] D_{\lambda}^{1/2} \|_2 \\ &\leq \|D_{\lambda}^{1/2} \|_2 \cdot \|(W^{\mathrm{ds}})^t - J\|_2 \cdot \|D_{\lambda}^{1/2} \|_2 \\ &= \lambda_{\max} \rho_J^t, \end{aligned}$$

where $\lambda_{\max} = \max_i \lambda_i$ and $\rho_J = \|W^{\mathrm{ds}} - J\|_2 < 1$ denotes the spectral radius of $W^{\mathrm{ds}} - J$.

To facilitate the subsequent proofs, we now introduce the following lemmas concerning series summations.

Lemma B.6. Consider the sequence ta^t for t = 0, 1, ..., n, where 0 < a < 1. The closed-form expression for its sum is given by

$$\sum_{t=0}^{n} ta^{2t} = \frac{a^2 \left(1 - (n+1)a^{2n} + na^{2(n+1)}\right)}{(1 - a^2)^2},$$

and the infinite sum is

$$\sum_{t=0}^{\infty} t a^{2t} = \frac{a^2}{(1-a^2)^2}.$$
(11)

Proof. Let $b = a^2$, the series can be rewritten as

$$\sum_{t=0}^{n} ta^{2t} = \sum_{t=0}^{n} tb^{t}.$$

We first consider the standard geometric series

$$G(b) = \sum_{t=0}^{n} b^t = \frac{1 - b^{(n+1)}}{1 - b}, \quad 0 < b < 1.$$

Differentiating both sides of the equation with respect to b yields

$$G'(b) = \sum_{t=0}^{n} tb^{t-1} = \frac{1 - (n+1)b^n + nb^{n+1}}{(1-b)^2}.$$

Multiplying both sides by b gives the desired sum:

$$\sum_{t=0}^{n} ta^{2t} = \sum_{t=0}^{n} tb^{t} = b\sum_{t=1}^{n} tb^{t-1} = \frac{a^{2}(1 - (n+1)a^{2n} + na^{2(n+1)})}{(1 - a^{2})^{2}}.$$

Taking the limit as $n \to \infty$ yields the infinite sum:

$$\sum_{t=0}^{\infty} t a^{2t} = \frac{a^2}{(1-a^2)^2}.$$

Lemma B.7. Consider the sequence t^2a^{2t} for $t=0,1,\ldots,n$, where 0< a< 1. The closed-form expression for its sum is given by

$$\sum_{t=0}^n t^2 a^{2t} = \frac{a^2(1+a^2) - (n+1)^2 a^{2(n+1)} + (2n^2 + 2n - 1)a^{2(n+2)} - n^2 a^{2(n+3)}}{(1-a^2)^3}.$$

Taking the limit as $n \to \infty$ yields the infinite sum:

$$\sum_{t=0}^{\infty} t^2 a^{2t} = \frac{a^2 (1+a^2)}{(1-a^2)^3}.$$
 (12)

Proof. Let $b = a^2$, the series can be rewritten as

$$\sum_{t=0}^{n} t^2 a^{2t} = \sum_{t=0}^{n} t^2 b^t.$$

We also begin with the standard geometric series

$$G(b) = \sum_{t=0}^{n} b^{t} = \frac{1 - b^{n+1}}{1 - b}, \quad 0 < b < 1.$$

Differentiating G(b) with respect to b yields

$$G'(b) = \sum_{t=1}^{n} tb^{t-1} = \frac{1 - (n+1)b^n + nb^{n+1}}{(1-b)^2}.$$
 (13)

Differentiating once more, we obtain

$$G''(b) = \sum_{t=2}^{n} t(t-1)b^{t-2} = \frac{2 - (n+1)nb^{n-1} + 2(n^2 - 1)b^n - n(n-1)b^{n+1}}{(1-b)^3}.$$
 (14)

Since $t^2 = t(t-1) + t$, we can decompose the sum as

$$\sum_{t=0}^{n} t^{2} b^{t} = \sum_{t=0}^{n} t(t-1)b^{t} + \sum_{t=0}^{n} tb^{t}$$
$$= b^{2} G''(b) + bG'(b). \tag{15}$$

Substituting (13) and (14) into (15) and replacing b with a^2 , we obtain

$$\sum_{t=0}^{n} t^2 a^{2t} = \frac{a^2 (1+a^2) - (n+1)^2 a^{2(n+1)} + (2n^2 + 2n - 1) a^{2(n+2)} - n^2 a^{2(n+3)}}{(1-a^2)^3}.$$

Finally, since $a^{2n} \to 0$ as $n \to \infty$ for 0 < a < 1, the infinite series converges to

$$\sum_{t=0}^{\infty} t^2 a^{2t} = \frac{a^2 (1+a^2)}{(1-a^2)^3}.$$

Lemma B.8. Consider the sequence t^3a^{2t} for t=0,1,..., where 0 < a < 1. The closed-form expression for its infinite sum is given by

$$\sum_{t=0}^{\infty} t^3 a^{2t} = \frac{a^2 (1 + 4a^2 + a^4)}{(1 - a^2)^4}.$$
 (16)

Proof. Following Lemma B.7, which states that

$$\sum_{t=0}^{\infty} t^2 a^{2t} = \frac{a^2 (1+a^2)}{(1-a^2)^3},$$

we differentiate both sides of the equation with respect to a^2 to obtain:

$$\frac{\mathrm{d} \sum_{t=0}^{\infty} t^2 a^{2t}}{\mathrm{d} a^2} = \sum_{t=0}^{\infty} t^3 a^{2(t-1)} = \frac{a^4 + 4a^2 + 1}{(1 - a^2)^4}.$$

Therefore, we can get the final result

$$\sum_{t=0}^{\infty} t^3 a^{2t} = a^2 \sum_{t=0}^{\infty} t^3 a^{2(t-1)} = \frac{a^2 (a^4 + 4a^2 + 1)}{(1 - a^2)^4}.$$

B.2. Descent lemma

In this subsection, we present the proof of the descent lemma to obtain the convergence rate with the two strategies. To begin with, we present the following descent lemma for the two strategies.

Lemma B.9. Under Assumptions 6.1 and 6.2 and a constant step size α , it holds for Algorithm 1 with both Strategy I and II that:

$$\mathbb{E}\left[F(\overline{\theta}_{*}^{(t+1)})\right] \leq \mathbb{E}\left[F\left(\overline{\theta}_{*}^{(t)}\right)\right] - \frac{\alpha}{2}\mathbb{E}\left[\left\|\nabla F(\overline{\theta}_{*}^{(t)})\right\|^{2}\right] - \frac{\alpha}{2}\mathbb{E}\left[\left\|\sum_{i=1}^{n} \frac{\lambda_{i}}{n} \nabla F_{i}(\theta_{i}^{(t)})\right\|^{2}\right] + \frac{c_{\lambda}\alpha^{2}\beta v^{2}}{2} + \frac{\alpha^{2}\beta}{2} \cdot \mathbb{E}\left[\left\|\sum_{i=1}^{n} \frac{\lambda_{i}}{n} \nabla F_{i}(\theta_{i}^{(t)})\right\|^{2}\right] + \frac{\alpha T_{3}}{2}, \tag{17}$$

where
$$T_3 = \mathbb{E}\left[\left\|\nabla F(\overline{\theta}_*^{(t)}) - \sum_{i=1}^n \frac{\lambda_i}{n} \nabla F_i(\theta_i^{(t)})\right\|^2\right]$$
, $\overline{\theta}_*^{(t)} = \overline{\theta}^{(t)}$ in Strategy I and $\overline{\theta}_*^{(t)} = \overline{\theta}_\lambda^{(t)}$ in Strategy II.

Proof. According to Assumption 6.1, we can derive

$$\mathbb{E}\left[F(\overline{\theta}_*^{(t+1)})\right] \leq \mathbb{E}\left[F\left(\overline{\theta}_*^{(t)}\right)\right] + \underbrace{\mathbb{E}\left[\left\langle\nabla F(\overline{\theta}_*^{(t)}), \overline{\theta}_*^{(t+1)} - \overline{\theta}_*^{(t)}\right\rangle\right]}_{:=T_1} + \underbrace{\mathbb{E}\left[\frac{\beta}{2}\left\|\overline{\theta}_*^{(t+1)} - \overline{\theta}_*^{(t)}\right\|^2\right]}_{:=T_2}.$$

Using $\overline{\theta}_*^{(t+1)} = \overline{\theta}_*^{(t)} - \frac{\alpha}{n} \sum_{i=1}^n \lambda_i g_i^{(t)}$, we can derive:

$$T_{1} = -\alpha \mathbb{E}\left[\left\langle \nabla F(\overline{\theta}_{*}^{(t)}), \sum_{i=1}^{n} \frac{\lambda_{i}}{n} g_{i}^{(t)} \right\rangle\right]$$

$$= -\alpha \mathbb{E}\left[\left\langle \nabla F(\overline{\theta}_{*}^{(t)}), \sum_{i=1}^{n} \frac{\lambda_{i}}{n} \nabla F_{i}(\theta_{i}^{(t)}) \right\rangle\right]$$

$$= \frac{\alpha}{2} \mathbb{E}\left[\left\|\nabla F(\overline{\theta}_{*}^{(t)}) - \sum_{i=1}^{n} \frac{\lambda_{i}}{n} \nabla F_{i}(\theta_{i}^{(t)})\right\|^{2}\right] - \frac{\alpha}{2} \mathbb{E}\left[\left\|\nabla F(\overline{\theta}_{*}^{(t)})\right\|^{2}\right] - \frac{\alpha}{2} \mathbb{E}\left[\left\|\sum_{i=1}^{n} \frac{\lambda_{i}}{n} \nabla F_{i}(\theta_{i}^{(t)})\right\|^{2}\right],$$
(18)

and

$$T_{2} = \frac{\alpha^{2} \beta}{2} \mathbb{E} \left[\left\| \sum_{i=1}^{n} \frac{\lambda_{i}}{n} g_{i}^{(t)} \right\|^{2} \right] = \frac{\alpha^{2} \beta}{2} \mathbb{E} \left[\mathbb{E}_{t} \left[\left\| \sum_{i=1}^{n} \frac{\lambda_{i}}{n} \left(g_{i}^{(t)} - \nabla F_{i}(\theta_{i}^{(t)}) + \nabla F_{i}(\theta_{i}^{(t)}) \right) \right\|^{2} \right] \right]$$

$$= \frac{\alpha^{2} \beta}{2} \left(\mathbb{E} \left[\left\| \sum_{i=1}^{n} \frac{\lambda_{i}}{n} \left(g_{i}^{(t)} - \nabla F_{i}(\theta_{i}^{(t)}) \right) \right\|^{2} \right] + \mathbb{E} \left[\left\| \sum_{i=1}^{n} \frac{\lambda_{i}}{n} \nabla F_{i}(\theta_{i}^{(t)}) \right\|^{2} \right] \right)$$

$$+ 2\mathbb{E} \left[\left\langle \sum_{i=1}^{n} \frac{\lambda_{i}}{n} \nabla F_{i}(\theta_{i}^{(t)}), \mathbb{E}_{t} \left[\sum_{i=1}^{n} \frac{\lambda_{i}}{n} \left(g_{i}^{(t)} - \nabla F_{i}(\theta_{i}^{(t)}) \right) \right] \right\rangle \right]$$

$$\leq \frac{\alpha^{2} \beta}{2} \left(\frac{1}{n^{2}} \sum_{i=1}^{n} \lambda_{i}^{2} v^{2} + \mathbb{E} \left[\left\| \sum_{i=1}^{n} \frac{\lambda_{i}}{n} \nabla F_{i}(\theta_{i}^{(t)}) \right\|^{2} \right] \right) = \frac{c_{\lambda} \alpha^{2} \beta v^{2}}{2} + \frac{\alpha^{2} \beta}{2} \cdot \mathbb{E} \left[\left\| \sum_{i=1}^{n} \frac{\lambda_{i}}{n} \nabla F_{i}(\theta_{i}^{(t)}) \right\|^{2} \right],$$

$$(19)$$

where we use the Assumption 6.2. Plugging (18) and (19) into (17) and using the definition of T_3 , we can prove that (17) holds for both strategies.

Here, we denote $c_{\lambda} = \sum_{i=1}^{n} \lambda_i^2/n^2 < 1$. Then with Lemma B.9, we can present a further descent lemma for the both communication strategies.

Lemma B.10 (Descent lemma of Strategy I). *Under Assumptions 6.1 and 6.2 and a constant step size* $\alpha \leq 1/\beta$, *it holds for Algorithm 1 with Strategy I that:*

$$\mathbb{E}[F(\bar{\theta}^{(t+1)})] \le \mathbb{E}[F(\bar{\theta}^{(t)})] - \frac{\alpha}{2} \mathbb{E}[\|\nabla F(\bar{\theta}^{(t)})\|^2] + \frac{\alpha\beta^2}{2n} \mathbb{E}[\|(I-J)\Theta^{(t)}\|_{F,\lambda}^2] + \frac{\alpha^2 c_{\lambda} \beta v^2}{2}. \tag{20}$$

Proof. We consider the term T_3 that has been definited in Lemma B.9. It holds under Assumption 6.1 that:

$$T_{3} = \mathbb{E}\left[\left\|\nabla F(\overline{\theta}^{(t)}) - \sum_{i=1}^{n} \frac{\lambda_{i}}{n} \nabla F_{i}(\theta_{i}^{(t)})\right\|^{2}\right] = \mathbb{E}\left[\left\|\sum_{i=1}^{n} \frac{\lambda_{i}}{n} \left(\nabla F_{i}(\overline{\theta}^{(t)}) - \nabla F_{i}(\theta_{i}^{(t)})\right)\right\|^{2}\right]$$

$$\leq \frac{\beta^{2}}{n} \sum_{i=1}^{n} \lambda_{i} \mathbb{E}\left[\left\|\overline{\theta}^{(t)} - \theta_{i}^{(t)}\right\|_{2}^{2}\right] = \frac{\beta^{2}}{n} \mathbb{E}\left[\left\|(I - J)\Theta^{(t)}\right\|_{F, \lambda}^{2}\right],$$
(21)

where the last inequality follows from Jensen's inequality. Substituting (21) into (17) and it holds that:

$$\begin{split} \mathbb{E}\left[F(\overline{\theta}^{(t+1)})\right] &\leq \mathbb{E}\left[F(\overline{\theta}^{(t)})\right] + \frac{\alpha\beta^2}{2n^2} \mathbb{E}\left[\left\|(I-J)\Theta^{(t)}\right\|_{F,\lambda}^2\right] + \frac{\alpha(\alpha\beta-1)}{2} \mathbb{E}\left[\left\|\sum_{i=1}^n \frac{\lambda_i}{n} \nabla F_i(\theta_i^{(t)})\right\|^2\right] \\ &- \frac{\alpha}{2} \mathbb{E}\left[\left\|\nabla F(\overline{\theta}^{(t)})\right\|^2\right] + \frac{c_\lambda \alpha^2 \beta \upsilon^2}{2} \\ &\stackrel{\alpha \leq \frac{1}{\beta}}{\leq} \mathbb{E}\left[F(\overline{\theta}^{(t)})\right] + \frac{\alpha\beta^2}{2n^2} \mathbb{E}\left[\left\|(I-J)\Theta^{(t)}\right\|_{F,\lambda}^2\right] - \frac{\alpha}{2} \mathbb{E}\left[\left\|\nabla F(\overline{\theta}^{(t)})\right\|^2\right] + \frac{c_\lambda \alpha^2 \beta \upsilon^2}{2}. \end{split}$$

Then we finish the proof of Eq. (20).

The following lemma is the descent lemma of strategy II.

Lemma B.11 (Descent lemma of Strategy II). *Under Assumptions 6.1 and 6.2 and a constant step size* $\alpha \le 1/\beta$, *it holds for Algorithm 1 with Strategy II that:*

$$\mathbb{E}[F(\bar{\theta}_{\lambda}^{(t+1)})] \leq \mathbb{E}[F(\bar{\theta}_{\lambda}^{(t)})] - \frac{\alpha}{2}\mathbb{E}[\|\nabla F(\bar{\theta}_{\lambda}^{(t)})\|^2] + \frac{\alpha\beta^2}{2n}\mathbb{E}[\|(I - \Lambda)\Theta^{(t)}\|_{F,\lambda}^2] + \frac{\alpha^2c_{\lambda}\beta\upsilon^2}{2}.$$
 (22)

Proof. We consider the term T_3 that has been definited in Lemma B.9. It holds under Assumption 6.1 that:

$$T_{3} = \mathbb{E}\left[\left\|\nabla F(\overline{\theta}_{\lambda}^{(t)}) - \sum_{i=1}^{n} \frac{\lambda_{i}}{n} \nabla F_{i}(\theta_{i}^{(t)})\right\|^{2}\right] = \mathbb{E}\left[\left\|\sum_{i=1}^{n} \frac{\lambda_{i}}{n} \left(\nabla F_{i}(\overline{\theta}_{\lambda}^{(t)}) - \nabla F_{i}(\theta_{i}^{(t)})\right)\right\|^{2}\right]$$

$$\leq \frac{\beta^{2}}{n} \sum_{i=1}^{n} \lambda_{i} \mathbb{E}\left[\left\|\overline{\theta}_{\lambda}^{(t)} - \theta_{i}^{(t)}\right\|_{2}^{2}\right] = \frac{\beta^{2}}{n} \mathbb{E}\left[\left\|(I - \Lambda)\Theta^{(t)}\right\|_{F, \lambda}^{2}\right],$$
(23)

Substituting (23) into (17) and it holds that:

$$\begin{split} \mathbb{E}\left[F(\overline{\theta}_{\lambda}^{(t+1)})\right] &\leq \mathbb{E}\left[F(\overline{\theta}_{\lambda}^{(t)})\right] + \frac{\alpha\beta^2}{2n^2}\mathbb{E}\left[\left\|(I-\Lambda)\Theta^{(t)}\right\|_{F,\lambda}^2\right] + \frac{\alpha(\alpha\beta-1)}{2}\mathbb{E}\left[\left\|\sum_{i=1}^n \frac{\lambda_i}{n}\nabla F_i(\theta_i^{(t)})\right\|^2\right] \\ &- \frac{\alpha}{2}\mathbb{E}\left[\left\|\nabla F(\overline{\theta}_{\lambda}^{(t)})\right\|^2\right] + \frac{\alpha^2c_{\lambda}\beta\upsilon^2}{2} \\ &\stackrel{\alpha\leq\frac{1}{\beta}}{\leq} \mathbb{E}\left[F(\overline{\theta}_{\lambda}^{(t)})\right] + \frac{\alpha\beta^2}{2n^2}\mathbb{E}\left[\left\|(I-\Lambda)\Theta^{(t)}\right\|_{F,\lambda}^2\right] - \frac{\alpha}{2}\mathbb{E}\left[\left\|\nabla F(\overline{\theta}_{\lambda}^{(t)})\right\|^2\right] + \frac{\alpha^2c_{\lambda}\beta\upsilon^2}{2}. \end{split}$$

Then we finish the proof of Eq. (22).

Remark B.12. We observe that, due to the heterogeneous node weights, the consensus error terms in the descent lemmas for both strategies, (21) and (23), naturally take the form of norms in the Hilbert space $L^2(\lambda; \mathbb{R}^d)$. This serves as an important motivation for introducing this weighted Hilbert space.

B.3. Consensus error analysis

In this subsection, we present the consensus error analysis for Algorithm 1 with different communication strategies.

B.3.1. PARAMETER DEVIATIONS AND SPECTRAL NORMS

Firstly, we present the following lemma to characterize the parameter and tracker deviations:

Lemma B.13. The parameter and tracker deviations satisfy the following recursive relations:

$$\begin{cases}
E_{\rm I}^{(t+1)} = A_{\rm I} E_{\rm I}^{(t)} + \alpha B_{\rm I}^{(t)}, & (Strategy I), \\
E_{\rm II}^{(t+1)} = A_{\rm II} E_{\rm II}^{(t)} + \alpha B_{\rm II}^{(t)}, & (Strategy II),
\end{cases}$$
(24)

where the matrices involved are defined as follows:

$$E_{\mathrm{I}}^{(t)} = \begin{bmatrix} (I-J)\Theta^{(t)} \\ \alpha(I-J)Y^{(t)} \end{bmatrix}, \quad E_{\mathrm{II}}^{(t)} = \begin{bmatrix} (I-\Lambda)\Theta^{(t)} \\ \alpha(I-\Lambda)Y^{(t)} \end{bmatrix}, \quad A_{\mathrm{I}} = \begin{bmatrix} W_J & -W_J \\ \mathbf{0} & W_J \end{bmatrix}, \quad A_{\mathrm{II}} = \begin{bmatrix} W_{\Lambda} & -W_{\Lambda} \\ \mathbf{0} & W_{\Lambda} \end{bmatrix},$$

$$B_{\mathrm{I}}^{(t)} = \begin{bmatrix} \mathbf{0} \\ (I-J)D_{\lambda} \left[\nabla F_{\xi}(\Theta^{(t+1)}) - \nabla F_{\xi}(\Theta^{(t)}) \right] \right], \quad B_{\mathrm{II}}^{(t)} = \begin{bmatrix} \mathbf{0} \\ (I-\Lambda) \left[\nabla F_{\xi}(\Theta^{(t+1)}) - \nabla F_{\xi}(\Theta^{(t)}) \right] \right].$$

Proof. For Strategy I, we have the following update form:

$$\begin{bmatrix} \Theta^{(t+1)} \\ \alpha \cdot Y^{(t+1)} \end{bmatrix} = \begin{bmatrix} W^{\mathrm{ds}} & -W^{\mathrm{ds}} \\ \mathbf{0} & W^{\mathrm{ds}} \end{bmatrix} \begin{bmatrix} \Theta^{(t)} \\ \alpha \cdot Y^{(t)} \end{bmatrix} + \alpha \begin{bmatrix} \mathbf{0} \\ D_{\lambda} [\nabla F_{\xi}(\Theta^{(t+1)}) - \nabla F_{\xi}(\Theta^{(t)})] \end{bmatrix}. \tag{25}$$

Then, we have the following equations:

$$(I-J)^2 = I - 2J + J^2 = I - 2J + J = I - J,$$

 $(I-J)^2 W^{\text{ds}} \stackrel{\mathbf{1}W^{\text{ds}}=\mathbf{1}}{=} (I-J)(W^{\text{ds}} - J) \stackrel{W^{\text{ds}}=\mathbf{1}}{=} (I-J)W^{\text{ds}}(I-J) = W_J(I-J).$

Multiplying both sides of (25) by $(I - J)^2$, we obtain:

$$\underbrace{\begin{bmatrix} (I-J)\Theta^{(t+1)} \\ \alpha \cdot (I-J)Y^{(t+1)} \end{bmatrix}}_{E_{\mathbf{I}}^{(t+1)}} = \underbrace{\begin{bmatrix} W_J & -W_J \\ \mathbf{0} & W_J \end{bmatrix}}_{A_{\mathbf{I}}} \underbrace{\begin{bmatrix} (I-J)\Theta^{(t)} \\ \alpha \cdot (I-J)Y^{(t)} \end{bmatrix}}_{E_{\mathbf{I}}^{(t)}} + \alpha \underbrace{\begin{bmatrix} \mathbf{0} \\ (I-J)D_{\lambda}[\nabla F_{\xi}(\Theta^{(t+1)}) - \nabla F_{\xi}(\Theta^{(t)})] \end{bmatrix}}_{B_{\mathbf{I}}^{(t)}}.$$

Similarly for Strategy II, we can give the following update from (2):

$$\begin{bmatrix} \Theta^{(t+1)} \\ \alpha \cdot Y^{(t+1)} \end{bmatrix} = \begin{bmatrix} W & -W \\ \mathbf{0} & W \end{bmatrix} \begin{bmatrix} \Theta^{(t)} \\ \alpha \cdot Y^{(t)} \end{bmatrix} + \alpha \begin{bmatrix} \mathbf{0} \\ \nabla F_{\xi}(\Theta^{(t+1)}) - \nabla F_{\xi}(\Theta^{(t)}) \end{bmatrix}.$$
 (26)

Then, we have the following equations:

$$(I - \Lambda)^2 = I - 2\Lambda + \Lambda^2 = I - 2\Lambda + \mathbf{1}\lambda \cdot \mathbf{1}\lambda \stackrel{\lambda \cdot \mathbf{1} = 1}{=} I - \Lambda,$$

$$(I - \Lambda)^2 W \stackrel{\lambda W = \lambda}{=} (I - \Lambda)(W - \Lambda) \stackrel{W \mathbf{1} = \mathbf{1}}{=} (I - \Lambda)W(I - \Lambda) = W_{\Lambda}(I - \Lambda).$$

Multiplying both sides of (26) by $(I - \Lambda)^2$ and substituting the two equations above, we arrive at the desired result:

$$\underbrace{ \begin{bmatrix} (I-\Lambda)\Theta^{(t+1)} \\ \alpha \cdot (I-\Lambda)Y^{(t+1)} \end{bmatrix}}_{E_{\mathrm{II}}^{(t+1)}} = \underbrace{ \begin{bmatrix} W_{\Lambda} & -W_{\Lambda} \\ \mathbf{0} & W_{\Lambda} \end{bmatrix}}_{A_{\mathrm{II}}} \underbrace{ \begin{bmatrix} (I-\Lambda)\Theta^{(t)} \\ \alpha \cdot (I-\Lambda)Y^{(t)} \end{bmatrix}}_{E_{\mathrm{II}}^{(t)}} + \alpha \underbrace{ \begin{bmatrix} \mathbf{0} \\ (I-\Lambda)[\nabla F_{\xi}(\Theta^{(t+1)}) - \nabla F_{\xi}(\Theta^{(t)})] \end{bmatrix}}_{B_{\mathrm{II}}^{(t)}}.$$

Thus Eq. (24) holds for both strategies.

From Lemma B.13, we obtain the following recursion:

$$\begin{cases} E_{\rm II}^{(t)} = A_{\rm II}^t E_{\rm II}^{(0)} + \alpha \sum_{j=1}^t A_{\rm II}^{t-j} B_{\rm II}^{(j-1)}, \text{ (Strategy II)}, \\ E_{\rm I}^{(t)} = A_{\rm I}^t E_{\rm I}^{(0)} + \alpha \sum_{j=1}^t A_{\rm I}^{t-j} B_{\rm I}^{(j-1)}, \text{ (Strategy I)}. \end{cases}$$

We next examine the spectral norms of $A_{\rm II}$ and $A_{\rm I}$. While both matrices have spectral radius strictly less than one, their spectral norms do not necessarily satisfy this property. The following proposition makes this distinction precise.

Proposition B.14. Let $A_{\rm II}$ and $A_{\rm I}$ be as defined in Lemma B.13. Then (i) $\rho(A_{\rm II}) < 1$ and $\rho(A_{\rm I}) < 1$; (ii) for any integer $t \ge 1$, the λ -weighted spectral norms satisfy

$$||A_{\text{II}}^t||_{\lambda}^2 = \frac{2+t+t\sqrt{t^2+4}}{2}\rho_{\Lambda}^{2t}, \quad ||A_{\text{I}}^t||_{\lambda}^2 = \frac{2+t+t\sqrt{t^2+4}}{2}\kappa_{\lambda}\rho_{J}^{2t}.$$
 (27)

Proof. We start with the traditional method for computing eigenvalues:

$$\det(\sigma I - A_{\rm II}) = \det \begin{bmatrix} \sigma I - W_{\Lambda} & \sigma I + W_{\Lambda} \\ \mathbf{0} & \sigma I - W_{\Lambda} \end{bmatrix} = [\det(\sigma I - W_{\Lambda})]^2.$$

Therefore, A has the same eigenvalues as W_{Λ} , each with algebraic multiplicity two, indicating that $\rho(A) = \rho_{\Lambda} < 1$.

As for the matrix $A_{\rm I}$, similarly, we can obtain:

$$\det(\sigma I - A_{\rm I}) = \det \begin{bmatrix} \sigma I - W_J & \sigma I + W_J \\ \mathbf{0} & \sigma I - W_J \end{bmatrix} = [\det(\sigma I - W_J)]^2.$$

Hence, $A_{\rm I}$ shares the same spectrum as W_J , and each eigenvalue of W_J appears twice in $A_{\rm I}$. This implies that the spectral radius of $A_{\rm I}$ satisfies $\rho(A_{\rm I}) = \rho_J < 1$.

Proof of $||A_{\rm II}^t||_{\lambda}^2$. Recall that the λ -weighted spectral norm is defined as

$$||M||_{\lambda} = ||D_{\lambda}^{1/2} M D_{\lambda}^{-1/2}||_{2}.$$

Consequently, in order to evaluate $||A_{II}^t||_{\lambda}$, it suffices to compute the spectral radius of the right normal matrix of its λ -similarity transform:

$$\|A_{\mathrm{II}}^t\|_{\lambda}^2 = \|A_{\mathrm{II,sim}}^t\|_2^2 = \rho \left((A_{\mathrm{II,sim}}^t)^\top A_{\mathrm{II,sim}}^t \right).$$

We start by calculating the power of A, by simple recursion, one obtains

$$A_{\mathrm{II}}^{t} = \begin{bmatrix} W_{\Lambda}^{t} & -tW_{\Lambda}^{t} \\ \mathbf{0} & W_{\Lambda}^{t} \end{bmatrix},$$

where t is a positive integer. To compute the λ -weighted spectral norm, we need to obtain the λ -similarity transform of A^t :

$$A_{\mathrm{II,sim}}^t = \begin{bmatrix} D_{\lambda}^{\frac{1}{2}} & \mathbf{0} \\ \mathbf{0} & D_{\lambda}^{\frac{1}{2}} \end{bmatrix} A_{\mathrm{II}}^t \begin{bmatrix} D_{\lambda}^{-\frac{1}{2}} & \mathbf{0} \\ \mathbf{0} & D_{\lambda}^{-\frac{1}{2}} \end{bmatrix} = \begin{bmatrix} \widetilde{W}_{\Lambda}^t & -t\widetilde{W}_{\Lambda}^t \\ \mathbf{0} & \widetilde{W}_{\Lambda}^t \end{bmatrix},$$

where $\widetilde{W}^t_{\Lambda}=D^{\frac{1}{2}}_{\lambda}W^t_{\Lambda}D^{-\frac{1}{2}}_{\lambda}$. The right normal matrix associated with $A^t_{\rm II,sim}$ is

$$(A_{\mathrm{II,sim}}^t)^\top A_{\mathrm{II,sim}}^t = \begin{bmatrix} (\widetilde{W}_{\Lambda}^t)^\top \widetilde{W}_{\Lambda}^t & -t (\widetilde{W}_{\Lambda}^t)^\top \widetilde{W}_{\Lambda}^t \\ -t (\widetilde{W}_{\Lambda}^t)^\top \widetilde{W}_{\Lambda}^t & (1+t^2) (\widetilde{W}_{\Lambda}^t)^\top \widetilde{W}_{\Lambda}^t \end{bmatrix}.$$

We denote $\mathcal{W}=(\widetilde{W}_{\Lambda}^t)^{\top}\widetilde{W}_{\Lambda}^t$ for simplicity. This matrix admits a Kronecker factorization

$$(A_{\mathrm{II,sim}}^t)^{\top} A_{\mathrm{II,sim}}^t = \begin{bmatrix} 1 & -t \\ -t & 1+t^2 \end{bmatrix} \otimes \mathcal{W}.$$

By the spectral property of Kronecker products (Horn & Johnson, 2012), the eigenvalues of $A \otimes B$ are given by the pairwise products of the eigenvalues of A and B.

We first compute the eigenvalues of the 2×2 coefficient matrix $M_t = \begin{bmatrix} 1 & -t \\ -t & 1+t^2 \end{bmatrix}$. Its characteristic polynomial is

$$\det \begin{bmatrix} 1 - \mu & -t \\ -t & 1 + t^2 - \mu \end{bmatrix} = (1 - \mu)(1 + t^2 - \mu) - t^2 = 0,$$

which yields

$$\mu_{1,2} = \frac{t^2 + 2 \pm t\sqrt{t^2 + 4}}{2}.$$

For the matrix $W = (\widetilde{W}_{\Lambda}^t)^{\top} \widetilde{W}_{\Lambda}^t$, the spectral mapping theorem together with the invariance of eigenvalues under similarity transformations implies

$$\sigma_i(\mathcal{W}) = (\sigma_i(W_{\Lambda}))^{2t}, \quad i = 1, \dots, n.$$

Therefore, the eigenvalues of $(A_{\text{II.sim}}^t)^{\top} A_{\text{II.sim}}^t$ are given by

$$\sigma(A_{\mathrm{II,sim}}^t) = \left\{ \mu_k(M_t) \cdot \left(\sigma_i(W_\Lambda)\right)^{2t} \middle| k = 1, 2, i = 1, \dots, n \right\}.$$

In particular, the spectral radius is

$$\rho((A_{\mathrm{II,sim}}^t)^\top A_{\mathrm{II,sim}}^t) = \max\{|\mu_1|, |\mu_2|\} \cdot \max_i (\sigma_i(W_\Lambda))^{2t} = \frac{t^2 + 2 + t\sqrt{t^2 + 4}}{2} \rho_\Lambda^{2t}.$$

Consequently, the λ -weighted spectral norm of A^t satisfies

$$||A_{\mathrm{II}}^t||_{\lambda}^2 = ||A_{\mathrm{II,sim}}^t||_2^2 = \rho((A_{\mathrm{II,sim}}^t)^{\top} A_{\mathrm{II,sim}}^t) = \frac{t^2 + 2 + t\sqrt{t^2 + 4}}{2} \rho_{\Lambda}^{2t},$$

and we obtain $\|A_{\rm II}\|_{\lambda}^2=\frac{3+\sqrt{5}}{2}\rho_{\Lambda}^{2t}\approx 2.62\rho_{\Lambda}^{2t}$, which can be greater than 1 when the network connectivity is poor.

Proof of $\|A_1^t\|_{\lambda}^2$. Since the matrix W^{ds} is self-adjoint in the standard Euclidean space, we can similarly obtain:

$$\|A_{\mathrm{I}}^t\|_2^2 = \frac{t^2 + 2 + t\sqrt{t^2 + 4}}{2}\rho_J^{2t}.$$

Therefore, the λ -weighted norm of $A_{\rm I}^t$ satisfies:

$$\begin{split} \|A_{\mathbf{I}}^t\|_{\lambda}^2 &= \left\| \begin{bmatrix} D_{\lambda}^{\frac{1}{2}} & \mathbf{0} \\ \mathbf{0} & D_{\lambda}^{\frac{1}{2}} \end{bmatrix} A_{\mathbf{I}}^t \begin{bmatrix} D_{\lambda}^{-\frac{1}{2}} & \mathbf{0} \\ \mathbf{0} & D_{\lambda}^{-\frac{1}{2}} \end{bmatrix} \right\|_2^2 \leq \left\| \begin{bmatrix} D_{\lambda}^{-\frac{1}{2}} & \mathbf{0} \\ \mathbf{0} & D_{\lambda}^{-\frac{1}{2}} \end{bmatrix} \right\|_2^2 \|A_{\mathbf{I}}^t\|_2^2 \left\| \begin{bmatrix} D_{\lambda}^{-\frac{1}{2}} & \mathbf{0} \\ \mathbf{0} & D_{\lambda}^{-\frac{1}{2}} \end{bmatrix} \right\|_2^2 \\ &\leq \kappa_{\lambda} \frac{t^2 + 2 + t\sqrt{t^2 + 4}}{2} \rho_J^{2t}. \end{split}$$

Thus Eq. (27) holds.

B.3.2. CONSENSUS ERROR FOR A SINGLE STEP

Then we can present the consensus error for the t-th step for both cases. Firstly, the following lemma gives the consensus error of Strategy II.

Lemma B.15 (Consensus error for Strategy II). Suppose that Assumptions 6.1, 6.3, and 6.2 hold, and the step size α satisfies that $\alpha \leq \frac{1}{9\beta} \sqrt{\frac{3(1-\rho_{\Lambda})}{(2-\rho_{\Lambda})}}$. Then for any t>0, the following bounds on $\mathbb{E}\left[\|E_{\mathrm{II}}^{(t)}\|_{F,\lambda}^2\right]$ are satisfied:

$$\mathbb{E}\left[\|E_{\Pi}^{(t)}\|_{F,\lambda}^{2}\right] \leq 3\left(2+t+t\sqrt{t^{2}+4}\right)\rho_{\Lambda}^{2t}\left\|E_{\Pi}^{(0)}\right\|_{F,\lambda}^{2} + 27\alpha^{2}\beta^{2}\mathbb{E}\left[\sum_{j=0}^{t-1}\left(H_{\Lambda}^{(t,j)}+\frac{11}{10}H_{\Lambda}^{(t,j+1)}\right)\left\|(I-\Lambda)\Theta^{(j)}\right\|_{F,\lambda}^{2}\right] \\ + 2n\alpha^{2}\mathbb{E}\left[\sum_{j=1}^{t}H_{\Lambda}^{(t,j)}\left\|\nabla F(\overline{\theta}_{\lambda}^{(j-1)})\right\|^{2}\right] + 18n\alpha^{2}\upsilon^{2}\sum_{j=1}^{t}\left(h_{\Lambda}^{(t,j)}+\frac{3}{2}c_{\lambda}\alpha^{2}\beta^{2}H_{\Lambda}^{(t,j)}\right).$$

$$\text{where } H_{\Lambda}^{(t,j)} := ((t-j)^{2}+1)\rho_{\Lambda}^{2(t-j)} + \left(\frac{\rho_{\Lambda}(t-j)}{1-\rho_{\Lambda}}+1\right)\frac{\rho_{\Lambda}^{t-j}}{1-\rho_{\Lambda}} \text{ and } h_{\Lambda}^{(t,j)} := ((t-j)^{2}+1)\rho_{\Lambda}^{2(t-j)}.$$

$$(28)$$

Proof. From (24), it can be obtained that:

$$E_{\text{II}}^{(t)} = A_{\text{II}}^t E_{\text{II}}^{(0)} + \alpha \sum_{j=1}^t A_{\text{II}}^{t-j} B_{\text{II}}(j-1).$$

Then we obtain

$$\mathbb{E}\left[\left\|E_{\Pi}^{(t)}\right\|_{F,\lambda}^{2}\right]^{lm.B.3} (1+2)\|A_{\Pi}^{t}\|_{\lambda}^{2} \left\|E_{\Pi}^{(0)}\right\|_{F,\lambda}^{2} + (1+\frac{1}{2})\alpha^{2}\mathbb{E}\left[\left\|\sum_{j=1}^{t} A_{\Pi}^{t-j} B_{\Pi}(j-1)\right\|_{F,\lambda}^{2}\right]$$

$$= 3\|A_{\Pi}^{t}\|_{\lambda}^{2} \left\|E_{\Pi}^{(0)}\right\|_{F,\lambda}^{2} + \frac{3}{2}\alpha^{2}\mathbb{E}\left[\left\|\left[-\sum_{j=1}^{t} (t-j)W_{\Lambda}^{t-j} I_{\Lambda}[\nabla F_{\xi}(\Theta^{(j)}) - \nabla F_{\xi}(\Theta^{(j-1)})]}{\sum_{j=1}^{t} W_{\Lambda}^{t-j} I_{\Lambda}[\nabla F_{\xi}(\Theta^{(j)}) - \nabla F_{\xi}(\Theta^{(j-1)})]}\right]\right\|_{F,\lambda}^{2}\right]$$

$$\leq 3\|A^{t}\|_{\lambda}^{2} \left\|E_{\Pi}^{(0)}\right\|_{F,\lambda}^{2} + \frac{3}{2}\alpha^{2}\mathbb{E}\left[\left\|\sum_{j=1}^{t} W_{\Lambda}^{t-j}[\nabla F_{\xi}(\Theta^{(j)}) - \nabla F_{\xi}(\Theta^{(j-1)})]\right\|_{F,\lambda}^{2}\right]$$

$$+ \frac{3}{2}\alpha^{2}\mathbb{E}\left[\left\|\sum_{j=1}^{t} (t-j)W_{\Lambda}^{t-j}[\nabla F_{\xi}(\Theta^{(j)}) - \nabla F_{\xi}(\Theta^{(j-1)})]\right\|_{F,\lambda}^{2}\right],$$

where we use $W_{\Lambda}^{t-j}I_{\Lambda}=I_{\Lambda}W_{\Lambda}^{t-j}$ and $\|I_{\Lambda}\|_{\lambda}\leq 1$. From Spectral Mapping Theorem, we have $\rho(W_{\Lambda}^{t-j})=\rho_{\Lambda}^{t-j}$. For matrix W_{Λ} , the λ -weighted spectral norm coincides with the spectral radius, implying $\|W_{\Lambda}^{t-j}\|_{\lambda}=\rho_{\Lambda}^{t-j}$. Therefore, we obtain

$$T_{1} \leq 3\mathbb{E}\left[\left\|\sum_{j=1}^{t} W_{\Lambda}^{t-j} \left[\nabla F(\Theta^{(j-1)}) - \nabla F_{\xi}(\Theta^{(j-1)})\right]\right\|_{F,\lambda}^{2}\right] + 3\mathbb{E}\left[\left\|\sum_{j=1}^{t} W_{\Lambda}^{t-j} \left[\nabla F(\Theta^{(j)}) - \nabla F_{\xi}(\Theta^{(j)})\right]\right\|_{F,\lambda}^{2}\right] + 3\mathbb{E}\left[\left\|\sum_{j=1}^{t} W_{\Lambda}^{t-j} \left[\nabla F(\Theta^{(j)}) - \nabla F(\Theta^{(j-1)})\right]\right\|_{F,\lambda}^{2}\right] + 3\mathbb{E}\left[\left\|\sum_{j=1}^{t} W_{\Lambda}^{t-j} \left[\nabla F(\Theta^{(j)}) - \nabla F(\Theta^{(j-1)})\right]\right\|_{F,\lambda}^{2}\right]\right]$$

Then from Lemma B.2 and the unbiasedness of the stochastic gradient, it comes that:

$$T_{1} \leq 3 \sum_{j=1}^{t} \left\| W_{\Lambda}^{t-j} \right\|_{\lambda}^{2} \mathbb{E} \left[\left\| \nabla F(\Theta^{(j-1)}) - \nabla F_{\xi}(\Theta^{(j-1)}) \right\|_{F,\lambda}^{2} \right]$$

$$+ 3 \sum_{j=1}^{t} \left\| W_{\Lambda}^{t-j} \right\|_{\lambda}^{2} \mathbb{E} \left[\left\| \nabla F(\Theta^{(j)}) - \nabla F_{\xi}(\Theta^{(j)}) \right\|_{F,\lambda}^{2} \right] + 3 \mathbb{E}[T_{3}]$$

$$\leq 3 \sum_{j=1}^{t} \rho_{\Lambda}^{2(t-j)} n v^{2} + 3 \sum_{j=1}^{t} \rho_{\Lambda}^{2(t-j)} n v^{2} + 3 \mathbb{E}[T_{3}] = 6 \sum_{j=1}^{t} \rho_{\Lambda}^{2(t-j)} n v^{2} + 3 \mathbb{E}[T_{3}],$$

$$(30)$$

As for the term T_3 , it holds that:

$$T_{3} = \mathbb{E} \left[\left\| \sum_{j=1}^{t} W_{\Lambda}^{t-j} [\nabla F(\Theta^{(j)}) - \nabla F(\Theta^{(j-1)})] \right\|_{F,\lambda}^{2} \right]$$

$$= \mathbb{E} \left[\sum_{j=1}^{t} \left\| W_{\Lambda}^{t-j} [\nabla F(\Theta^{(j)}) - \nabla F(\Theta^{(j-1)})] \right\|_{F,\lambda}^{2} \right]$$

$$+ \mathbb{E} \left[\sum_{j \neq \iota} \left\langle W_{\Lambda}^{t-j} [\nabla F(\Theta^{(j)}) - \nabla F(\Theta^{(j-1)})], W_{\Lambda}^{t-\iota} [\nabla F(\Theta^{(\iota)}) - \nabla F(\Theta^{(\iota-1)})] \right\rangle_{\lambda,d} \right].$$

$$(31)$$

We bound T_4 :

$$T_{4} = \sum_{j \neq \iota}^{t} \left\langle W_{\Lambda}^{t-j} [\nabla F(\Theta^{(j)}) - \nabla F(\Theta^{(j-1)})], W_{\Lambda}^{t-\iota} [\nabla F(\Theta^{(\iota)}) - \nabla F(\Theta^{(\iota-1)})] \right\rangle_{\lambda, d}$$

$$\leq \sum_{j \neq \iota}^{t} \left\| W_{\Lambda}^{t-j} \right\|_{\lambda} \left\| \nabla F(\Theta^{(j)}) - \nabla F(\Theta^{(j-1)}) \right\|_{F, \lambda} \left\| W_{\Lambda}^{t-\iota} \right\|_{\lambda} \left\| \nabla F(\Theta^{(\iota)}) - \nabla F(\Theta^{(\iota-1)}) \right\|_{F, \lambda}$$

$$\leq \sum_{j \neq \iota}^{t} \rho_{\Lambda}^{2t-(j+\iota)} \frac{\left\| \nabla F(\Theta^{(j)}) - \nabla F(\Theta^{(j-1)}) \right\|_{F, \lambda}^{2}}{2} + \sum_{j \neq \iota}^{t} \rho_{\Lambda}^{2t-(j+\iota)} \frac{\left\| \nabla F(\Theta^{(\iota)}) - \nabla F(\Theta^{(\iota-1)}) \right\|_{F, \lambda}^{2}}{2}$$

$$= \sum_{j \neq \iota}^{t} \rho_{\Lambda}^{2t-(j+\iota)} \left\| \nabla F(\Theta^{(j)}) - \nabla F(\Theta^{(j-1)}) \right\|_{F, \lambda}^{2} = \sum_{j=1}^{t} \sum_{\substack{\iota=1 \ \iota \neq j}}^{t} \rho_{\Lambda}^{2t-(j+\iota)} \left\| \nabla F(\Theta^{(j)}) - \nabla F(\Theta^{(j-1)}) \right\|_{F, \lambda}^{2}$$

$$\leq \frac{1}{1-\rho_{\Lambda}} \sum_{i=1}^{t} \rho_{\Lambda}^{t-j} \left\| \nabla F(\Theta^{(j)}) - \nabla F(\Theta^{(j-1)}) \right\|_{F, \lambda}^{2}.$$

$$(32)$$

Combing (31) and (32), we can get the upper bound for $\mathbb{E}[T_3]$:

$$T_3 \le \sum_{j=1}^t \left(\rho_{\Lambda}^{2(t-j)} + \frac{1}{1 - \rho_{\Lambda}} \rho_{\Lambda}^{t-j} \right) \mathbb{E} \left[\left\| \nabla F(\Theta^{(j)}) - \nabla F(\Theta^{(j-1)}) \right\|_{F,\lambda}^2 \right]. \tag{33}$$

Similarly, we can bound T_2 as:

$$T_{2} \leq 6 \sum_{j=1}^{t} (t-j)^{2} \rho_{\Lambda}^{2(t-j)} n v^{2} + 3 \mathbb{E} \left[\underbrace{\left\| \sum_{j=1}^{t} (t-j) W_{\Lambda}^{t-j} [\nabla F(\Theta^{(j)}) - \nabla F(\Theta^{(j-1)})] \right\|_{F, \lambda}^{2}}_{T_{3}'} \right]$$
(34)

As for T_3' , we have

$$T_{3}' \leq \sum_{j=1}^{t} (t-j)^{2} \rho_{\Lambda}^{2(t-j)} \left\| \nabla F(\Theta^{(j)}) - \nabla F(\Theta^{(j-1)}) \right\|_{F,\lambda}^{2}$$

$$+ \sum_{j=1}^{t} (t-j) \sum_{\substack{\iota=1\\\iota \neq j}}^{t} (t-\iota) \rho_{\Lambda}^{2t-(j+\iota)} \left\| \nabla F(\Theta^{(j)}) - \nabla F(\Theta^{(j-1)}) \right\|_{F,\lambda}^{2}$$

$$\leq \sum_{j=1}^{t} \left((t-j)^{2} \rho_{\Lambda}^{2(t-j)} + \frac{\rho_{\Lambda}}{(1-\rho_{\Lambda})^{2}} (t-j) \rho_{\Lambda}^{t-j} \right) \left\| \nabla F(\Theta^{(j)}) - \nabla F(\Theta^{(j-1)}) \right\|_{F,\lambda}^{2} .$$

$$(35)$$

Therefore, it holds from (30), (33), (34), and (35) that

$$T_{1} + T_{2} \leq 6 \sum_{j=1}^{t} ((t-j)^{2} + 1) \rho_{\Lambda}^{2(t-j)} n v^{2}$$

$$+ 3 \sum_{j=1}^{t} \left[((t-j)^{2} + 1) \rho_{\Lambda}^{2(t-j)} + \left(\frac{\rho_{\Lambda}(t-j)}{1 - \rho_{\Lambda}} + 1 \right) \frac{\rho_{\Lambda}^{t-j}}{1 - \rho_{\Lambda}} \right] \mathbb{E} \left[\underbrace{\left\| \nabla F(\Theta^{(j)}) - \nabla F(\Theta^{(j-1)}) \right\|_{F, \lambda}^{2}}_{T_{5}} \right]$$

$$\leq 3 \sum_{j=1}^{t} H_{\Lambda}^{(t,j)} \mathbb{E}[T_{5}] + 6 \sum_{j=1}^{t} h_{\Lambda}^{(t,j)} n v^{2},$$

$$(36)$$

 $\text{where we denote } H_{\Lambda}^{(t,j)} := ((t-j)^2 + 1)\rho_{\Lambda}^{2(t-j)} + \left(\frac{\rho_{\Lambda}(t-j)}{1-\rho_{\Lambda}} + 1\right)\frac{\rho_{\Lambda}^{t-j}}{1-\rho_{\Lambda}} \text{ and } h_{\Lambda}^{(t,j)} := ((t-j)^2 + 1)\rho_{\Lambda}^{2(t-j)}.$

As for the term T_5 , we can derive

$$T_{5} \leq 3 \left\| \nabla F(\Theta^{(j)}) - \nabla F(\overline{\Theta}_{\lambda}(j)) \right\|_{F,\lambda}^{2} + 3 \left\| \nabla F(\Theta^{(j-1)}) - \nabla F(\overline{\Theta}_{\lambda}^{(j-1)}) \right\|_{F,\lambda}^{2} + 3 \left\| \nabla F(\overline{\Theta}_{\lambda}^{(j-1)}) - \nabla F(\overline{\Theta}_{\lambda}(j)) \right\|_{F,\lambda}^{2}$$

$$\leq 3\beta^{2} \left[\left\| (I - \Lambda)\Theta^{(j)} \right\|_{F,\lambda}^{2} + \left\| (I - \Lambda)\Theta^{(j-1)} \right\|_{F,\lambda}^{2} + \left\| \overline{\Theta}_{\lambda}(j) - \overline{\Theta}_{\lambda}^{(j-1)} \right\|_{F,\lambda}^{2} \right]. \tag{37}$$

We consider the last term of (37) and obtain that:

$$\mathbb{E}\left[\left\|\overline{\Theta}_{\lambda}(j) - \overline{\Theta}_{\lambda}^{(j-1)}\right\|_{F,\lambda}^{2}\right] = \sum_{i=1}^{n} \lambda_{i} \mathbb{E}\left[\left\|\overline{\theta}_{\lambda}(j) - \overline{\theta}_{\lambda}^{(j-1)}\right\|^{2}\right] = n\alpha^{2} \mathbb{E}\left[\left\|\sum_{i=1}^{n} \frac{\lambda_{i}}{n} g_{i}^{(j-1)}\right\|^{2}\right] \\
\leq n\alpha^{2} \mathbb{E}\left[\left\|\sum_{i=1}^{n} \frac{\lambda_{i}}{n} \nabla F_{i}(\theta_{i}^{(j-1)})\right\|^{2} + \left\|\sum_{i=1}^{n} \frac{\lambda_{i}}{n} [g_{i}^{(j-1)} - \nabla F_{i}(\theta_{i}^{(j-1)})]\right\|^{2}\right] \\
\leq n\alpha^{2} \mathbb{E}\left[\left\|\sum_{i=1}^{n} \frac{\lambda_{i}}{n} \nabla F_{i}(\theta_{i}^{(j-1)})\right\|^{2}\right] + c_{\lambda} n\alpha^{2} v^{2} \\
\leq 2n\alpha^{2} \left(\mathbb{E}\left[\left\|\sum_{i=1}^{n} \frac{\lambda_{i}}{n} \left[\nabla F_{i}(\theta_{i}^{(j-1)}) - \nabla F_{i}(\overline{\theta}_{\lambda}^{(j-1)})\right]\right\|^{2} + \left\|\nabla F_{\lambda}(\overline{\theta}_{\lambda}^{(j-1)})\right\|^{2}\right] + \frac{c_{\lambda} v^{2}}{2}\right)$$
(38)

Combining (37) and (38) together, it holds that:

$$\mathbb{E}[T_5] = 3\beta^2 \mathbb{E}\left[\left\| (I - \Lambda)\Theta^{(j)} \right\|_{F,\lambda}^2 \right] + 3\beta^2 (1 + 2\alpha^2 \beta^2) \mathbb{E}\left[\left\| (I - \Lambda)\Theta^{(j-1)} \right\|_{F,\lambda}^2 \right] + 6n\alpha^2 \beta^2 \mathbb{E}\left[\left\| \nabla F_{\lambda}(\overline{\theta}_{\lambda}^{(j-1)}) \right\|^2 \right]$$

$$+ 3c_{\lambda} n\alpha^2 \beta^2 v^2.$$
(39)

Substituting (39) and (36) into (29), it holds that:

$$\mathbb{E}\left[\left\|E^{(t)}\right\|_{F,\lambda}^{2}\right] \leq 3\left\|A^{t}\right\|_{\lambda}^{2}\left\|E_{\Pi}^{(0)}\right\|_{F,\lambda}^{2} + \frac{27}{2}\alpha^{2}\beta^{2}\mathbb{E}\left[\sum_{j=0}^{t-1}\left(H_{\Lambda}^{(t,j)} + (1+2\alpha^{2}\beta^{2})H^{(t,j+1)}\right)\left\|(I-\Lambda)\Theta^{(j)}\right\|_{F,\lambda}^{2}\right] \\
+ \frac{27(2-\rho_{\Lambda})}{2(1-\rho_{\Lambda})}\alpha^{2}\beta^{2}\mathbb{E}\left[\left\|(I-\Lambda)\Theta^{(t)}\right\|_{F,\lambda}^{2}\right] + 27n\alpha^{4}\beta^{2}\mathbb{E}\left[\sum_{j=1}^{t}H_{\Lambda}^{(t,j)}\left\|\nabla F_{\lambda}(\overline{\theta}_{\lambda}^{(j-1)})\right\|^{2}\right] \\
+ 9n\alpha^{2}v^{2}\sum_{j=1}^{t}\left(h_{\Lambda}^{(t,j)} + \frac{3}{2}c_{\lambda}\alpha^{2}\beta^{2}H_{\Lambda}^{(t,j)}\right).$$
(40)

Furthermore, by noting that $\mathbb{E}\left[\left\|(I-\Lambda)\Theta^{(t)}\right\|_{F,\lambda}^2\right] \leq \mathbb{E}\left[\left\|E^{(t)}\right\|_{F,\lambda}^2\right]$ and assuming that $\alpha \leq \frac{1}{9\beta}\sqrt{\frac{3(1-\rho_\Lambda)}{2-\rho_\Lambda}}$, we can further derive from (40) that:

$$\mathbb{E}\left[\|E(t)\|_{F,\lambda}^{2}\right] \leq 3\left(2 + t + t\sqrt{t^{2} + 4}\right)\rho_{\Lambda}^{2t} \left\|E_{\Pi}^{(0)}\right\|_{F,\lambda}^{2} + 27\alpha^{2}\beta^{2}\mathbb{E}\left[\sum_{j=0}^{t-1} \left(H_{\Lambda}^{(t,j)} + \frac{11}{10}H^{(t,j+1)}\right) \left\|(I - \Lambda)\Theta^{(j)}\right\|_{F,\lambda}^{2}\right] + 2n\alpha^{2}\mathbb{E}\left[\sum_{j=1}^{t} H_{\Lambda}^{(t,j)} \left\|\nabla F(\overline{\theta}_{\lambda}^{(j-1)})\right\|^{2}\right] + 18n\alpha^{2}v^{2}\sum_{j=1}^{t} \left(h_{\Lambda}^{(t,j)} + \frac{3}{2}c_{\lambda}\alpha^{2}\beta^{2}H_{\Lambda}^{(t,j)}\right).$$

Thus we prove that (28) holds.

The following lemma present the single-step consensus error for Strategy I.

Lemma B.16 (Consensus error for Strategy I). Suppose that Assumptions 6.1, 6.3, and 6.2 hold, and the step size α satisfies that $\alpha \leq \frac{1}{9\beta} \sqrt{\frac{3(1-\rho_J)}{(2-\rho_J)\lambda_{\max}^2}}$. Then for any t>0, the following bounds on $\mathbb{E}\left[\|E_{\mathrm{I}}^{(t)}\|_{F,\lambda}^2\right]$ are satisfied:

$$\mathbb{E}\left[\left\|E_{\mathrm{I}}^{(t)}\right\|_{F,\lambda}^{2}\right] \leq 3\kappa_{\lambda}\left(2+t+t\sqrt{t^{2}+4}\right)\rho_{J}^{2t}\left\|E_{\mathrm{I}}^{(0)}\right\|_{F,\lambda}^{2}+27\alpha^{2}\beta^{2}\mathbb{E}\left[\sum_{j=0}^{t-1}\left(H_{J}^{(t,j)}+\frac{11}{10}H_{J}^{(t,j+1)}\right)\left\|(I-J)\Theta^{(j)}\right\|_{F,\lambda}^{2}\right] \\ +2n\alpha^{2}\mathbb{E}\left[\sum_{j=1}^{t}H_{J}^{(t,j)}\left\|\nabla F(\overline{\theta}_{\lambda}^{(j-1)})\right\|^{2}\right]+18n\alpha^{2}v^{2}\sum_{j=1}^{t}\left(h_{J}^{(t,j)}+\frac{3}{2}c_{\lambda}\alpha^{2}\beta^{2}H_{J}^{(t,j)}\right),$$

$$\text{where }H_{J}^{(t,j)}:=\lambda_{\max}^{2}\left[\left((t-j)^{2}+1\right)\rho_{J}^{2(t-j)}+\left(\frac{\rho_{J}(t-j)}{1-\rho_{J}}+1\right)\frac{\rho_{J}^{t-j}}{1-\rho_{J}}\right]\text{ and }h_{J}^{(t,j)}:=\lambda_{\max}^{2}((t-j)^{2}+1)\rho_{J}^{2(t-j)}.$$

Proof. Similar to that of Strategy II, we can derive:

$$\mathbb{E}\left[\left\|E_{\mathbf{I}}^{(t)}\right\|_{F,\lambda}^{2}\right] \leq 3\|A_{\mathbf{I}}^{t}\|_{\lambda}^{2} \left\|E_{\mathbf{I}}^{(0)}\right\|_{F,\lambda}^{2} + \frac{3}{2}\alpha^{2}\mathbb{E}\left[\left\|\sum_{j=1}^{t}A^{t-j}B(j-1)\right\|_{F,\lambda}^{2}\right] \\
\leq 3\|A_{\mathbf{I}}^{t}\|_{\lambda}^{2} \left\|E_{\mathbf{I}}^{(0)}\right\|_{F,\lambda}^{2} + \frac{3}{2}\alpha^{2}\mathbb{E}\left[\left\|\sum_{j=1}^{t}W_{J}^{t-j}I_{J}D_{\lambda}[\nabla F_{\xi}(\Theta^{(j)}) - \nabla F_{\xi}(\Theta^{(j-1)})]\right\|_{F,\lambda}^{2}\right] \\
+ \frac{3}{2}\alpha^{2}\mathbb{E}\left[\left\|\sum_{j=1}^{t}(t-j)W_{J}^{t-j}I_{J}D_{\lambda}[\nabla F_{\xi}(\Theta^{(j)}) - \nabla F_{\xi}(\Theta^{(j-1)})]\right\|_{F,\lambda}^{2}\right], \tag{42}$$

For the term T_1 , we can present an upper bound as follows:

$$T_{1} = \mathbb{E}\left[\left\|\sum_{j=1}^{t} W_{J}^{t-j} I_{J} D_{\lambda} \left[\nabla F_{\xi}(\Theta^{(j)}) - \nabla F_{\xi}(\Theta^{(j-1)})\right]\right\|_{F,\lambda}^{2}\right]$$

$$\leq \sum_{j=1}^{t} \left\|W_{J}^{t-j} I_{J} D_{\lambda}\right\|_{\lambda}^{2} \mathbb{E}\left[\left\|\nabla F_{\xi}(\Theta^{(j)}) - \nabla F_{\xi}(\Theta^{(j-1)})\right\|_{F,\lambda}^{2}\right]$$

$$+ \mathbb{E}\left[\sum_{\substack{j\neq \iota}\\ J\neq \iota}} \left\langle W_{J}^{t-j} I_{J} D_{\lambda} \left[\nabla F(\Theta^{(j)}) - \nabla F(\Theta^{(j-1)})\right], W_{J}^{t-\iota} I_{J} D_{\lambda} \left[\nabla F(\Theta^{(\iota)}) - \nabla F(\Theta^{(\iota-1)})\right]\right\rangle_{\lambda,d}\right].$$

$$(43)$$

The proof is essentially identical to that of Strategy II, except that every W_{Λ} term is replaced by W_{J} , and an extra factor $I_{J}D_{\lambda}$ is applied. Consequently, the argument reduces to bounding the corresponding λ -weighted spectral norm. Applying Lemma B.5, we obtain:

$$\|W_J^{t-j}I_JD_\lambda\|_\lambda \le \lambda_{\max}\rho_J^{t-j}, \quad \|(t-j)W_J^{t-j}I_JD_\lambda\|_\lambda \le (t-j)\lambda_{\max}\rho_J^{t-j}$$

If α satisfies that $\alpha \leq \frac{1}{9\beta} \sqrt{\frac{3(1-\rho_J)}{(2-\rho_J)\lambda_{\max}^2}}$, we can obtain from (42) and (43) that:

$$\begin{split} \mathbb{E}\left[\left\| E_{\mathrm{I}}^{(t)} \right\|_{F,\lambda}^{2} \right] \leq & 3\kappa_{\lambda} \left(2 + t + t\sqrt{t^{2} + 4} \right) \rho_{J}^{2t} \left\| E_{\mathrm{I}}^{(0)} \right\|_{F,\lambda}^{2} + 27\alpha^{2}\beta^{2} \mathbb{E}\left[\sum_{j=0}^{t-1} \left(H_{J}^{(t,j)} + \frac{11}{10} H_{J}^{(t,j+1)} \right) \left\| (I - J)\Theta^{(j)} \right\|_{F,\lambda}^{2} \right] \\ & + 2n\alpha^{2} \mathbb{E}\left[\sum_{j=1}^{t} H_{J}^{(t,j)} \left\| \nabla F(\overline{\theta}_{\lambda}^{(j-1)}) \right\|^{2} \right] + 18n\alpha^{2} v^{2} \sum_{j=1}^{t} \left(h_{J}^{(t,j)} + \frac{3}{2} c_{\lambda} \alpha^{2} \beta^{2} H_{J}^{(t,j)} \right), \\ \text{where } H_{\Lambda}^{(t,j)} := ((t-j)^{2} + 1)\rho_{\Lambda}^{2(t-j)} + \left(\frac{\rho_{\Lambda}(t-j)}{1-\rho_{\Lambda}} + 1 \right) \frac{\rho_{\Lambda}^{t-j}}{1-\rho_{\Lambda}} \text{ and } h_{\Lambda}^{(t,j)} := ((t-j)^{2} + 1)\rho_{\Lambda}^{2(t-j)}. \text{ Thus (41) holds.} \quad \Box \\ & \frac{1}{2} \left(\frac{1}{2} \left(\frac{1}{2} \right) \left(\frac{1}{2} \left(\frac{1}{2} \right) \left(\frac{1}{2} \right) \left(\frac{1}{2} \right) \left(\frac{1}{2} \right) \left(\frac{1}{2} \left(\frac{1}{2} \right) \left(\frac{1}{2}$$

B.3.3. TOTAL CONSENSUS ERROR ANALYSIS

Finally, we can present total consensus error analysis and complete the proof of Proposition 6.4.

Proof. Proof of Strategy II. By taking the summation on both sides of Eq. (28) from t=0 to T-1, we obtain:

$$\sum_{t=0}^{T-1} \mathbb{E}\left[\left\|E_{\Pi}^{(t)}\right\|_{F,\lambda}^{2}\right] \\
\leq 6 \sum_{t=0}^{T-1} \frac{2+t+t\sqrt{t^{2}+4}}{2} \rho_{\Lambda}^{2t} \left\|E_{\Pi}^{(0)}\right\|_{F,\lambda}^{2} + 27\alpha^{2}\beta^{2} \sum_{t=0}^{T-1} \sum_{j=0}^{t-1} \left(H_{\Lambda}^{(t,j)} + \frac{11}{10}H^{(t,j+1)}\right) \mathbb{E}\left[\left\|(I-\Lambda)\Theta^{(j)}\right\|_{F,\lambda}^{2}\right] \\
+ 2n\alpha^{2} \sum_{t=0}^{T-1} \sum_{j=1}^{t} H_{\Lambda}^{(t,j)} \mathbb{E}\left[\left\|\nabla F(\overline{\theta}_{\lambda}^{(-1)})\right\|^{2}\right] + 18n\alpha^{2}v^{2} \sum_{t=0}^{T-1} \sum_{j=1}^{t} \left(h_{\Lambda}^{(t,j)} + \frac{3}{2}c_{\lambda}\alpha^{2}\beta^{2}H_{\Lambda}^{(t,j)}\right) \\
\leq 6 \sum_{t=0}^{T-1} \frac{2+t+t\sqrt{t^{2}+4}}{2} \rho_{\Lambda}^{2t} \left\|E_{\Pi}^{(0)}\right\|_{F,\lambda}^{2} + 27\alpha^{2}\beta^{2} \sum_{j=0}^{T-2} \mathbb{E}\left[\left\|(I-\Lambda)\Theta^{(j)}\right\|_{F,\lambda}^{2}\right] \sum_{t=j+1}^{T-1} \left(H_{\Lambda}^{(t,j)} + \frac{11}{10}H^{(t,j+1)}\right) \\
+ 2n\alpha^{2} \sum_{j=1}^{T-1} \mathbb{E}\left[\left\|\nabla F(\overline{\theta}_{\lambda}^{(-1)})\right\|^{2}\right] \sum_{t=j}^{T-1} H_{\Lambda}^{(t,j)} + 18n\alpha^{2}v^{2} \sum_{t=0}^{T-1} \sum_{j=1}^{t} \left(h_{\Lambda}^{(t,j)} + \frac{3}{2}c_{\lambda}\alpha^{2}\beta^{2}H_{\Lambda}^{(t,j)}\right) \\
+ 2n\alpha^{2} \sum_{j=1}^{T-1} \mathbb{E}\left[\left\|\nabla F(\overline{\theta}_{\lambda}^{(-1)})\right\|^{2}\right] \sum_{t=j}^{T-1} H_{\Lambda}^{(t,j)} + 18n\alpha^{2}v^{2} \sum_{t=0}^{T-1} \sum_{j=1}^{t} \left(h_{\Lambda}^{(t,j)} + \frac{3}{2}c_{\lambda}\alpha^{2}\beta^{2}H_{\Lambda}^{(t,j)}\right) \\
\cdot T_{4} \cdot \left(\frac{1}{2} \sum_{t=0}^{T-1} \frac{1}{2} \left(\frac{1}{2} \sum_{t=0}^{T-1} \frac{1}{2} \sum_{t=0}^{T-1} \frac{1}{2} \sum_{t=0}^{T-1} \frac{1}{2} \sum_{t=0}^{T-1} \frac{1}{2} \left(\frac{1}{2} \sum_{t=0}^{T-1} \frac{1}{2} \sum_{t=0}^{T-1} \frac{1}{2} \left(\frac{1}{2} \sum_{t=0}^{T-1} \frac{1}{2} \sum_{t=0}^{T-1} \frac{1}{2} \sum_{t=0}^{T-1} \frac{1}{2} \left(\frac{1}{2} \sum_{t=0}^{T-1} \frac{1}{2} \sum_{t=0}^{T-1} \frac{1}{2} \sum_{t=0}^{T-1} \frac{1}{2} \sum_{t=0}^{T-1} \frac{1}{2} \left(\frac{1}{2} \sum_{t=0}^{T-1} \frac{1}{2} \sum_{t=0}^{T-1}$$

We first consider the term T_1 . From (11) and (12) it holds that:

$$T_{1} = \sum_{t=0}^{T-1} \frac{2+t+t\sqrt{t^{2}+4}}{2} \rho_{\Lambda}^{2t} \leq \sum_{t=0}^{\infty} \frac{t^{2}+t+6}{2} \rho_{\Lambda}^{2t} = \frac{\rho_{\Lambda}^{2} (1+\rho_{\Lambda}^{2})}{2(1-\rho_{\Lambda}^{2})^{3}} + \frac{\rho_{\Lambda}^{2}}{2(1-\rho_{\Lambda}^{2})^{2}} + \frac{3}{(1-\rho_{\Lambda}^{2})} = \frac{3(1-\rho_{\Lambda}^{2})^{2}+\rho_{\Lambda}^{2}}{(1-\rho_{\Lambda}^{2})^{3}}.$$

$$(45)$$

Then, the term T_2 holds from (11) and (12) that:

$$T_{2} = \sum_{t=j+1}^{T-1} \left(H_{\Lambda}^{(t,j)} + \frac{11}{10} H^{(t,j+1)} \right)$$

$$\leq \frac{11}{10} \sum_{m=1}^{T-j-1} \left((m^{2}+1)\rho_{\Lambda}^{2m} + \left(\frac{\rho_{\Lambda}m}{1-\rho_{\Lambda}} + 1 \right) \frac{\rho_{\Lambda}^{m}}{1-\rho_{\Lambda}} + ((m-1)^{2}+1)\rho_{\Lambda}^{2(m-1)} + \left(\frac{\rho_{\Lambda}(m-1)}{1-\rho_{\Lambda}} + 1 \right) \frac{\rho_{\Lambda}^{(m-1)}}{1-\rho_{\Lambda}} \right)$$

$$\leq \frac{11}{5} \sum_{m=0}^{T-j-1} \left((m^{2}+1)\rho_{\Lambda}^{2m} + \left(\frac{\rho_{\Lambda}m}{1-\rho_{\Lambda}} + 1 \right) \frac{\rho_{\Lambda}^{m}}{1-\rho_{\Lambda}} \right)$$

$$\leq \frac{11}{5} \left(\frac{\rho_{\Lambda}^{2}(1+\rho_{\Lambda}^{2})}{(1-\rho_{\Lambda}^{2})^{3}} + \frac{1}{1-\rho_{\Lambda}^{2}} + \frac{\rho_{\Lambda}^{2}}{(1-\rho_{\Lambda})^{4}} + \frac{1}{(1-\rho_{\Lambda})^{2}} \right) \leq \frac{22}{5} \cdot \frac{1+3\rho_{\Lambda}^{4}}{(1-\rho_{\Lambda}^{2})^{3}(1-\rho_{\Lambda})}.$$

$$(46)$$

The term T_3 holds from (11) and (12) that:

$$T_{3} = \sum_{t=j}^{T-1} H_{\Lambda}^{(t,j)} = \sum_{t=j}^{T-1} \left(((t-j)^{2} + 1)\rho_{\Lambda}^{2(t-j)} + \left(\frac{\rho_{\Lambda}(t-j)}{1 - \rho_{\Lambda}} + 1 \right) \frac{\rho_{\Lambda}^{t-j}}{1 - \rho_{\Lambda}} \right)$$

$$= \sum_{m=0}^{T-j-1} \left((m^{2} + 1)\rho_{\Lambda}^{2m} + \left(\frac{\rho_{\Lambda}m}{1 - \rho_{\Lambda}} + 1 \right) \frac{\rho_{\Lambda}^{m}}{1 - \rho_{\Lambda}} \right)$$

$$\leq \left(\frac{\rho_{\Lambda}^{2}(1 + \rho_{\Lambda}^{2})}{(1 - \rho_{\Lambda}^{2})^{3}} + \frac{1}{1 - \rho_{\Lambda}^{2}} + \frac{\rho_{\Lambda}^{2}}{(1 - \rho_{\Lambda})^{4}} + \frac{1}{(1 - \rho_{\Lambda})^{2}} \right) \leq \frac{2(1 + 3\rho_{\Lambda}^{4})}{(1 - \rho_{\Lambda}^{2})^{3}(1 - \rho_{\Lambda})}$$

$$(47)$$

The last term T_4 holds from (11), (12), and (16) that:

$$T_{4} = \sum_{t=0}^{T-1} \sum_{j=1}^{t} \left(h_{\Lambda}^{(t,j)} + \frac{3}{2} c_{\lambda} \alpha^{2} \beta^{2} H_{\Lambda}^{(t,j)} \right)$$

$$= \sum_{t=0}^{T-1} \sum_{j=1}^{t} \left(((t-j)^{2} + 1) \rho_{\Lambda}^{2(t-j)} + \frac{3}{2} c_{\lambda} \alpha^{2} \beta^{2} \left(((t-j)^{2} + 1) \rho_{\Lambda}^{2(t-j)} + \left(\frac{\rho_{\Lambda}(t-j)}{1 - \rho_{\Lambda}} + 1 \right) \frac{\rho_{\Lambda}^{t-j}}{1 - \rho_{\Lambda}} \right) \right)$$

$$= \sum_{k=0}^{T-2} \sum_{t=k+1}^{T-1} \left((k^{2} + 1) \rho_{\Lambda}^{2k} + \frac{3}{2} c_{\lambda} \alpha^{2} \beta^{2} \left((k^{2} + 1) \rho_{\Lambda}^{2k} + \left(\frac{\rho_{\Lambda}k}{1 - \rho_{\Lambda}} + 1 \right) \frac{\rho_{\Lambda}^{k}}{1 - \rho_{\Lambda}} \right) \right)$$

$$= \sum_{k=0}^{T-2} (T - k - 2) \left((k^{2} + 1) \rho_{\Lambda}^{2k} + \frac{3}{2} c_{\lambda} \alpha^{2} \beta^{2} \left((k^{2} + 1) \rho_{\Lambda}^{2k} + \left(\frac{\rho_{\Lambda}k}{1 - \rho_{\Lambda}} + 1 \right) \frac{\rho_{\Lambda}^{k}}{1 - \rho_{\Lambda}} \right) \right)$$

$$\leq \left(\frac{\rho_{\Lambda}^{2} (1 + \rho_{\Lambda}^{2})}{(1 - \rho_{\Lambda}^{2})^{3}} + \frac{1}{1 - \rho_{\Lambda}^{2}} + \frac{3}{2} c_{\lambda} \alpha^{2} \beta^{2} \left(\frac{\rho_{\Lambda}^{2} (1 + \rho_{\Lambda}^{2})}{(1 - \rho_{\Lambda}^{2})^{3}} + \frac{1}{1 - \rho_{\Lambda}^{2}} + \frac{1}{(1 - \rho_{\Lambda})^{2}} \right) \right) T$$

$$\leq \frac{1 + \rho_{\Lambda}^{2}}{(1 - \rho_{\Lambda}^{2})^{3}} + \frac{3c_{\lambda} \alpha^{2} \beta^{2} (1 + 3\rho_{\Lambda}^{4})}{(1 - \rho_{\Lambda}^{2})^{3} (1 - \rho_{\Lambda})}$$

For simplicity of notation, we denote $A(\rho_{\Lambda}) := \frac{1 + \rho_{\Lambda}^2}{(1 - \rho_{\Lambda}^2)^3}$ and $B(\rho_{\Lambda}) := \frac{2(1 + 3\rho_{\Lambda}^4)}{(1 - \rho_{\Lambda}^2)^3(1 - \rho_{\Lambda})}$. Plugging (45), (46), (47),

and (48) into (44), then we can derive:

$$\sum_{t=0}^{T-1} \mathbb{E}\left[\left\|E_{\text{II}}^{(t)}\right\|_{F,\lambda}^{2}\right] \leq \frac{18(1-\rho_{\Lambda}^{2})^{2}+6\rho_{\Lambda}^{2}}{(1-\rho_{\Lambda}^{2})^{3}} \left\|E_{\text{II}}^{(0)}\right\|_{F,\lambda}^{2} + 60\alpha^{2}\beta^{2}B(\rho_{\Lambda}) \sum_{t=0}^{T-1} \mathbb{E}\left[\left\|(I-\Lambda)\Theta^{(t)}\right\|_{F,\lambda}^{2}\right] + 2n\alpha^{2}B(\rho_{\Lambda}) \sum_{j=0}^{T-1} \mathbb{E}\left[\left\|\nabla F(\overline{\theta}_{\lambda}^{(t)})\right\|^{2}\right] + 18n\alpha^{2}v^{2} \left(A(\rho_{\Lambda}) + \frac{3}{2}c_{\lambda}\alpha^{2}\beta^{2}B(\rho_{\Lambda})\right)T.$$
(49)

Rearranging (49) and using that $\|(I - \Lambda)\Theta^{(t)}\|_{F,\lambda}^2 \leq \|E_{II}^{(t)}\|_{F,\lambda}^2$, we can derive

$$(1 - 60\alpha^{2}\beta^{2}B(\rho_{\Lambda})) \sum_{t=0}^{T-1} \mathbb{E}\left[\left\| E_{\text{II}}^{(t)} \right\|_{F,\lambda}^{2} \right] \leq \frac{18(1 - \rho_{\Lambda}^{2})^{2} + 6\rho_{\Lambda}^{2}}{(1 - \rho_{\Lambda}^{2})^{3}} \left\| E_{\text{II}}^{(0)} \right\|_{F,\lambda}^{2} + 2n\alpha^{2}B(\rho_{\Lambda}) \sum_{j=0}^{T-1} \mathbb{E}\left[\left\| \nabla F(\overline{\theta}_{\lambda}^{(t)}) \right\|^{2} \right] + 18n\alpha^{2}v^{2} \left(A(\rho_{\Lambda}) + \frac{3}{2}c_{\lambda}\alpha^{2}\beta^{2}B(\rho_{\Lambda}) \right) T.$$

Thus, Eq. (5) holds.

Proof of Strategy I. The modification is purely mechanical: replace ρ_{Λ} with ρ_{J} , multiply the summation term by λ_{\max}^{2} , and multiply the E'_{0} term by κ_{λ} . The derivation mirrors the previous case and is omitted for brevity. The resulting expression is:

$$(1 - 60\lambda_{\max}^{2} \alpha^{2} \beta^{2} B(\rho_{J})) \sum_{t=0}^{T-1} \mathbb{E} \left[\left\| E_{\mathbf{I}}^{(t)} \right\|_{F,\lambda}^{2} \right]$$

$$\leq \frac{18(1 - \rho_{J}^{2})^{2} + 6\rho_{J}^{2}}{(1 - \rho_{J}^{2})^{3}} \kappa_{\lambda} \left\| E_{\mathbf{I}}^{(0)} \right\|_{F,\lambda}^{2} + 2n\lambda_{\max}^{2} \alpha^{2} B(\rho_{J}) \sum_{j=0}^{T-1} \mathbb{E} \left[\left\| \nabla F(\overline{\theta}^{(t)}) \right\|_{F,\lambda}^{2} \right]$$

$$+ 18n\lambda_{\max}^{2} \alpha^{2} v^{2} \left(A(\rho_{J}) + \frac{3}{2} c_{\lambda} \alpha^{2} \beta^{2} B(\rho_{J}) \right) T.$$

Thus Eq. (4) also holds. We finish the proof of Proposition 6.4.

Proof of step size. We show that the two upper bounds of the step size satisfy $M_1(\rho) > M_2(\rho)$ for all $0 < \rho < 1$, where

$$M_1(\rho) = \frac{1}{9} \sqrt{\frac{3(1-\rho)}{2-\rho}}, \qquad M_2(\rho) = \frac{1}{2} \sqrt{\frac{1}{15B(\rho)}}, \quad B(\rho) = \frac{2(1+3\rho^4)}{(1-\rho^2)^3(1-\rho)}.$$

Since both terms are positive, it suffices to show $[M_1(\rho)]^2 > [M_2(\rho)]^2$. Direct computation yields

$$[M_1(\rho)]^2 = \frac{1-\rho}{27(2-\rho)}, \qquad [M_2(\rho)]^2 = \frac{(1-\rho^2)^3(1-\rho)}{120(1+3\rho^4)}.$$

Hence

$$[M_1(\rho)]^2 - [M_2(\rho)]^2 = (1 - \rho) \left[\frac{1}{27(2 - \rho)} - \frac{(1 - \rho^2)^3}{120(1 + 3\rho^4)} \right] = \frac{(1 - \rho)Q(\rho)}{1080(2 - \rho)(1 + 3\rho^4)},$$

where

$$Q(\rho) = -9\rho^7 + 18\rho^6 + 27\rho^5 + 66\rho^4 - 27\rho^3 + 54\rho^2 + 9\rho + 22.$$

Since the denominator is positive on (0,1), it suffices to check $Q(\rho) > 0$. Noting that $\rho^7 < \rho^6$ and $\rho^3 < \rho^2$ for $0 < \rho < 1$, we have

$$Q(\rho) > 9\rho^6 + 27\rho^5 + 66\rho^4 + 27\rho^2 + 9\rho + 22 > 0.$$

Thus, $M_1(\rho) > M_2(\rho)$ holds for all $0 < \rho < 1$. Consequently, the step size α should satisfy

$$\alpha < \frac{1}{\lambda_{\max}\beta} \min \left\{ \frac{1}{9} \sqrt{\frac{3(1-\rho_J)}{2-\rho_J}}, \frac{1}{2} \sqrt{\frac{1}{15B(\rho_J)}} \right\} = \frac{1}{2\lambda_{\max}\beta} \sqrt{\frac{1}{15B(\rho_J)}},$$

for Strategy I, and

$$\alpha < \frac{1}{\beta} \min \left\{ \frac{1}{9} \sqrt{\frac{3(1-\rho_{\Lambda})}{2-\rho_{\Lambda}}}, \frac{1}{2} \sqrt{\frac{1}{15B(\rho_{\Lambda})}} \right\} = \frac{1}{2\beta} \sqrt{\frac{1}{15B(\rho_{\Lambda})}},$$

for Strategy II.

B.4. Obtaining of the final convergence error.

In this subsection, we combine the consensus error analysis and the single-step convergence analysis and present the final convergence error and complete the proof of Theorem 6.5.

The following lemma present the convergence rate under Strategy II.

Lemma B.17 (Convergence rate under Strategy II). Suppose Assumptions 6.1–6.3 are all hold and the step-size $\alpha < \frac{1}{\beta} \sqrt{\frac{1}{62B(\rho_{\Lambda})}}$, then

$$\frac{1}{T} \sum_{t=0}^{T-1} \mathbb{E} \left[\|\nabla F(\overline{\theta}_{\lambda}^{(t)})\|^{2} \right] \leq \frac{2[F(\overline{\theta}_{\lambda}^{(0)}) - F(\theta^{*})]}{\alpha C_{2}T} + \frac{6[3(1 - \rho_{\Lambda}^{2})^{2} + \rho_{\Lambda}^{2}]\beta^{2}}{(1 - \rho_{\Lambda}^{2})^{3} C_{1} C_{2} n T} \left\| E_{\text{II}}^{(0)} \right\|_{F,\lambda}^{2} + \frac{\alpha c_{\lambda} \beta v^{2}}{C_{2}} + \frac{18\alpha^{2} \beta^{2} v^{2}}{C_{1} C_{2}} \left(A(\rho_{\Lambda}) + \frac{3}{2} c_{\lambda} \alpha^{2} \beta^{2} B(\rho_{\Lambda}) \right),$$

where
$$C_2 = 1 - \frac{2\alpha^2 \beta^2 B(\rho_{\Lambda})}{C_1} > 0$$
.

Proof. By taking the summation on both sides of (22) from t = 0 to T - 1 and use (28), we can derive:

$$\begin{split} \frac{1}{T} \sum_{t=0}^{T-1} \mathbb{E} \left[\| \nabla F(\overline{\theta}_{\lambda}^{(t)}) \|^2 \right] &\leq \frac{2}{\alpha T} \sum_{t=0}^{T-1} \left(\mathbb{E} \left[F(\overline{\theta}_{\lambda}^{(t)}) \right] - \mathbb{E} \left[F(\overline{\theta}_{\lambda}^{(t+1)}) \right] \right) + \frac{\beta^2}{n T} \sum_{t=0}^{T-1} \mathbb{E} \left[\| (I - \Lambda) \Theta^{(t)} \|_{F, \lambda}^2 \right] + \alpha c_{\lambda} \beta v^2 \\ &\leq \frac{2 [F(\overline{\theta}_{\lambda}^{(0)}) - F(\theta^*)]}{\alpha T} + \frac{\beta^2}{n T} \sum_{t=0}^{T-1} \mathbb{E} \left[\| E_{\text{II}}^{(t)} \|_{F, \lambda}^2 \right] + \alpha c_{\lambda} \beta v^2 \\ &\leq \frac{2 [F(\overline{\theta}_{\lambda}^{(0)}) - F(\theta^*)]}{\alpha T} + \frac{6 [3 (1 - \rho_{\Lambda}^2)^2 + \rho_{\Lambda}^2] \beta^2}{(1 - \rho_{\Lambda}^2)^3 C_1 n T} \left\| E_{\text{II}}^{(0)} \right\|_{F, \lambda}^2 + \alpha c_{\lambda} \beta v^2 \\ &+ \frac{2 \alpha^2 \beta^2 B(\rho_{\Lambda})}{C_1 T} \sum_{j=0}^{T-1} \mathbb{E} \left[\| \nabla F(\overline{\theta}_{\lambda}^{(t)}) \|^2 \right] + \frac{18 \alpha^2 \beta^2 v^2}{C_1} \left[A(\rho_{\Lambda}) + \frac{3}{2} c_{\lambda} \alpha^2 \beta^2 B(\rho_{\Lambda}) \right]. \end{split}$$

Then it follows that:

$$\begin{split} & \left(1 - \frac{2\alpha^2\beta^2B(\rho_{\Lambda})}{C_1}\right)\frac{1}{T}\sum_{t=0}^{T-1}\mathbb{E}\left[\left\|\nabla F(\overline{\theta}_{\lambda}^{(t)})\right\|^2\right] \\ & \leq & \frac{2[F(\overline{\theta}_{\lambda}^{(0)}) - F(\theta^*)]}{\alpha T} + 18\alpha^2\beta^2v^2\left(A(\rho_{\Lambda}) + \frac{3}{2}c_{\lambda}\alpha^2\beta^2B(\rho_{\Lambda})\right) + \alpha c_{\lambda}\beta v^2 + \frac{6[3(1-\rho_{\Lambda}^2)^2 + \rho_{\Lambda}^2]\beta^2}{(1-\rho_{\Lambda}^2)^3C_1nT}\left\|E_{\text{II}}^{(0)}\right\|_{F,\lambda}^2, \end{split}$$
 which yields Eq. (7).

Similarly, we can present the following lemma to present the convergence rate under Strategy I.

Lemma B.18 (Convergence rate under Strategy I). Suppose Assumptions 6.1–6.3 are all hold and the step-size $\alpha < \frac{1}{\lambda_{\max}\beta}\sqrt{\frac{1}{62B(\rho_J)}}$, then

$$\frac{1}{T} \sum_{t=0}^{T-1} \mathbb{E}[\|\nabla F(\overline{\theta}^{(t)})\|^{2}] \leq \frac{2[F(\overline{\theta}^{(0)}) - F(\theta^{\star})]}{\alpha C_{2}^{\prime} T} + \frac{6\kappa_{\lambda}[3(1-\rho_{J}^{2})^{2} + \rho_{J}^{2}]\beta^{2}}{(1-\rho_{J}^{2})^{3} C_{1}^{\prime} C_{2}^{\prime} n T} \|E_{I}^{(0)}\|_{F,\lambda}^{2} + \frac{\alpha c_{\lambda} \beta v^{2}}{C_{2}^{\prime}} + \frac{18\lambda_{\max}^{2} \alpha^{2} \beta^{2} v^{2}}{C_{1}^{\prime} C_{2}^{\prime}} \left(A(\rho_{J}) + \frac{3}{2}c_{\lambda} \alpha^{2} \beta^{2} B(\rho_{J})\right),$$

where
$$C_2' = 1 - \frac{2\lambda_{\max}^2 \alpha^2 \beta^2 B(\rho_J)}{C_1'} > 0.$$

B.5. Proof of Corollary 6.6

Proof. According to (6) and (7), the convergence rate for both strategies under uniform weight can be given as:

$$\frac{1}{T} \sum_{t=0}^{T-1} \mathbb{E}[\|\nabla F(\overline{\theta}^{(t)})\|^{2}] \leq \frac{2[F(\overline{\theta}^{(0)}) - F(\theta^{\star})]}{\alpha C_{2}T} + \frac{6[3(1 - \rho_{J}^{2})^{2} + \rho_{J}^{2}]\beta^{2}}{(1 - \rho_{J}^{2})^{3} C_{1} C_{2} n T} \|E_{I}^{(0)}\|_{F, \lambda}^{2} + \frac{\alpha \beta v^{2}}{n C_{2}} + \frac{18\alpha^{2}\beta^{2}v^{2}}{C_{1}C_{2}} \left(A(\rho_{J}) + \frac{3}{2n}\alpha^{2}\beta^{2}B(\rho_{J})\right).$$

We first consider the terms C_1 and C_2 , we set:

$$C_1 = 1 - 60\alpha^2 \beta^2 B(\rho_J) \ge \frac{1}{2} \text{ and } C_2 = 1 - \frac{2\alpha^2 \beta^2 B(\rho_J)}{C_1} \ge \frac{1}{2} \implies \alpha \le \frac{1}{2\beta} \sqrt{\frac{1}{30B(\rho_J)}}.$$

Then, we let $\Delta = F(\overline{\theta}^{(0)}) - F(\theta^*)$ and define

$$\alpha_1 = \left(\frac{2n\Delta}{\beta v^2 T}\right)^{\frac{1}{2}}, \quad \alpha_2 = \left(\frac{n\Delta}{18\beta v^2 A(\rho_J) T}\right)^{\frac{1}{3}}, \quad \alpha_3 = \left(\frac{n\Delta}{27\beta^4 v^2 B(\rho_\Lambda) T}\right)^{\frac{1}{5}}.$$

If we set

$$\alpha := \frac{1}{\frac{1}{\alpha_1} + \frac{1}{\alpha_2} + \frac{1}{\alpha_3} + 2\beta\sqrt{30B(\rho_J)}},$$

we can obtain the following convergence rate:

$$\begin{split} \frac{1}{T} \sum_{t=0}^{T-1} \mathbb{E}[\|\nabla F(\overline{\theta}^{(t)})\|^2] \leq & \frac{4\Delta}{T} \left(\frac{1}{\alpha_1} + \frac{1}{\alpha_2} + \frac{1}{\alpha_3} + 2\beta\sqrt{30B(\rho_J)} \right) + \frac{2\alpha_1\beta v^2}{n} + 72\alpha_2^2\beta^2 v^2 A(\rho_J) + \frac{108\alpha_3^4\beta^4 v^2 B(\rho_J)}{n} \\ & + \frac{24[3(1-\rho_J^2)^2 + \rho_J^2]\beta^2}{(1-\rho_J^2)^3 nT} \|E_{\mathrm{I}}^{(0)}\|_{F,\lambda}^2 \\ \lesssim_{n,T} \frac{1}{\sqrt{nT}}. \end{split}$$

Thus, we finish the proof of this corollary.

C. Missing proofs in the comparison for the convergence under two strategies

In this section, we present the missing proofs in Section 7, which are used for the comparsion of the convergence rate of Algorithm 1 under two communication strategies.

C.1. Proof of Theorem 7.1

Proof. As all nodes share the same initial states in Algorithm 1, we have $\overline{\theta}_{\lambda}^{(0)} = \overline{\theta}^{(0)}$ and $\|E_{\mathrm{I}}^{(0)}\|_{F,\lambda} = \|E_{\mathrm{II}}^{(0)}\|_{F,\lambda}$. From the two convergence results, we obtain that strategy II achieves a faster convergence than strategy I if the following inequalities hold:

$$\lambda_{\max}^2 \frac{1 + 3\rho_J^4}{(1 - \rho_J^2)^3 (1 - \rho_J)} \ge \frac{1 + 3\rho_J^4}{(1 - \rho_\Lambda^2)^3 (1 - \rho_\Lambda)},\tag{50a}$$

$$\lambda_{\max}^{2} \frac{1 + \rho_{J}^{2}}{(1 - \rho_{J}^{2})^{3}} \ge \frac{1 + \rho_{\Lambda}^{2}}{(1 - \rho_{\Lambda}^{2})^{3}},$$

$$\kappa_{\lambda} \frac{3(1 - \rho_{J}^{2})^{2} + \rho_{J}^{2}}{(1 - \rho_{\Lambda}^{2})^{3}C_{1}} \ge \frac{3(1 - \rho_{\Lambda}^{2})^{2} + \rho_{\Lambda}^{2}}{(1 - \rho_{\Lambda}^{2})^{3}C_{1}}.$$
(50b)

It is clear that when $\rho_{\Lambda} \leq \rho_{J}$, the three inequalities hold trivially; thus we focus on the case $\rho_{\Lambda} > \rho_{J}$.

Analysis for inequality (50a). It can be obtained that:

$$(1 - \rho_{\Lambda})^4 \ge \frac{\phi_1(\rho_{\Lambda})}{\lambda_{\max}^2 \phi_1(\rho_J)} (1 - \rho_J)^4,$$

where $\phi_1(\rho) := \frac{1+3\rho^4}{(1+\rho^2)^3}$. We now study the monotonicity of $\phi_1(\rho)$ for $\rho \in (0,1)$. It holds that:

$$\phi_1'(\rho) = \frac{6\rho\left(-(\rho^2-1)^2\right)}{(1+\rho^2)^4} = -\frac{6\rho(\rho^2-1)^2}{(1+\rho^2)^4} < 0 \quad \text{for all } \rho \in (0,1),$$

which proves strict monotonic decrease. Since $\rho_{\Lambda} > \rho_{J}$, we obtain

$$(1 - \rho_{\Lambda})^4 \ge \frac{\phi_1(\rho_{\Lambda})}{\lambda_{\max}^2 \phi_1(\rho_J)} (1 - \rho_J)^4 \ge \frac{1}{\lambda_{\max}^2} (1 - \rho_J)^4 \implies (1 - \rho_{\Lambda}) \ge \lambda_{\max}^{-1/2} (1 - \rho_J).$$

Analysis for inequality (50b). Similarly, we obtain

$$(1 - \rho_{\Lambda})^3 \ge \frac{\phi_2(\rho_{\Lambda})}{\lambda_{\text{max}}^2 \phi_2(\rho_J)} (1 - \rho_J)^3,$$

where $\phi_2(\rho) = \frac{1+\rho^2}{(1+\rho)^3}$. Consider the differentiation of $\phi_2(\rho) = (1+\rho^2)(1+\rho)^{-3}$:

$$\phi_2'(\rho) = 2\rho(1+\rho)^{-3} - 3(1+\rho^2)(1+\rho)^{-4} = \frac{2\rho(1+\rho) - 3(1+\rho^2)}{(1+\rho)^4}.$$

The numerator simplifies to

$$2\rho(1+\rho) - 3(1+\rho^2) = 2\rho + 2\rho^2 - 3 - 3\rho^2 = -\left(\rho^2 - 2\rho + 3\right) = -\left((\rho - 1)^2 + 2\right) < 0,$$

and the denominator $(1 + \rho)^4 > 0$ for $\rho \in (0, 1)$. Hence $\phi_2'(\rho) < 0$ on (0, 1), proving strict monotone decrease. We can obtain

$$(1 - \rho_{\Lambda})^3 \ge \frac{\phi_2(\rho_{\Lambda})}{\lambda_{\max}^2 \phi_2(\rho_J)} (1 - \rho_J)^3 \ge \frac{1}{\lambda_{\max}^2} (1 - \rho_J)^3 \implies (1 - \rho_{\Lambda}) \ge \lambda_{\max}^{-2/3} (1 - \rho_J).$$

Analysis for inequality (50b). We have

$$(1 - \rho_{\Lambda})^3 \ge \frac{\phi_3(\rho_{\Lambda})}{\kappa_{\lambda}\phi_3(\rho_J)} (1 - \rho_J)^3,$$

where $\phi_3(\rho) = \frac{3(1-\rho^2)^2 + \rho^2}{(1+\rho)^3}$. Write $\phi_3(\rho) = u(\rho)(1+\rho)^{-3}$ with $u(\rho) = 3 - 5\rho^2 + 3\rho^4$. Then

$$\phi_3'(\rho) = \frac{u'(\rho)(1+\rho) - 3u(\rho)}{(1+\rho)^4} = \frac{H(\rho)}{(1+\rho)^4},$$

where

$$H(\rho) = 3\rho^4 + 12\rho^3 + 5\rho^2 - 10\rho - 9.$$

Since $(1+\rho)^4 > 0$ on (0,1), the sign of ϕ_3' equals that of H. We have

$$H''(\rho) = 36\rho^2 + 72\rho + 10 > 0$$
 for all $\rho \in (0, 1)$,

so H is strictly convex and hence has at most two zeros. Moreover, H(0) = -9 < 0 and H(1) = 1 > 0, implying a unique zero $\rho_{\star} \in (0,1)$. Numerically, $\rho_{\star} \approx 0.978609$. Therefore, $\phi_3'(\rho) < 0$ on $(0,\rho_{\star})$ and $\phi_3'(\rho) > 0$ on $(\rho_{\star},1)$.

Now we consider the Bounds and extremum: $\phi_3(0)=3$, $\phi_3(1)=\frac{1}{8}$, and $\phi_3(\rho_\star)\approx 0.124328<\frac{1}{8}$. Consequently,

$$\phi_3(\rho) \in (\phi_3(\rho_*), 3] \subset (0.1243, 3]$$
 for $\rho \in (0, 1)$.

Therefore, we can derive:

$$\sup_{0<\rho_J<\rho_\Lambda<1} \frac{\phi_3(\rho_\Lambda)}{\phi_3(\rho_J)} = \frac{\phi_3(1)}{\phi_3(\rho_\star)} = \frac{1/8}{0.12432794} \approx 1.00541,$$

yielding that

$$(1 - \rho_{\Lambda})^{3} \ge \frac{\phi_{3}(\rho_{\Lambda})}{\kappa_{\lambda}\phi_{3}(\rho_{J})}(1 - \rho_{J})^{3} \ge \frac{(1 + \eta)^{3}}{\kappa_{\lambda}}(1 - \rho_{J})^{3} \implies (1 - \rho_{\Lambda}) \ge (1 + \eta)\kappa_{\lambda}^{-1/3}(1 - \rho_{J}).$$

where

$$\eta := \sup_{0 < \rho_J < \rho_\Lambda < 1} \left(\frac{\phi_3(\rho_\Lambda)}{\phi_3(\rho_J)} \right)^{1/3} - 1 \approx 1.8 \times 10^{-3}.$$

In summary, we obtain the final condition under which Strategy II converges faster than Strategy I as:

$$(1 - \rho_{\Lambda}) \ge \max \left\{ (1 + \eta) \kappa_{\lambda}^{-1/3}, \ \lambda_{\max}^{-1/2} \right\} (1 - \rho_{J}).$$

C.2. Proof of Theorem 7.2

Proof. We first consider the matrix \widetilde{W} obtained from W via a similarity transformation, $\widetilde{W} := D_{\lambda}^{1/2}WD_{\lambda}^{-1/2}$, where $D_{\lambda} = \operatorname{diag}(\lambda_1, \dots, \lambda_n)$. By construction, \widetilde{W} and W share the same spectrum. We can get the entries of \widetilde{W} as

$$\widetilde{W}_{i,j} = \begin{cases} W_{i,i} & \text{if } i = j \\ \frac{1-\varepsilon}{d_i} \sqrt{\frac{\lambda_i}{\lambda_j}} \min\left(1, \frac{\lambda_j d_i}{\lambda_i d_j}\right) & \text{if } i \neq j \text{ and } j \in \mathcal{N}_i \\ 0 & \text{otherwise}. \end{cases}$$

We then define the Laplacian matrix as

$$\mathcal{L}(\lambda) := I - \widetilde{W},$$

whose elements can be given by:

$$\mathcal{L}(\lambda)_{i,j} = \begin{cases} -\widetilde{W}_{i,j} & \text{if } i \neq j, \\ 1 - \widetilde{W}_{i,i} = \sum_{k \neq i} \widetilde{W}_{i,k} & \text{if } i = j. \end{cases}$$

It follows that the spectrum of \mathcal{L} satisfies

$$\sigma(\mathcal{L}(\lambda)) = 1 - \sigma(\widetilde{W}) = 1 - \sigma(W) \ge 0.$$

Moreover, we note that $|\sigma_{\min}(W)| \leq |\sigma_2(W)|$, and thus the second largest eigenvalue in absolute value of W corresponds to the second smallest eigenvalue of $\mathcal{L}(\lambda)$, i.e., $1-\sigma_2(W)=\sigma_{n-1}(\mathcal{L}(\lambda))$. According to the Courant–Fischer theorem, the variational characterization of \widetilde{W} can be expressed in terms of the Rayleigh quotient (Mohar et al., 1991; Chung, 1997). In particular, the second smallest eigenvalue corresponds to the minimum Rayleigh quotient over the subspace orthogonal to the trivial eigenvector, which is $D_{\lambda}^{\frac{1}{2}}$:

$$\mathcal{L}(\lambda)D_{\lambda}^{1/2}\mathbf{1} = (I - D_{\lambda}^{1/2}WD_{\lambda}^{-1/2})D_{\lambda}^{1/2}\mathbf{1} = D_{\lambda}^{1/2}\mathbf{1} - D_{\lambda}^{1/2}W\mathbf{1} = 0.$$

For the weighted case, this yields:

$$\sigma_{n-1}(\mathcal{L}(\lambda)) = \inf_{\substack{z \neq 0 \\ \langle z, D_{\lambda}^{1/2} \mathbf{1} \rangle = 0}} \frac{z^{\top} \mathcal{L}(\lambda) z}{\|z\|_{2}^{2}}, \quad \forall z \in \mathbb{R}^{n},$$
(51)

whereas in the uniform-weight case $(\lambda \equiv 1)$ we have

$$\sigma_{n-1}(\mathcal{L}(\mathbf{1})) = \inf_{\substack{z' \neq 0 \\ \langle z', \mathbf{1} \rangle = 0}} \frac{z'^{\top} \mathcal{L}(\mathbf{1}) z'}{\|z'\|_2^2}, \qquad z' \in \mathbb{R}^n.$$
 (52)

The quadratic form $z^{\top} \mathcal{L}(\lambda)z$ can be expanded as follows:

$$z^{\top} \mathcal{L}(\lambda) z = \sum_{i,j} z_i \mathcal{L}(\lambda)_{i,j} z_j = \sum_{i} z_i^2 \mathcal{L}(\lambda)_{i,i} + \sum_{i \neq j} z_i \mathcal{L}(\lambda)_{i,j} z_j$$
$$= \sum_{i} z_i^2 \sum_{j \neq i} \widetilde{W}_{i,j} - \sum_{i \neq j} z_i \widetilde{W}_{i,j} z_j = \sum_{i \neq j} \widetilde{W}_{i,j} z_i^2 - \sum_{i \neq j} \widetilde{W}_{i,j} z_i z_j.$$

By interchanging the summation indices, we obtain

$$\sum_{i \neq j} \widetilde{W}_{i,j} z_i^2 = \sum_{i \neq j} \widetilde{W}_{j,i} z_j^2,$$

which leads to

$$z^{\top} \mathcal{L}(\lambda) z = \frac{1}{2} \sum_{i} \sum_{j \neq i} \sum_{i \neq j} (\widetilde{W}_{i,j} z_{i}^{2} + \widetilde{W}_{j,i} z_{j}^{2}) - \sum_{i \neq j} \widetilde{W}_{i,j} z_{i} z_{j} = \frac{1}{2} \sum_{i \neq j} \widetilde{W}_{i,j} (z_{i}^{2} + z_{j}^{2}) - \sum_{i \neq j} \widetilde{W}_{i,j} z_{i} z_{j}$$

$$= \frac{1}{2} \sum_{i \neq j} \widetilde{W}_{i,j} (z_{i}^{2} + z_{j}^{2} - 2z_{i} z_{j}) = \frac{1}{2} \sum_{i \neq j} \widetilde{W}_{i,j} (z_{i} - z_{j})^{2},$$
(53)

where the symmetry property of \widetilde{W} is utilized, i.e., $\widetilde{W}_{j,i} = \widetilde{W}_{i,j}$. For simplicity ,we denote $R = \max\left\{(1+\eta)\kappa_{\lambda}^{-1/3},\ \lambda_{\max}^{-1/2}\right\}$.

According to (51) and (52), we have

$$\inf_{\substack{z\neq 0\\ \langle z, D_1^{1/2}\mathbf{1}\rangle = 0}} \frac{z^\top \mathcal{L}(\lambda)z}{\|z\|_2^2} \geq R \inf_{\substack{z'\neq 0\\ \langle z', \mathbf{1}\rangle = 0}} \frac{z'^\top \mathcal{L}(\mathbf{1})z'}{\|z'\|_2^2} \iff \sigma_{n-1}(\mathcal{L}(\lambda)) \geq R \cdot \sigma_{n-1}(\mathcal{L}(\mathbf{1})).$$

By substituting the explicit form of the quadratic terms and noting that $1 - \rho_{\Lambda} = \sigma_{n-1}(\mathcal{L}(\lambda))$ and $1 - \rho_{J} = \sigma_{n-1}(\mathcal{L}(\mathbf{1}))$, we obtain the necessary and sufficient condition of $\rho_{\Lambda} \leq \rho_{J}$:

$$\inf_{\substack{z\neq 0\\ \langle z, D_{\lambda}^{1/2}\mathbf{1}\rangle = 0}} \frac{\sum_{i,j} \min\left\{\frac{1}{d_i} \sqrt{\frac{\lambda_i}{\lambda_j}}, \frac{1}{d_j} \sqrt{\frac{\lambda_j}{\lambda_i}}\right\} (z_i - z_j)^2}{\|z\|_2^2} \geq R\inf_{\substack{z'\neq 0\\ \langle z', \mathbf{1}\rangle}} \frac{\sum_{i,j} \min\left\{\frac{1}{d_i}, \frac{1}{d_j}\right\} (z_i' - z_j')^2}{\|z'\|_2^2},$$

which yields the final result.

C.3. Proof of Corollary 7.3

Proof. We consider the Loewner order (Horn & Johnson, 2012) between the two Laplacian matrices $\mathcal{L}(\lambda)$ and $R\mathcal{L}(1)$

$$\mathcal{L}(\lambda) \succeq R\mathcal{L}(1) \tag{54}$$

holds, which means that the matrix difference $\mathcal{L}(\lambda) - R\mathcal{L}(1)$ is positive semi-definite, then by standard eigenvalue monotonicity under the Loewner order (Fan, 1949) we have

$$\sigma_i(\mathcal{L}(\lambda)) \geq R\sigma_i(\mathcal{L}(\mathbf{1})), \quad \forall i = 1, \dots, n.$$

In particular,

$$1 - \rho_{\Lambda} = \sigma_{n-1}(\mathcal{L}(\lambda)) \ge R\sigma_{n-1}(\mathcal{L}(\mathbf{1})) = R(1 - \rho_J),$$

which implies $\rho_{\Lambda} \leq \rho_{J}$ and yields exactly the scaled spectral-gap relation required in Theorem 7.1.

It remains to translate the Loewner-order relation (54) into conditions on the node degrees and weights. By definition of the semidefinite order.

$$\mathcal{L}(\lambda) \succeq R \cdot \mathcal{L}(\mathbf{1}) \iff z^{\top} \left[\mathcal{L}(\lambda) - R \cdot \mathcal{L}(\mathbf{1}) \right] z \geq 0 \quad \forall z \in \mathbb{R}^n$$

Substituting the quadratic-form representation (53) into the above inequality yields a sufficient condition that can be checked elementwise:

$$\min\left\{\frac{1}{d_i}\sqrt{\frac{\lambda_i}{\lambda_j}}, \frac{1}{d_j}\sqrt{\frac{\lambda_j}{\lambda_i}}\right\} \ge R\min\left\{\frac{1}{d_i}, \frac{1}{d_j}\right\}, \qquad \forall i, j.$$
 (55)

Let $r:=\sqrt{\lambda_i/\lambda_j}$ and define

$$I(r) := \min \left\{ \frac{r}{d_i}, \frac{1}{rd_j} \right\}.$$

Then (55) is equivalent to

$$I(r) \ge R \min \left\{ \frac{1}{d_i}, \frac{1}{d_j} \right\}.$$

We now analyze the range of r for which this inequality holds.

Case 1: $d_i \ge d_j$. In this case, $\min\{1/d_i, 1/d_j\} = 1/d_i$, and I(r) is piecewise:

$$I(r) = \begin{cases} \frac{r}{d_i}, & r \leq \frac{d_i}{d_j}, \\ \frac{1}{rd_j}, & r \geq \frac{d_i}{d_j}. \end{cases}$$

The inequality $I(r) \ge R/d_i$ holds if and only if

$$\frac{r}{d_i} \ge \frac{R}{d_i}$$
 and $\frac{1}{rd_j} \ge \frac{R}{d_i}$,

which simplifies to

$$R \le r \le \frac{d_i}{Rd_j}.$$

Case 2: $d_i < d_j$. Now $\min\{1/d_i, 1/d_j\} = 1/d_j$, and a symmetric argument shows that $I(r) \ge R/d_j$ holds if and only if

$$\frac{Rd_i}{d_j} \le r \le \frac{1}{R}.$$

Combining the two cases yields the unified condition

$$R\min\left\{\frac{d_i}{d_j},1\right\} \le r \le R^{-1}\max\left\{\frac{d_i}{d_j},1\right\} \implies R\min\left\{\frac{d_i}{d_j},1\right\} \le \sqrt{\frac{\lambda_i}{\lambda_j}} \le R^{-1}\max\left\{\frac{d_i}{d_j},1\right\},$$

which is exactly (10). This proves the sufficient condition for $1 - \rho_{\Lambda} \ge R(1 - \rho_{J})$.

Finally, we show that the spectral gap of W is maximized when λ is proportional to the degree vector d. This corresponds to maximizing the edge weights, or equivalently maximizing I(r) with respect to r > 0. Since

$$I(r) = \min\left\{\frac{r}{d_i}, \frac{1}{rd_i}\right\},\,$$

the two branches intersect when

$$\frac{r}{d_i} = \frac{1}{rd_j} \Longleftrightarrow r^2 = \frac{d_i}{d_j} \Longleftrightarrow r^* = \sqrt{\frac{d_i}{d_j}}.$$

At this point,

$$I(r^{\star}) = \frac{1}{\sqrt{d_i d_j}},$$

which is the maximum possible value of I(r) over r > 0. In terms of λ , this corresponds exactly to

$$\frac{\lambda_i}{\lambda_j} = (r^*)^2 = \frac{d_i}{d_j},$$

i.e., λ is proportional to d. This proves the "moreover" part of the corollary.

D. Details of Algorithm 2

This appendix provides the pseudocode of the four subroutines used in Algorithm 2. SCALETODEGREES rescales the weight vector into an integer degree sequence with an even total sum. HAVELHAKIMICONSTRUCT attempts to realize this degree sequence as a simple graph via a Havel—Hakimi procedure. MAKECONNECTED then applies degree-preserving edge swaps to connect different components while keeping all node degrees fixed. Finally, FALLBACKCONNECTEDGRAPH gives a simple ring-based construction used when the previous steps fail to produce a connected realization.

Algorithm 3 SCALETODEGREES

```
Require: Weight vector \lambda = (\lambda_1, \dots, \lambda_n), target average degree \bar{d}

Ensure: Integer degree sequence d_1, \dots, d_n

1: S \leftarrow nearest even integer to n\bar{d}

2: c \leftarrow S/\sum_{i=1}^n \lambda_i

3: for i=1 to n do

4: d_i \leftarrow \operatorname{round}(c\lambda_i)

5: d_i \leftarrow \min\{n-1, \max\{1, d_i\}\} {clip to [1, n-1]}

6: end for

7: if \sum_{i=1}^n d_i is odd then

8: Choose an index k with 1 \leq d_k < n-1

9: d_k \leftarrow d_k + 1 {make the total degree sum even}

10: end if

11: return (d_1, \dots, d_n)
```

Algorithm 4 HAVELHAKIMICONSTRUCT

```
Require: Degree sequence d_1, \ldots, d_n with even total sum
Ensure: Simple graph \mathcal{G}_{\lambda} = (\mathcal{V}, \mathcal{E}_{\lambda}) realizing d or failure
 1: \mathcal{V} \leftarrow \{1, \dots, n\}, \mathcal{E}_{\lambda} \leftarrow \emptyset
 2: rem \leftarrow \{(d_i, i) : i = 1, \dots, n\} {residual degrees}
 3: while some vertex has positive residual degree do
        Sort rem in non-increasing order by residual degree
        (r, u) \leftarrow first element of rem; remove it from rem
 5:
        if r > |\text{rem}| then
 6:
           fail {degree sequence is not graphical}
 7:
 8:
        Let (v_1, \ldots, v_r) be the indices of the r vertices in rem with largest residual degrees such that (u, v_i) \notin \mathcal{E}_{\lambda} for all j
 9:
        if fewer than r such vertices exist then
10:
11:
           fail {cannot add edges without violating simplicity}
        end if
12:
        for j = 1 to r do
13:
14:
           Add edge (u, v_i) to \mathcal{E}_{\lambda}
15:
           Decrease the residual degree of v_i in rem by 1
16:
           if some residual degree becomes negative then
               fail
17:
           end if
18:
        end for
19:
20: end while
21: return \mathcal{G}_{\lambda} = (\mathcal{V}, \mathcal{E}_{\lambda})
```

Algorithm 5 MAKECONNECTED

```
Require: Simple graph \mathcal{G}_{\lambda} = (\mathcal{V}, \mathcal{E}_{\lambda}) realizing the target degrees
Ensure: Connected simple graph \mathcal{G}'_{\lambda} = (\mathcal{V}, \mathcal{E}'_{\lambda}) with the same degrees
 1: \mathcal{G}'_{\lambda} \leftarrow \mathcal{G}_{\lambda}
 2: for iter = 1, 2, ..., K do
 3:
          Compute the connected components of \mathcal{G}'_{\lambda}
          if there is only one component then
 4:
 5:
              return \mathcal{G}'_{\lambda}
          end if
 6:
          Select two distinct components C_1 and C_2
 7:
          Select an internal edge (a,b) \in \mathcal{E}'_{\lambda} with a,b \in C_1 {e.g., uniformly at random} Select an internal edge (c,d) \in \mathcal{E}'_{\lambda} with c,d \in C_2 {e.g., uniformly at random}
 8:
 9:
10:
          success \leftarrow false
          for each choice of pairing, i.e., (e_1, e_2) \in \{\{(a, c), (b, d)\}, \{(a, d), (b, c)\}\}\ do
11:
12:
              if neither e_1 nor e_2 already belongs to \mathcal{E}'_{\lambda} and they are not self-loops then
                   \mathcal{E}'_{\lambda} \leftarrow \mathcal{E}'_{\lambda} \setminus \{(a,b),(c,d)\} 
 \mathcal{E}'_{\lambda} \leftarrow \mathcal{E}'_{\lambda} \cup \{e_1,e_2\} 
13:
14:
15:
                  success \leftarrow true
                  break {degrees are preserved by this edge swap}
16:
              end if
17:
18:
          end for
19:
          if not success then
20:
              {no valid pairing for this choice of edges; try different edges in the next iteration}
21:
          end if
22: end for
23: return \mathcal{G}'_{\lambda} {may still be disconnected in the worst case}
```

Algorithm 6 FALLBACKCONNECTEDGRAPH

```
Require: Target degree sequence d_1, \ldots, d_n
Ensure: Connected simple graph \mathcal{G}_{\lambda} = (\mathcal{V}, \mathcal{E}_{\lambda}) approximating d
 1: \mathcal{V} \leftarrow \{1, \dots, n\}, \mathcal{E}_{\lambda} \leftarrow \emptyset
 2: Initialize \mathcal{E}_{\lambda} as a simple ring:
 3: for i = 1 to n - 1 do
          add edge (i, i + 1)
 5: end for
 6: add edge (n,1)
 7: for i = 1 to n do
          \operatorname{need}_i \leftarrow d_i - \deg_{\mathcal{G}_{\lambda}}(i) {remaining degree to be assigned}
 9: end for
10: for t = 1 to n(n-1)/2 do
11:
          Choose u with maximal need<sub>u</sub>
12:
          if need_u \leq 0 then
13:
              break
14:
          end if
          Choose v \neq u with maximal need<sub>v</sub>, need<sub>v</sub> > 0, and (u, v) \notin \mathcal{E}_{\lambda}
15:
          if such v exists then
16:
17:
              Add edge (u, v) to \mathcal{E}_{\lambda}
18:
              \operatorname{need}_u \leftarrow \operatorname{need}_u - 1, \operatorname{need}_v \leftarrow \operatorname{need}_v - 1
19:
          else
20:
              break
21:
          end if
22: end for
23: return \mathcal{G}_{\lambda} = (\mathcal{V}, \mathcal{E}_{\lambda})
```

E. Experimental details and additional results

In this section, we provide the details on the experiment as well as additional experimental results.

E.1. Topology

In the experiments, we use three types of topologies that commonly used in existing works including *ring graphs*, *static exponential graphs*, and *grid graphs*. Moreover, we also introduce $Erd\delta s$ - $R\acute{e}nyi$ random graph and random geometric graph to the experiments, as well as the customized topology constructed according to the weight λ described in Section 7.2. Each of them represents a distinct level of sparsity and connectivity structure:

- 1. **Ring graph.** Each node i is connected only to its two immediate neighbors (i-1) and (i+1) with cyclic wrapping, forming a one-dimensional circular structure. This topology is regular and sparse, and is often used to study information propagation under limited local communication. Formally, the adjacency satisfies $\mathcal{V}_{\text{ring}} = \{(i, (i \pm 1) \mod n)\}$.
- 2. Static exponential graph. (Ying et al., 2021) Each node i is connected to nodes whose distances are powers of two, i.e., $(i \pm 2^p) \mod n$ for integer $p \ge 0$ up to $\lfloor \log_2(n/2) \rfloor$. This design introduces logarithmic shortcut links while maintaining deterministic sparsity, improving the spectral gap compared with the ring topology.
- 3. **Grid graph.** Nodes are arranged on a $\sqrt{n} \times \sqrt{n}$ two-dimensional lattice, where each node connects to its four orthogonal neighbors (up, down, left, right) with periodic boundary conditions. This structure is widely used to model spatially local communication and resembles decentralized sensor or mesh networks.
- 4. **Erdős–Rényi random graph.** (Beveridge & Youngblood, 2016) A stochastic topology where each undirected edge between any pair of nodes is independently included with probability $p \in (0,1)$. The resulting graph $\mathcal{G}_{ER}(n,p)$ is connected with high probability when $p > \frac{\log n}{n}$, and exhibits an expected node degree of (n-1)p. This topology captures random and dynamic communication patterns often observed in large-scale or unreliable networks.
- 5. Random geometric graph. (Boyd et al., 2005) Nodes are uniformly sampled from the unit square $[0,1]^2$, and an undirected edge is established between any two nodes whose Euclidean distance is less than a given radius r=0.3. Formally, the adjacency satisfies $\mathcal{V}_{RGG}=\{(i,j)\mid \|x_i-x_j\|_2\leq r\}$. This topology captures spatial locality in communication and is commonly used to model wireless or sensor networks, where connectivity depends on physical proximity rather than explicit node indices. When $r=\Theta\left(\sqrt{\frac{\log n}{n}}\right)$, the graph is connected with high probability.
- 6. Custom graph $\mathcal{G}_{\lambda} = (\mathcal{V}, \mathcal{E}_{\lambda})$. (Section 7.2)

Next, we consider the first set of randomly generated node weights given by

$$\lambda_A = [0.3, 0.8, 1.0, 0.9, 0.7, 1.0, 2, 2.2, 1.2, 1.4, 0.8, 0.5, 1.5, 0.6, 0.6, 0.5]^{\top}$$

The corresponding communication topology $\mathcal{G}_{\lambda_A} = (\mathcal{V}, \mathcal{E}_{\lambda_A})$ generated based on these weights is shown in the Figure 4.

The node degrees are, in order:

$$[2, 5, 6, 5, 4, 6, 12, 13, 7, 8, 5, 3, 9, 4, 4, 3].$$

The second set of randomly generated node weights are:

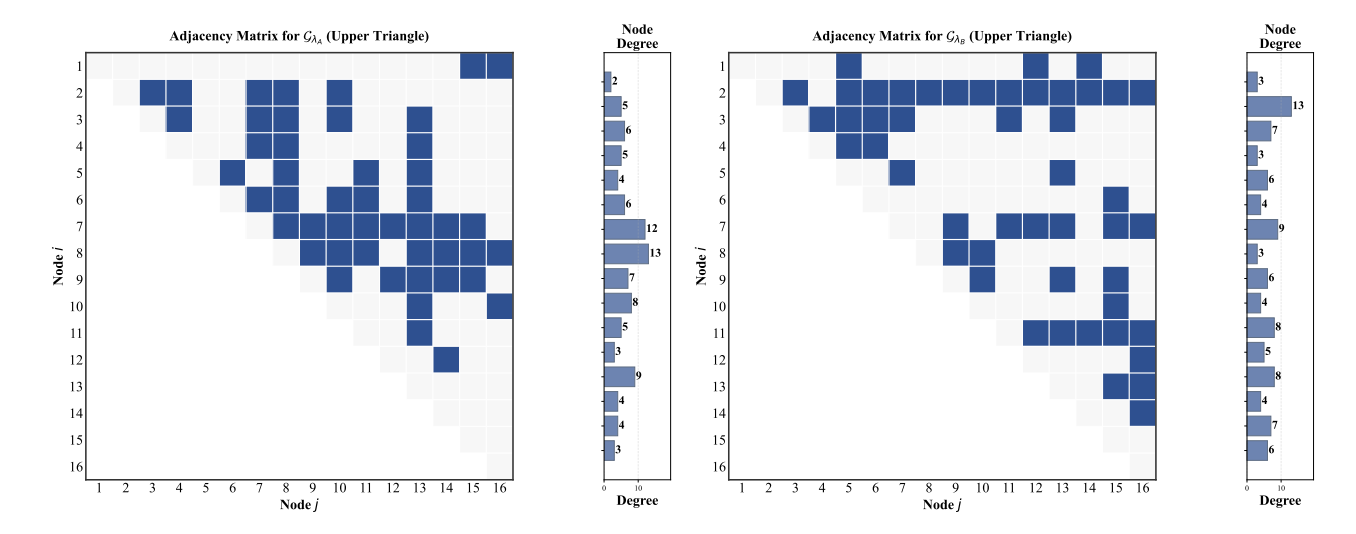
$$\lambda_B = [0.4, 2.3, 1.2, 0.5, 1.0, 0.6, 1.5, 0.8, 1.1, 0.7, 1.8, 0.9, 1.4, 0.6, 1.2, 1.0]^{\mathsf{T}}$$

The corresponding topology $\mathcal{G}_{\lambda_B} = (\mathcal{V}, \mathcal{E}_{\lambda_B})$ is shown in the Figure 5.

E.2. Comparison on Spectral Gaps

Existing studies typically adopt a conservative choice of the inertia coefficient (e.g., $\varepsilon = 0.5$) (Alghunaim & Yuan, 2022; Yuan et al., 2023). In contrast, we set $\varepsilon = 0.3$, which achieves a more balanced trade-off between stability and convergence speed (Levin & Peres, 2017).

The results in Table 1 validate the observation discussed in Section 7: for regular graphs, uniform weights yield the largest spectral gap. Moreover, the matrices designed using the proposed weighting strategy achieve a substantially larger spectral gap in heterogeneous settings.



node j, the (i, j) block is blue.

Figure 4. Adjacency matrix of \mathcal{G}_{λ_A} . If node i is connected with Figure 5. Adjacency matrix of \mathcal{G}_{λ_B} . If node i is connected with node j, the (i, j) block is blue.

Table 1. Spectral gaps of different network topologies under weights λ_1 and λ_2 .

| Topology | Mixing matrices | | |
|---------------------------|-----------------|-------------|----------------|
| | $W(\lambda_1)$ | $W^{ m ds}$ | $W(\lambda_2)$ |
| Ring | 0.034 | 0.053 | 0.027 |
| Grid | 0.075 | 0.119 | 0.086 |
| Exp | 0.248 | 0.400 | 0.202 |
| \mathcal{G}_{λ_A} | 0.311 | 0.108 | / |
| \mathcal{G}_{λ_B} | / | 0.130 | 0.293 |

The boldface numbers highlight the largest spectral gaps within each row.

E.3. Synthetic Quadratic Experiment

We consider a decentralized least-squares loss with heterogeneous local optima and optional gradient noise (Koloskova et al., 2020). For each node $i \in \{1, ..., n\}$, the local loss is

$$F_i(\theta) = \frac{1}{2} ||A_i \theta - b_i||_2^2 + \frac{\rho}{2} ||\theta||_2^2, \qquad A_i \in \mathbb{R}^{d \times d}, \ b_i \in \mathbb{R}^d.$$

In our construction we take $A_i = \zeta_i I_d$ (no directional heterogeneity) with $\theta_i^* := A_i^{-1} b_i$ being the local minimizer.

E.3.1. DATA GENERATION

We synthesize problem instances as follows.

- 1. Curvature (no directional heterogeneity). For each node, sample a scalar curvature $\zeta_i \sim \mathcal{U}[\zeta_{\min}, \zeta_{\max}]$ and set $A_i = \zeta_i I_d$. In our default setting, $\zeta_{\min} = 5.5$ and $\zeta_{\max} = 12.5$.
- 2. Local offsets (heterogeneous optima). Draw a shared reference center $c_{\text{base}} \sim \mathcal{N}(0, I_d)$. For each node i, assign $c_i = c_{\text{base}} + \mu_i$, where $\mu_i = \mu_0 v_i$, $v_i \sim \mathcal{N}(0, I_d) / ||v_i||_2$.
- 3. Initialization (heterogeneous). Each node starts from an independent random vector $\theta_i^{(0)} \sim \mathcal{N}(0, I_d)$.

4. Global weighted optimum (closed form). For an explicit loss-weight vector λ , the weighted global minimizer is

$$\theta^* = \left(\sum_{i=1}^n \lambda_i \zeta_i I_d + \rho I_d\right)^{-1} \left(\sum_{i=1}^n \lambda_i \zeta_i c_i\right).$$

E.3.2. GRADIENT EVALUATION

At iteration t, node i computes a local stochastic gradient by adding noise:

$$g_i^{(t)} = \nabla F_i \left(\theta_i^{(t)} \right) + \sigma \xi_{i,t} = \zeta_i (x_i^{(t)} - c_i) + \rho x_i^{(t)} + \sigma \xi_{i,t}, \quad \xi_{i,t} \sim \mathcal{N}(0, I_d).$$

To ensure reproducibility while keeping node- and iteration-wise diversity, $\xi_{i,t}$ is drawn using a deterministic composite seed $s_{i,t} = s_0 + 1000i + 10t$ for a base seed s_0 (cf. the code). This makes the sequence $\{\xi_{i,t}\}$ independent across nodes/iterations and exactly reproducible across runs with the same s_0 .

E.3.3. IMPLEMENTATION DETAILS

Unless otherwise stated, we use:

- Number of nodes: n = 16, dimension: d = 10
- Step size: $\alpha = 0.12$ for V_1 and V_2 , $\alpha = 0.09$ for ring, iterations: T = 240, evaluation interval: 3
- Regularization: $\rho = 0.01$, gradient-noise std: $\sigma = 1.0$
- Curvature range: $\zeta_i \in [5.5, 12.5]$, local offsets: $\mu_0 = 3.0$

E.3.4. EVALUATION METRICS

We monitor the global gradient norm defined as:

$$\left\| \frac{\lambda^{\top}}{n} \nabla F(\Theta^{(t)}) \right\| = \left\| \frac{1}{n} \sum_{i=1}^{n} \lambda_i \nabla F_i(\theta_i^{(t)}) \right\|.$$

Each experiment is repeated 10 times over independent seeds and the results are averaged.

E.4. CIFAR-10 Classification Experiment

We evaluate the proposed methods on the CIFAR-10 (Krizhevsky et al., 2009) dataset using a ResNet-18 (He et al., 2016) architecture with Batch Normalization (ResNet18WithBN). The network adopts the standard four-stage structure with channel widths $\{64, 128, 256, 512\}$, ReLU activations, and global average pooling. Following common practice (He et al., 2016; Zhang et al., 2019), we apply a weight decay of 5×10^{-4} to convolutional and linear weights, while excluding BatchNorm parameters and bias terms from regularization.

The dataset is randomly partitioned across n nodes according to a weighting vector $\lambda = [\lambda_1, \dots, \lambda_n]$, so that each node receives a fraction λ_i/n of the total samples. All models are trained for 2500 iterations using vanilla stochastic gradient descent with a mini-batch size of 128. Every 30 iterations, all nodes are jointly evaluated on the full test set. The reported metrics include both accuracy and loss, where the loss (interval loss) is computed as the average over each 30-iteration interval, and both accuracy and loss are aggregated across nodes via λ -weighted averaging.

The detailed experimental results are as follows.

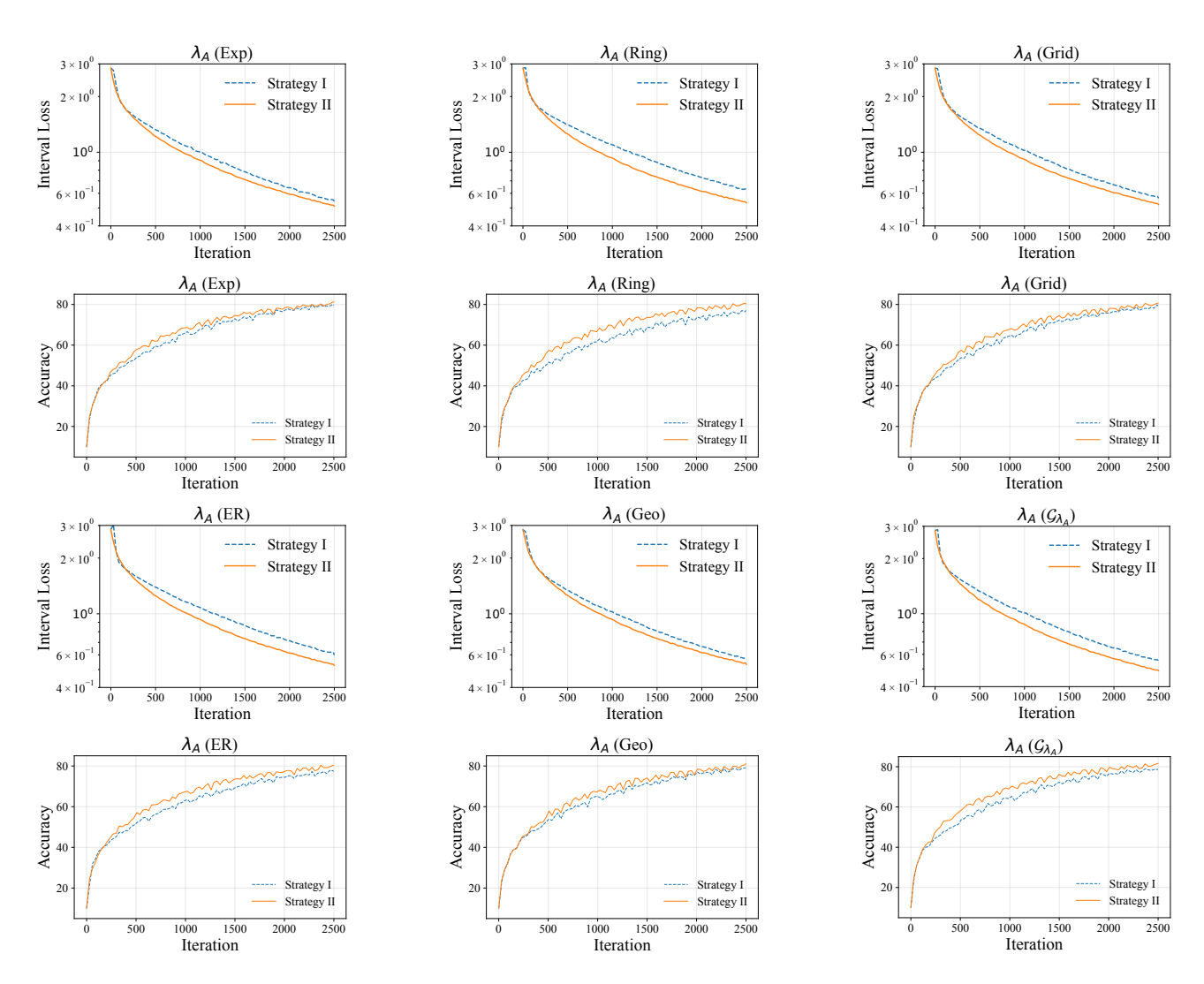


Figure 6. Training loss and test accuracy for models trained by Strategy I and II on CIFAR-10 dataset under weight λ_1 . Strategy II outperforms on all topologies.

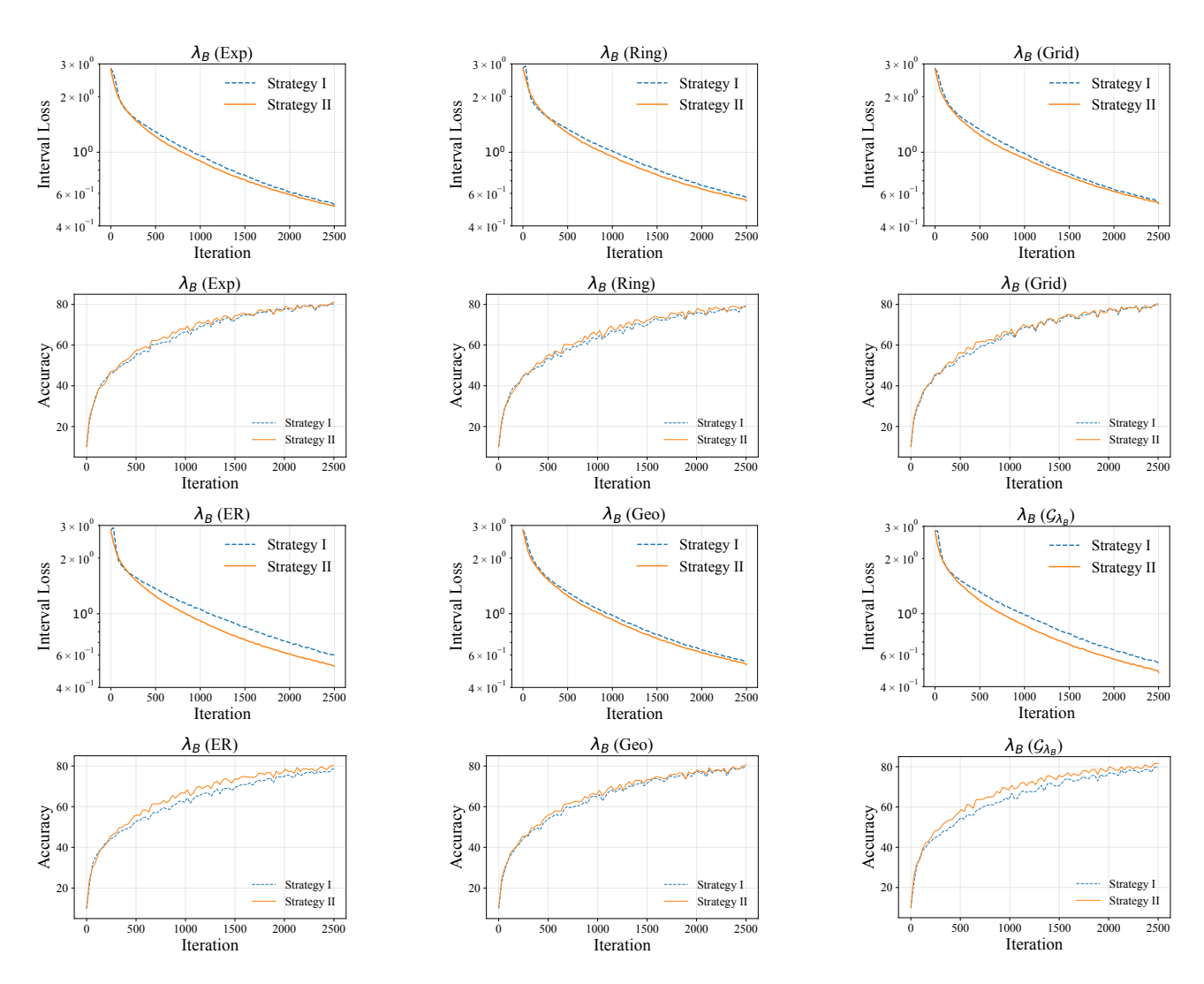


Figure 7. Training loss and test accuracy for models trained by Strategy I and II on CIFAR-10 dataset under weight λ_2 . Strategy II outperforms on all topologies.